

Muon g-2 and EDM

cLFV school

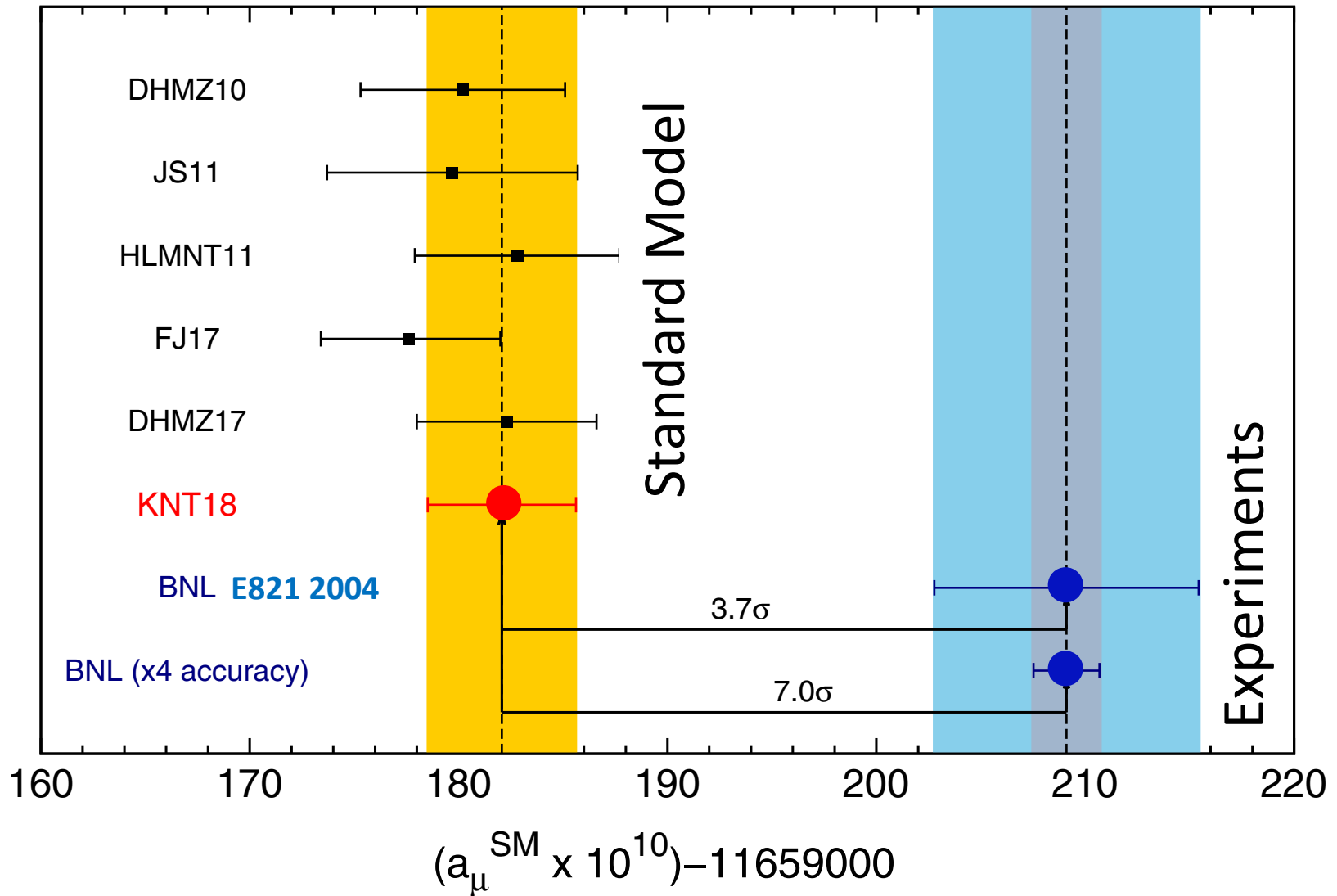
July 5-6, 2019

Tsutomu Mibe (IPNS, KEK)



Comparison between SM and a_μ

A. Keshavarzi, D. Nomura, T. Teubner, Phys. Rev. D 97, 114025 (2018)



Note that electron $g-2$ is consistent with the SM.

Comparison of experiments

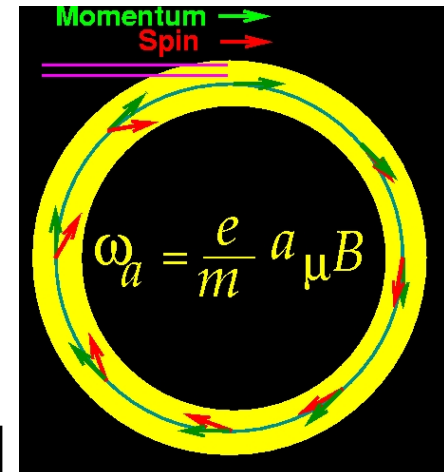
| | BNL-E821 | Fermilab-E989 | Our experiment |
|---------------------------|-------------------------------------------|----------------------|--------------------------------------------|
| Muon momentum | | 3.09 GeV/ c | 300 MeV/ c |
| Lorentz γ | | 29.3 | 3 |
| Polarization | | 100% | 50% |
| Storage field | | $B = 1.45$ T | $B = 3.0$ T |
| Focusing field | | Electric quadrupole | Very weak magnetic |
| Cyclotron period | | 149 ns | 7.4 ns |
| Spin precession period | | 4.37 μ s | 2.11 μ s |
| Number of detected e^+ | 5.0×10^9 | 1.6×10^{11} | 5.7×10^{11} |
| Number of detected e^- | 3.6×10^9 | – | – |
| a_μ precision (stat.) | 460 ppb | 100 ppb | 450 ppb |
| (syst.) | 280 ppb | 100 ppb | <70 ppb |
| EDM precision (stat.) | 0.2×10^{-19} $e \cdot \text{cm}$ | – | 1.5×10^{-21} $e \cdot \text{cm}$ |
| (syst.) | 0.9×10^{-19} $e \cdot \text{cm}$ | – | 0.36×10^{-21} $e \cdot \text{cm}$ |

Contents

- Spin properties of muon
- Building a magnet from SM
- Measurement of $g-2$
- Searching for EDM
- Technical advances for higher precision
- Auxiliary measurements with muonium

muon g-2 and EDM measurements

In uniform magnetic field, muon spin rotates ahead of momentum due to $g-2 \neq 0$



general form of spin precession vector:

$$\vec{\omega} = -\frac{e}{m} \left[a_\mu \vec{B} - \left(a_\mu - \frac{1}{\gamma^2 - 1} \right) \frac{\vec{\beta} \times \vec{E}}{c} + \frac{\eta}{2} \left(\vec{\beta} \times \vec{B} + \frac{\vec{E}}{c} \right) \right]$$

BNL E821 approach
 $\gamma=30$ ($P=3$ GeV/c)

$$\vec{\omega} = -\frac{e}{m} \left[a_\mu \vec{B} + \frac{\eta}{2} \left(\vec{\beta} \times \vec{B} + \frac{\vec{E}}{c} \right) \right]$$

FNAL E989

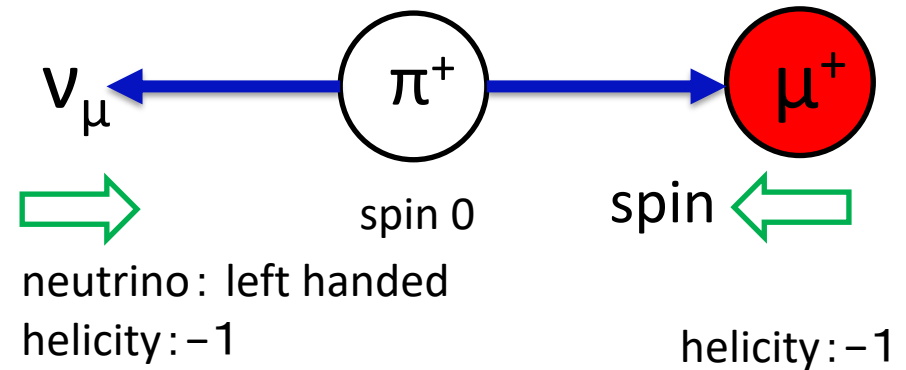
J-PARC approach
 $E = 0$ at any γ

$$\vec{\omega} = -\frac{e}{m} \left[a_\mu \vec{B} + \frac{\eta}{2} \left(\vec{\beta} \times \vec{B} \right) \right]$$

J-PARC E34

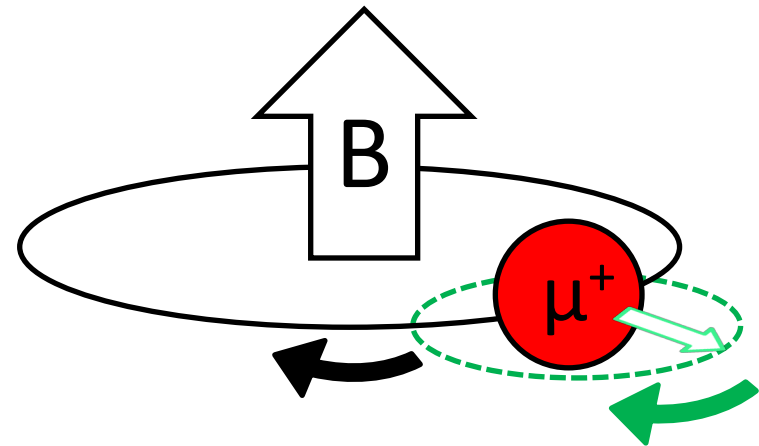
Three steps of g-2 measurement

1. Prepare a polarized muon beam.

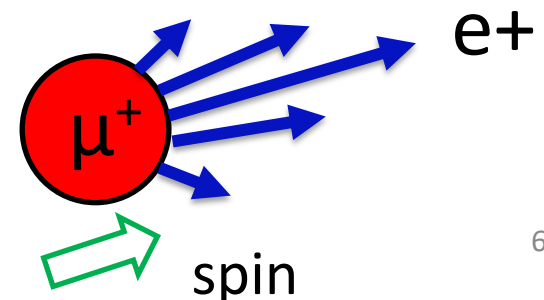


2. Store in a magnetic field (muon's spin precesses)

$$\vec{\omega} = -\frac{e}{m} \left[a_\mu \vec{B} - \left(a_\mu - \frac{1}{\gamma^2 - 1} \right) \frac{\vec{\beta} \times \vec{E}}{c} + \frac{\eta}{2} \left(\vec{\beta} \times \vec{B} + \frac{\vec{E}}{c} \right) \right]$$



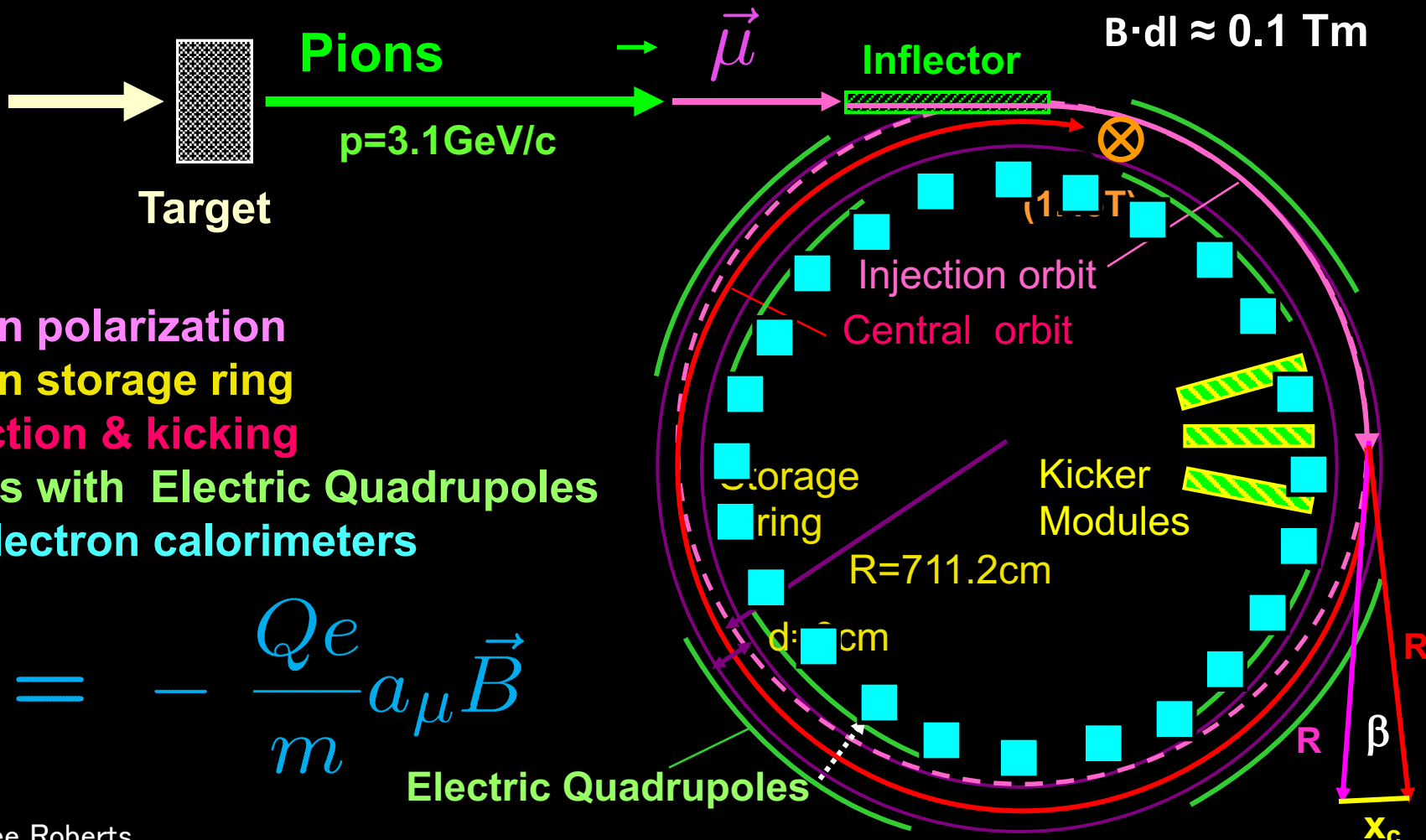
3. Measure decay positron



Experimental Technique

narrow bunch of protons

$x_c \approx 77$ mm
 $\beta \approx 10$ mrad
 $B \cdot dl \approx 0.1$ Tm



- Muon polarization
- Muon storage ring
- injection & kicking
- focus with Electric Quadrupoles
- 24 electron calorimeters

$$\vec{\omega}_a = - \frac{Qe}{m} a_\mu \vec{B}$$

Electric Quadrupoles

AGS

TABLE III. Selected AGS proton beam and secondary pion beamline characteristics.

| Proton Beam | Value | Pion Beamline | Value |
|--------------------------|--------------------|-----------------------------------|-----------------|
| Protons per AGS cycle | 5×10^{13} | Horizontal emittance | 42π mm-mrad |
| Cycle repetition rate | 0.37 Hz | Vertical emittance | 56π mm-mrad |
| Proton momentum | 24 GeV/c | Inflector horizontal aperture | ± 9 mm |
| Bunches per cycle | 6–12 | Inflector vertical aperture | ± 28 mm |
| Bunch width (σ) | 25 ns | Pions per proton ^a | 10^{-5} |
| Bunch spacing | 33 ms | Muons per pion decay ^b | 0.012 |

U–V line

VD3

VD4

V line

Pion Production Target (Nickel)
 $5E+12$ proton/spill

U line

Q2

Q1

D1,D2

D3,D4

Pion Decay Channel

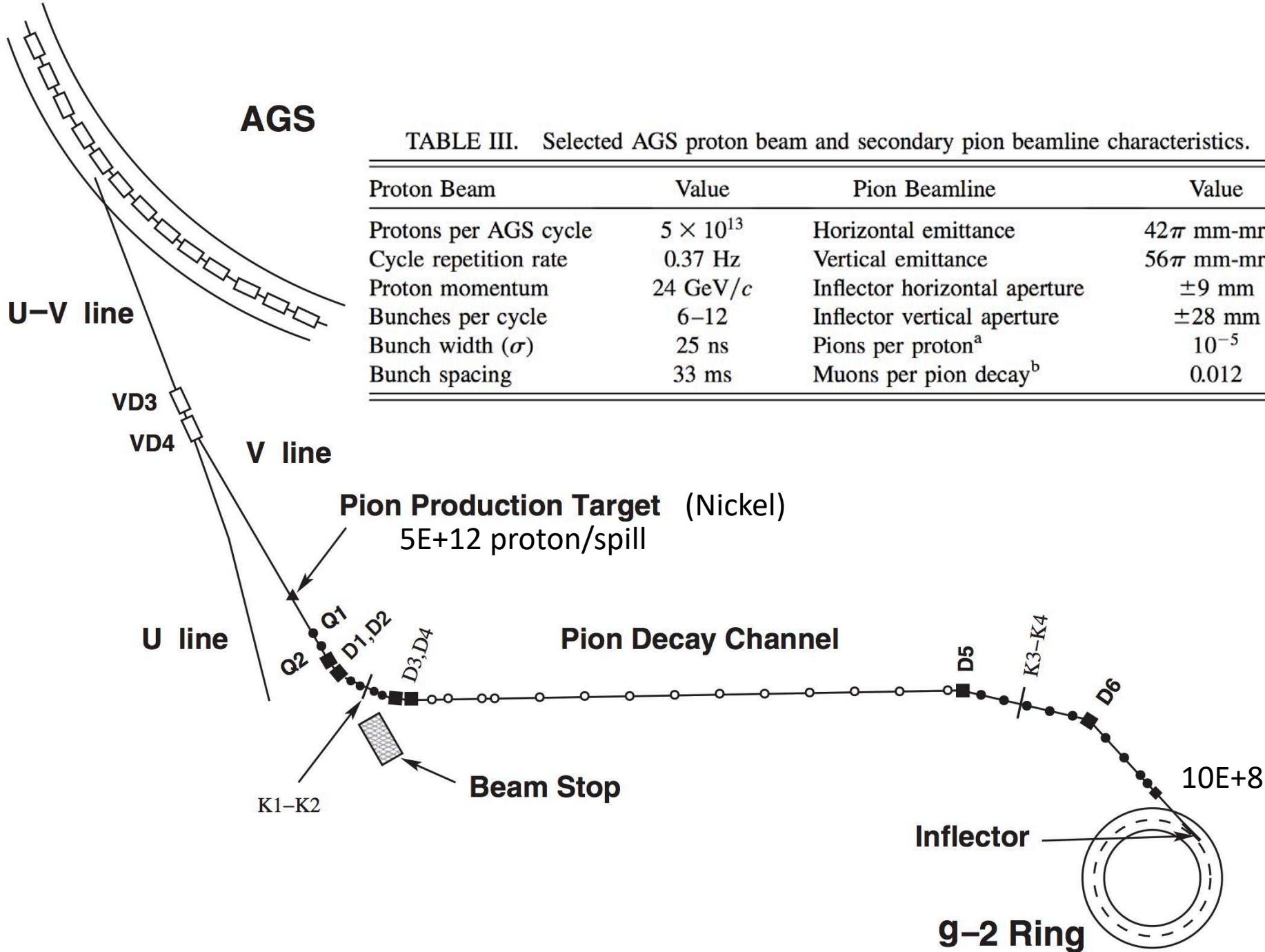
K1–K2

Beam Stop

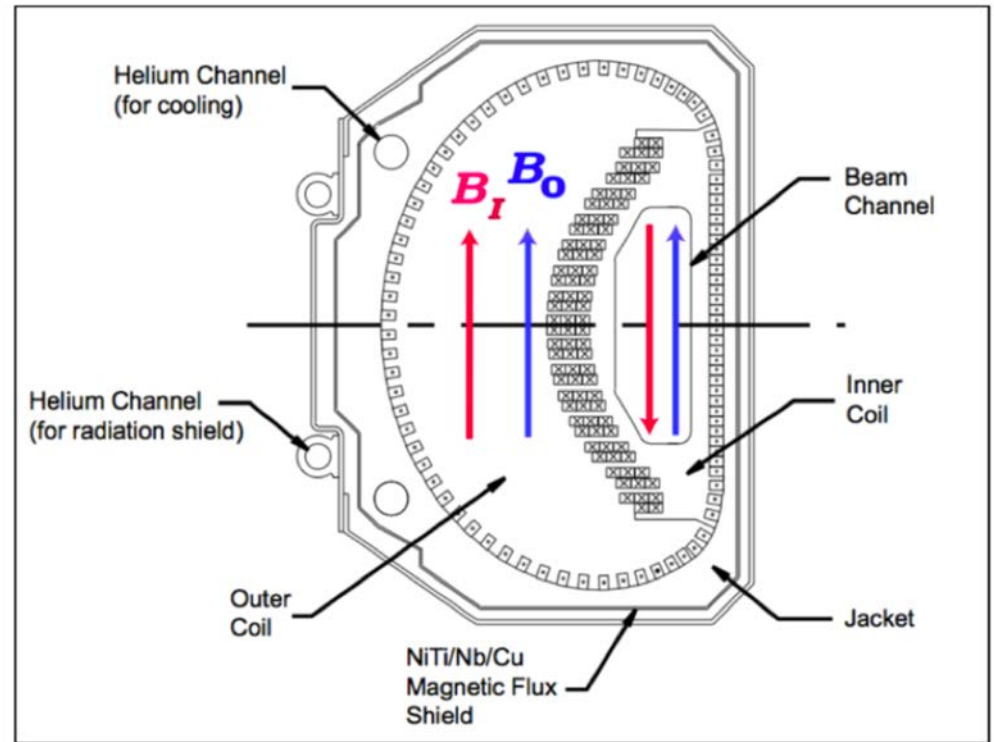
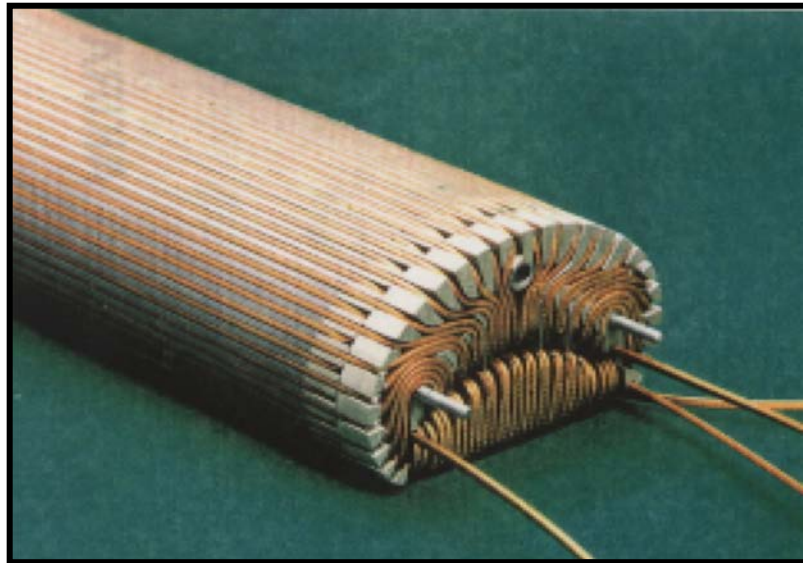
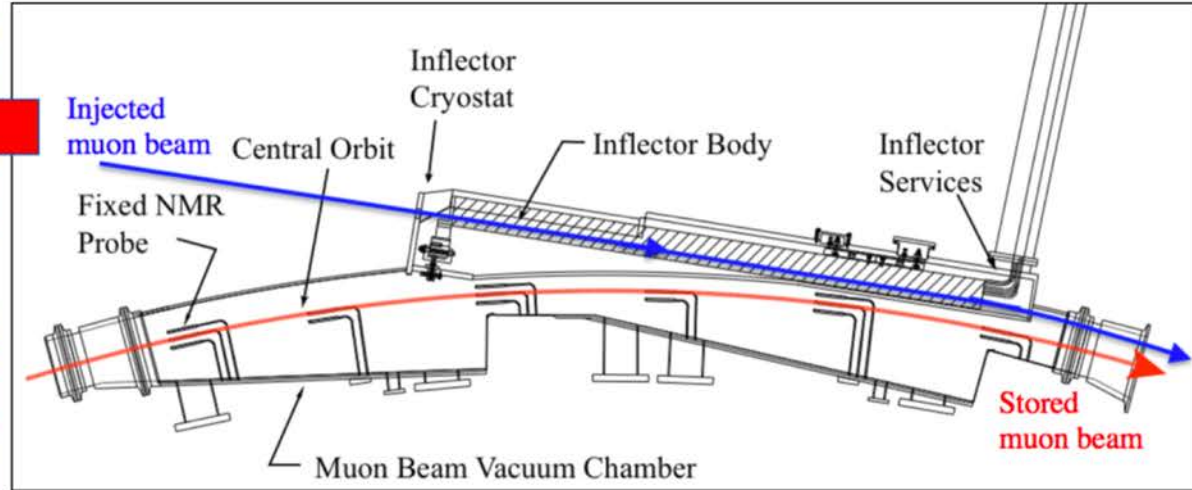
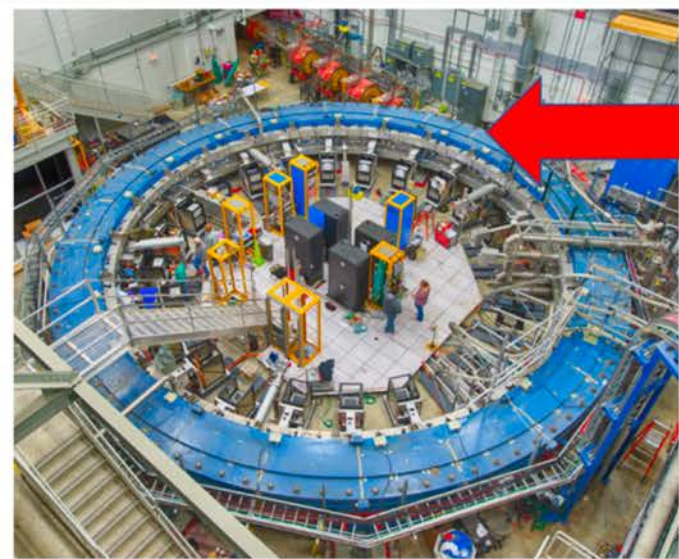
D5

K3–K4

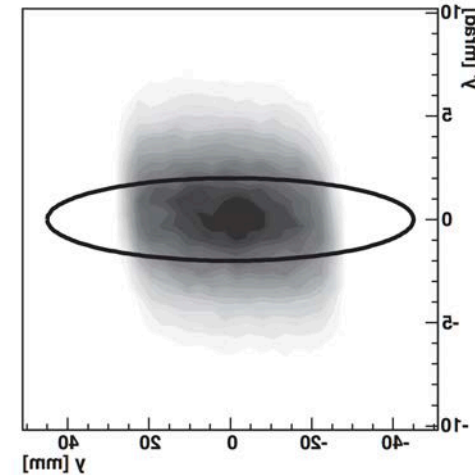
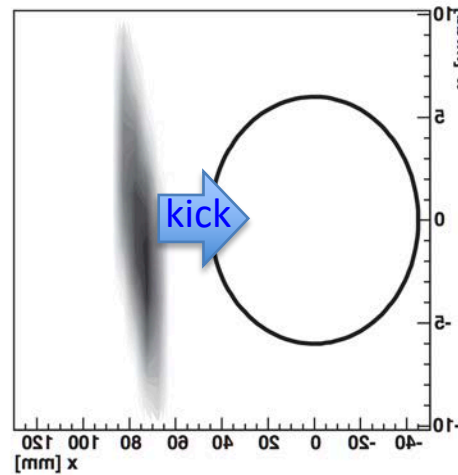
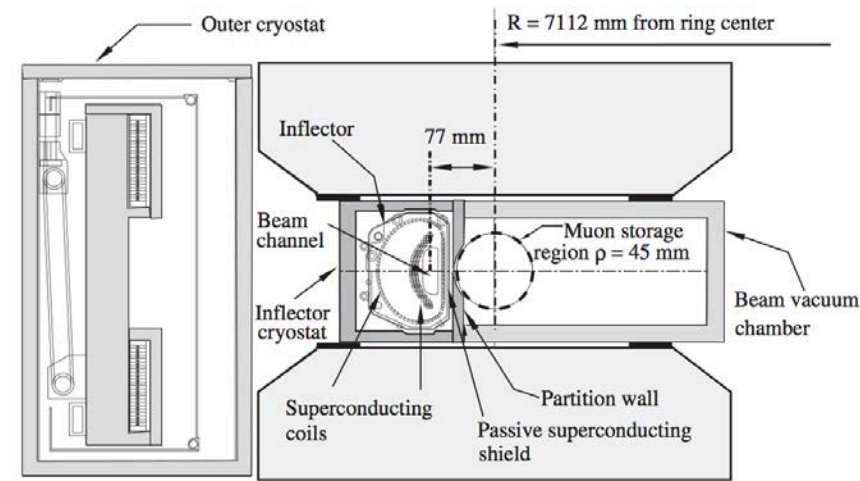
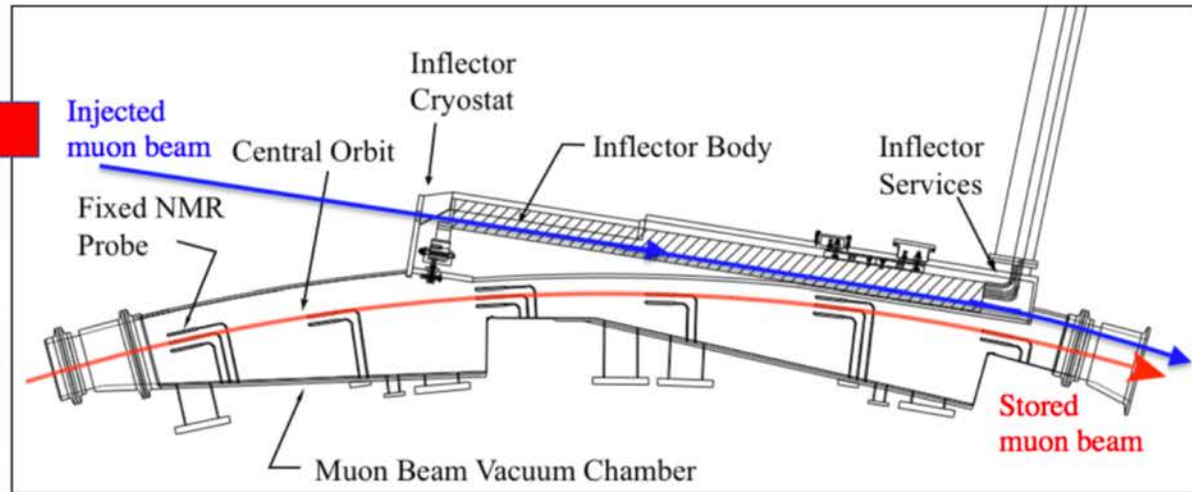
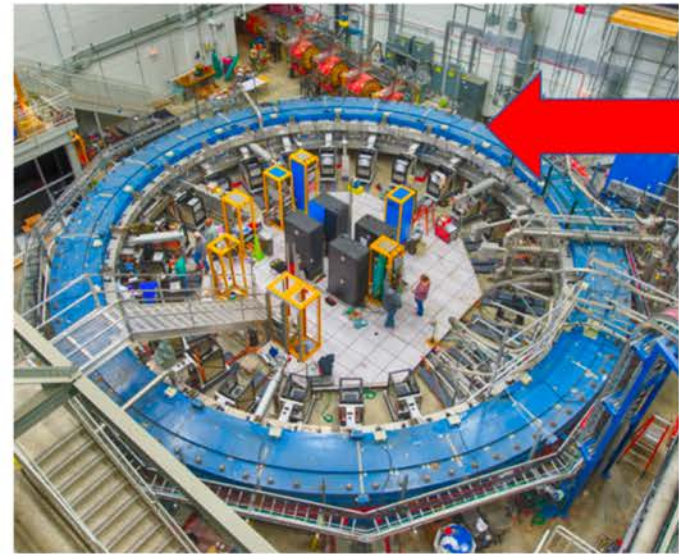
D6

 $10E+8$ **Inflector****g–2 Ring**

Injection



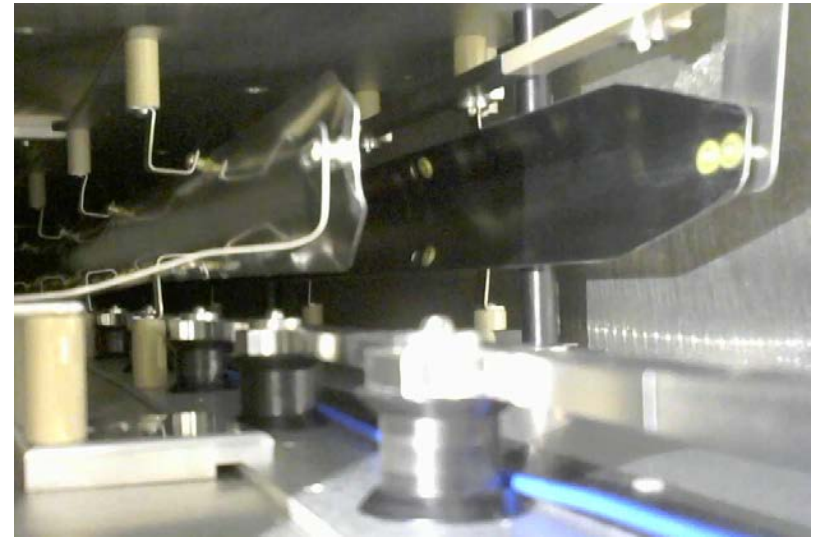
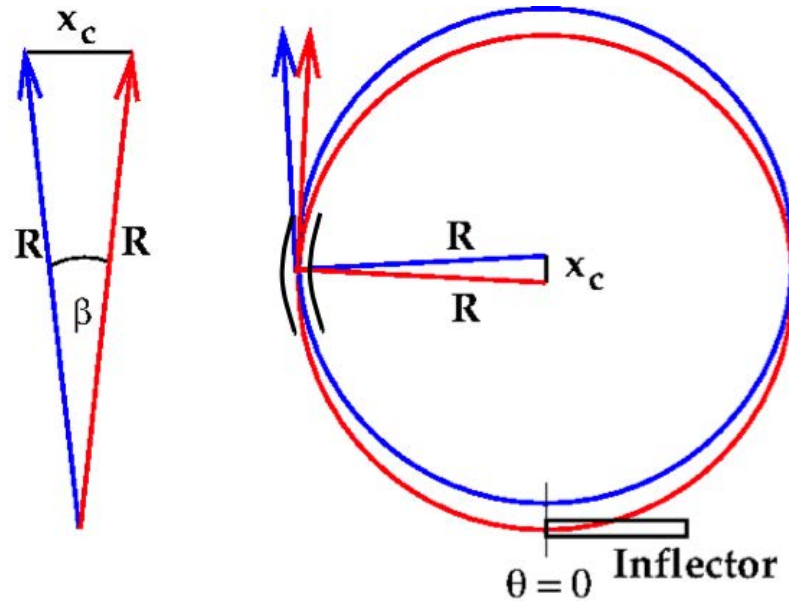
Injection



Injection efficiency 3-5%

Kicker

Slide by D. Kawall

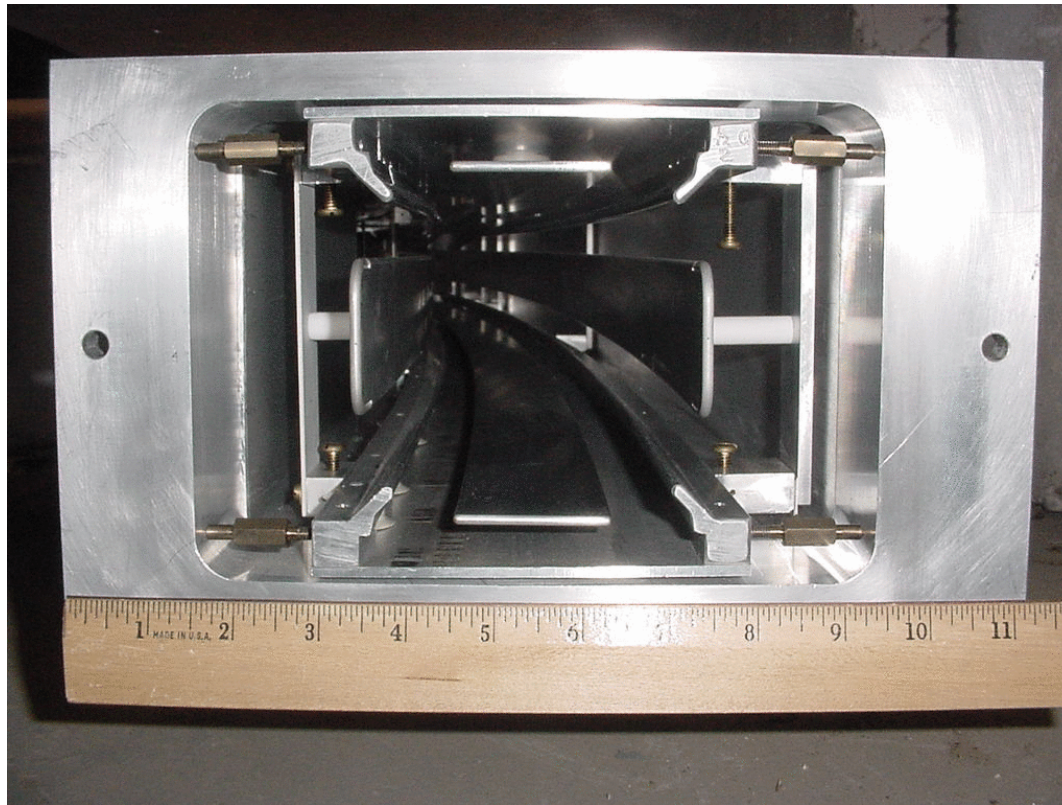


- Muons enter 77 mm outside ideal closed orbit with radius 7112 mm
- Muons cross ideal orbit at 90° , angle off by $77 \text{ mm} / 7112 \text{ mm} \approx 11 \text{ mrad}$
- ⇒ Reduce \mathbf{B} by $\approx 300 \text{ Gauss}$ over 4 metres for 149 ns at 100 Hz, 10% homogeneity
- Kicker steers muons onto stored orbit with $\approx 50 \text{ kV}$, 5000 Amp pulse

Electric quadrupoles

Slide by D. Kawall

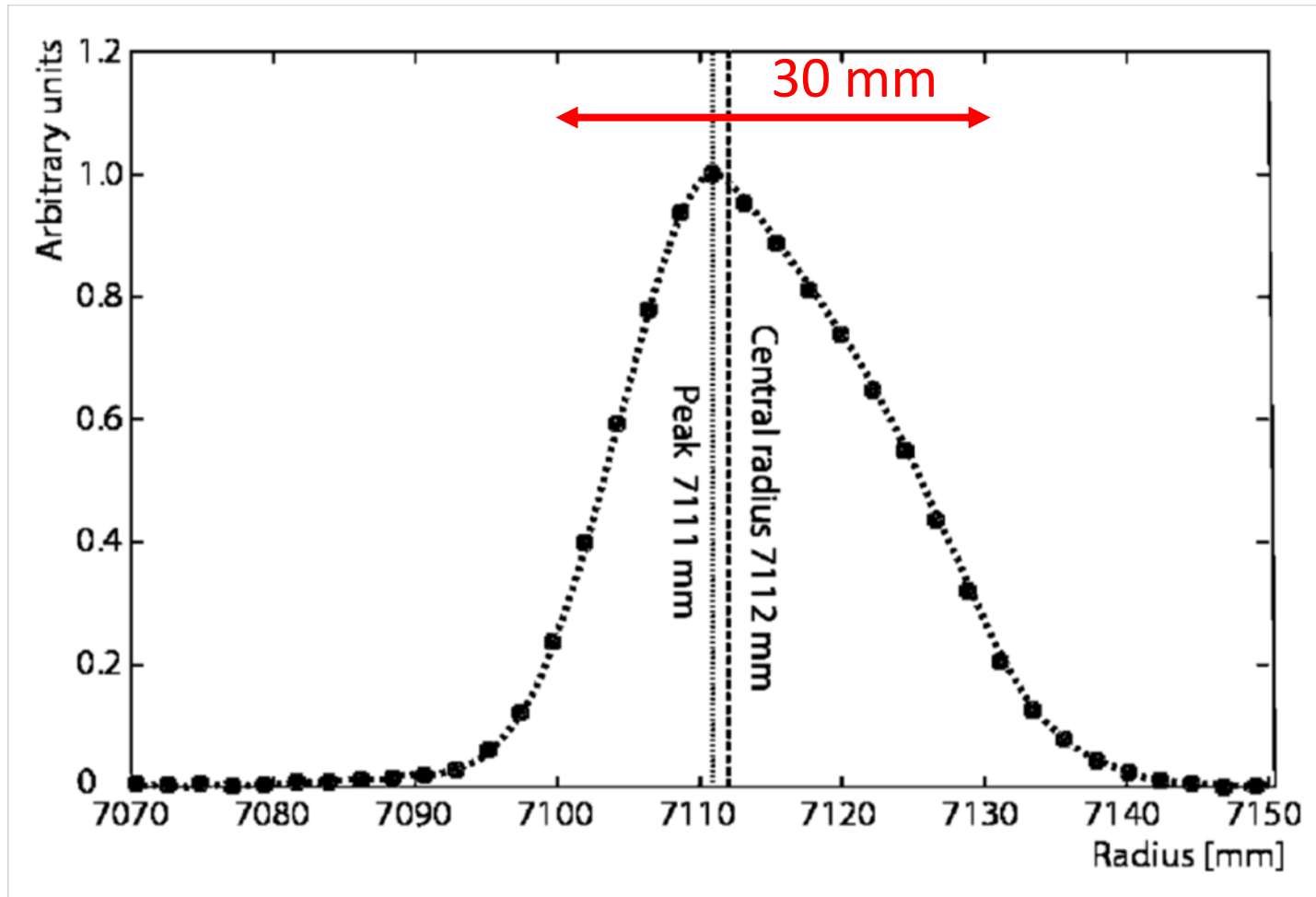
- Use electric quadrupoles for linear restoring force in vertical
- Uniform quadrupole field leads to simple harmonic motion about closed orbit



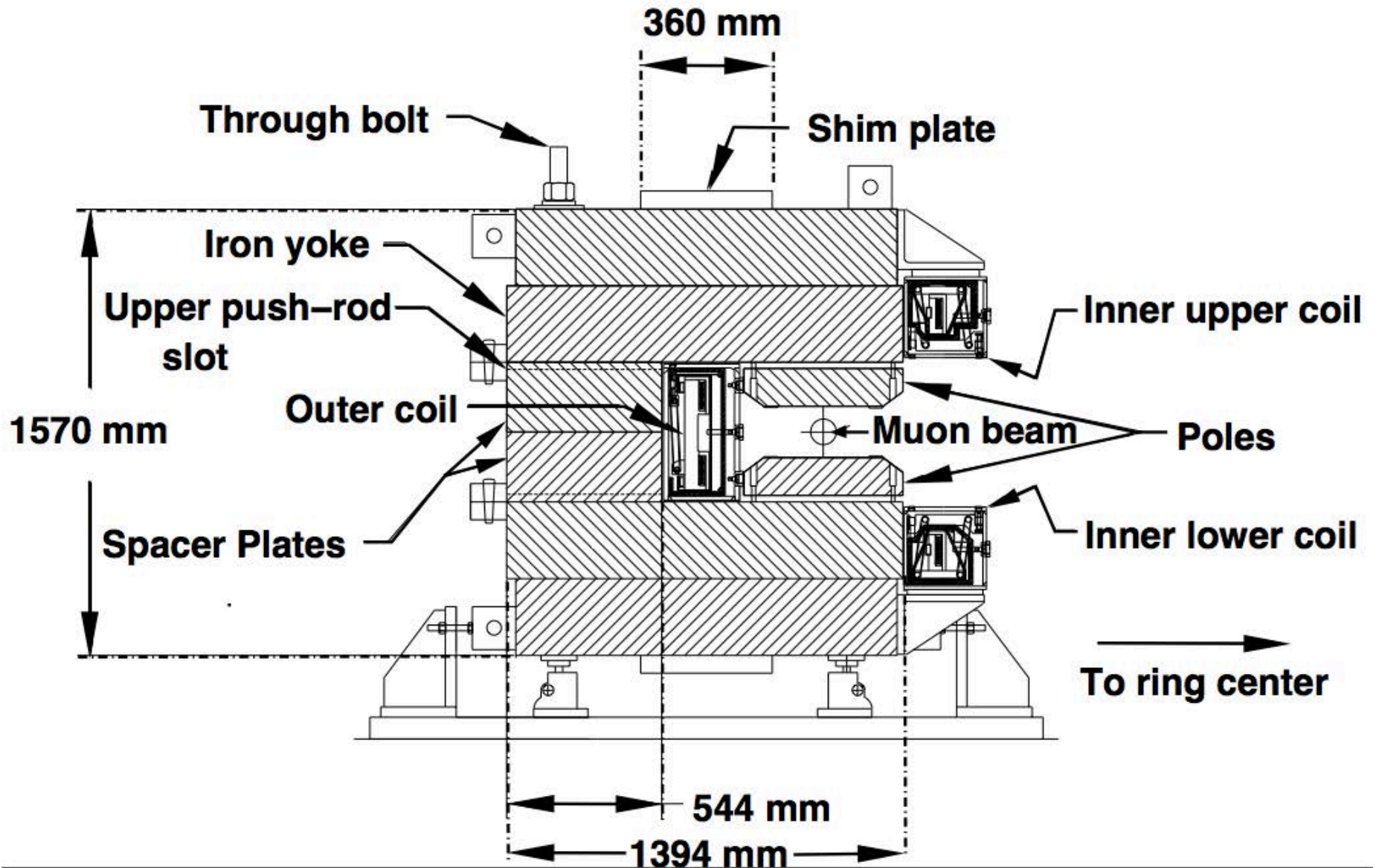
$V \approx 24 \text{ kV}$
 $n \approx 0.14$

$$x = x_e + A_x \cos \left(\nu_x \frac{s}{R_0} + \delta_x \right), \quad y = A_y \cos \left(\nu_y \frac{s}{R_0} + \delta_y \right)$$

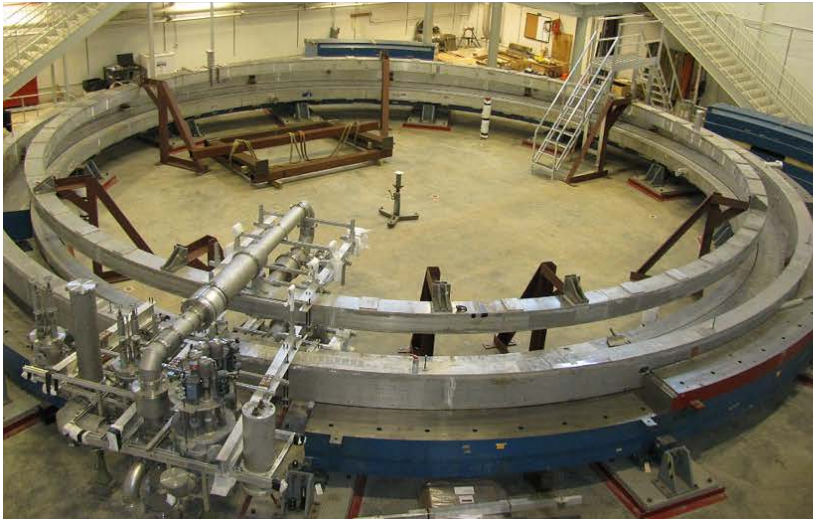
Beam distribution at storage



Storage magnet



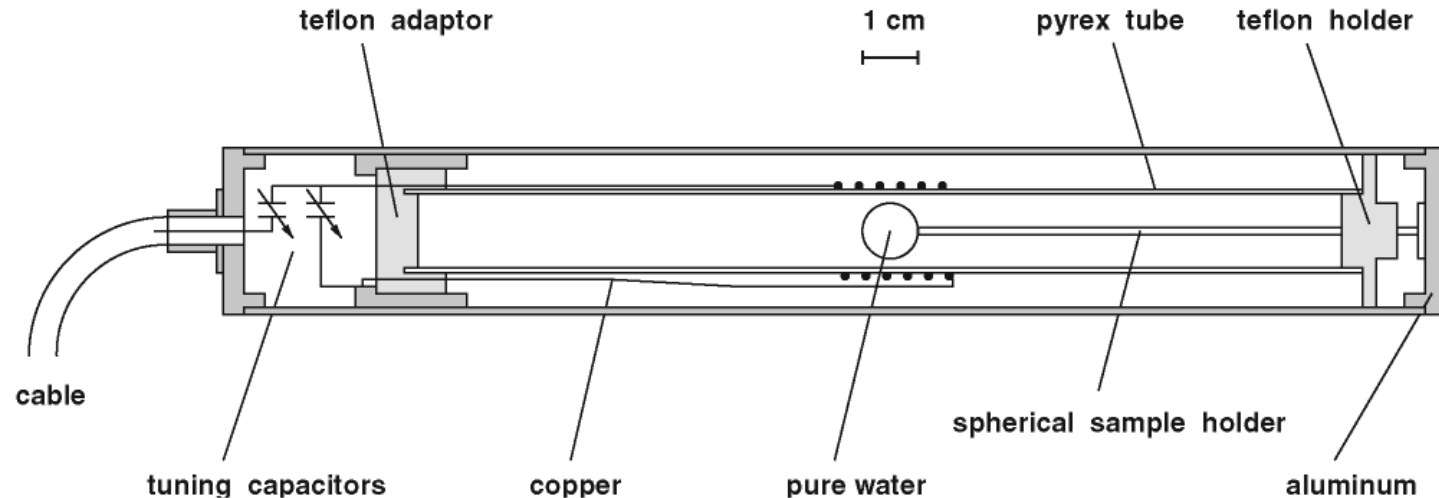
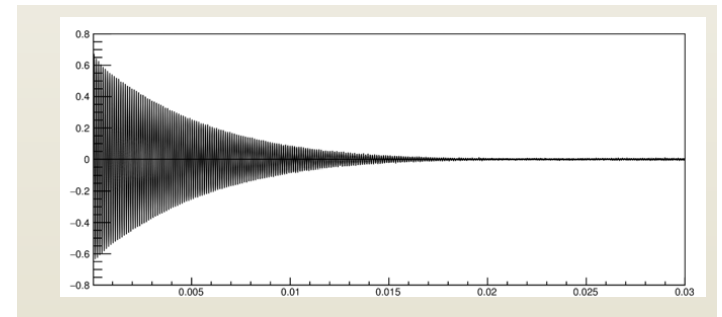
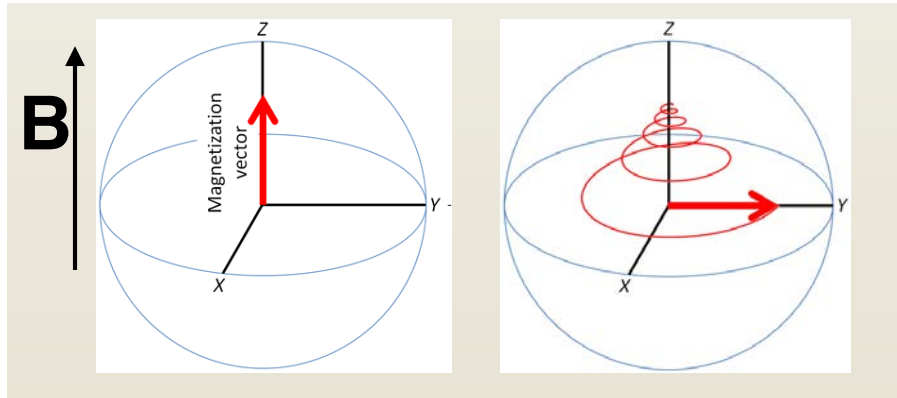
Magnet Reassembly at Fermilab June 2014 - June 2015



Measurement of magnetic field

NMR (Nuclear Magnetic Resonance)

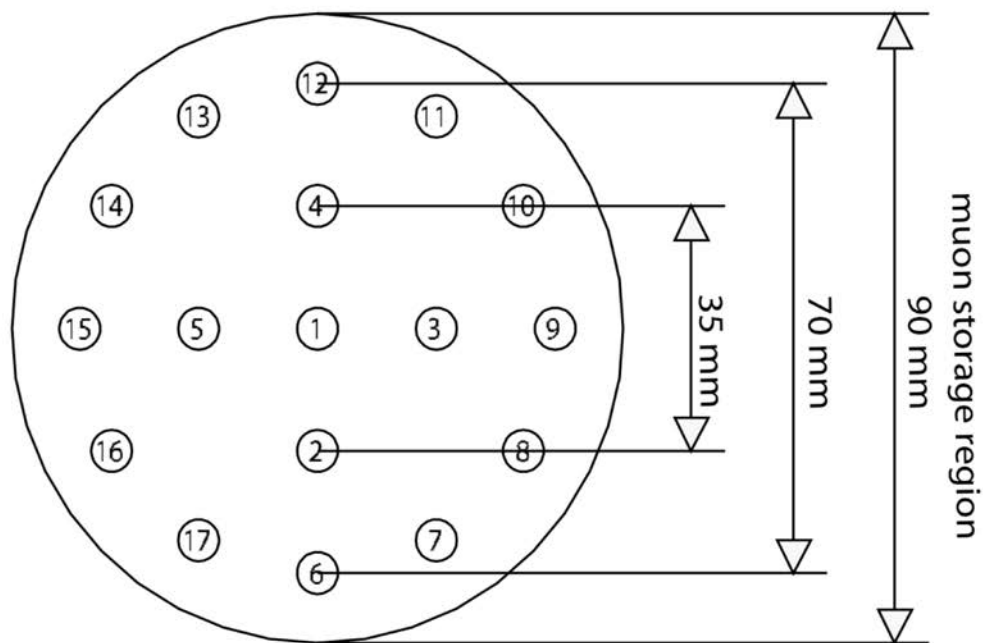
$$\omega_p = \mu_p B$$



Field mapping trolley

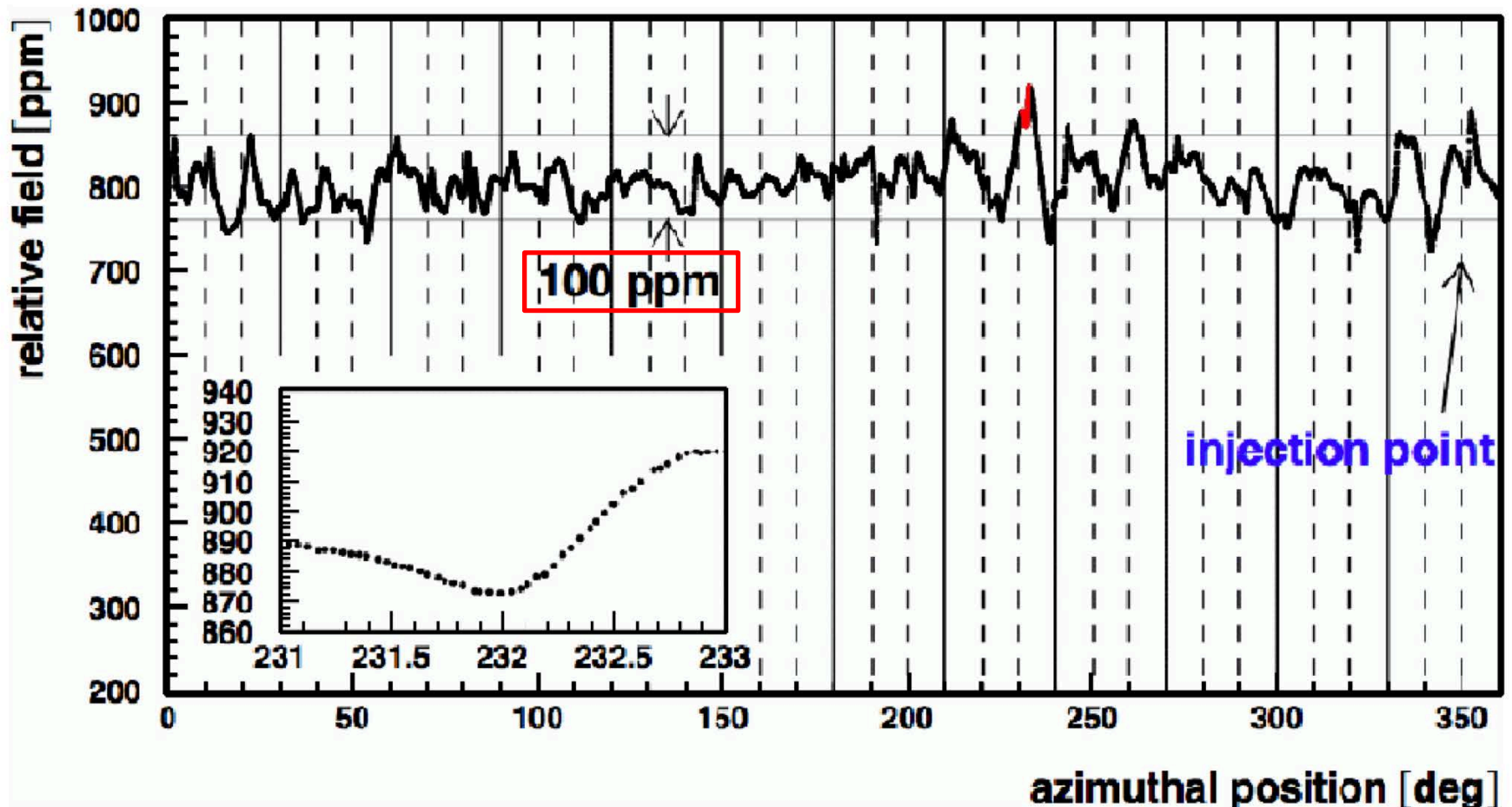


(a) NMR Trolley



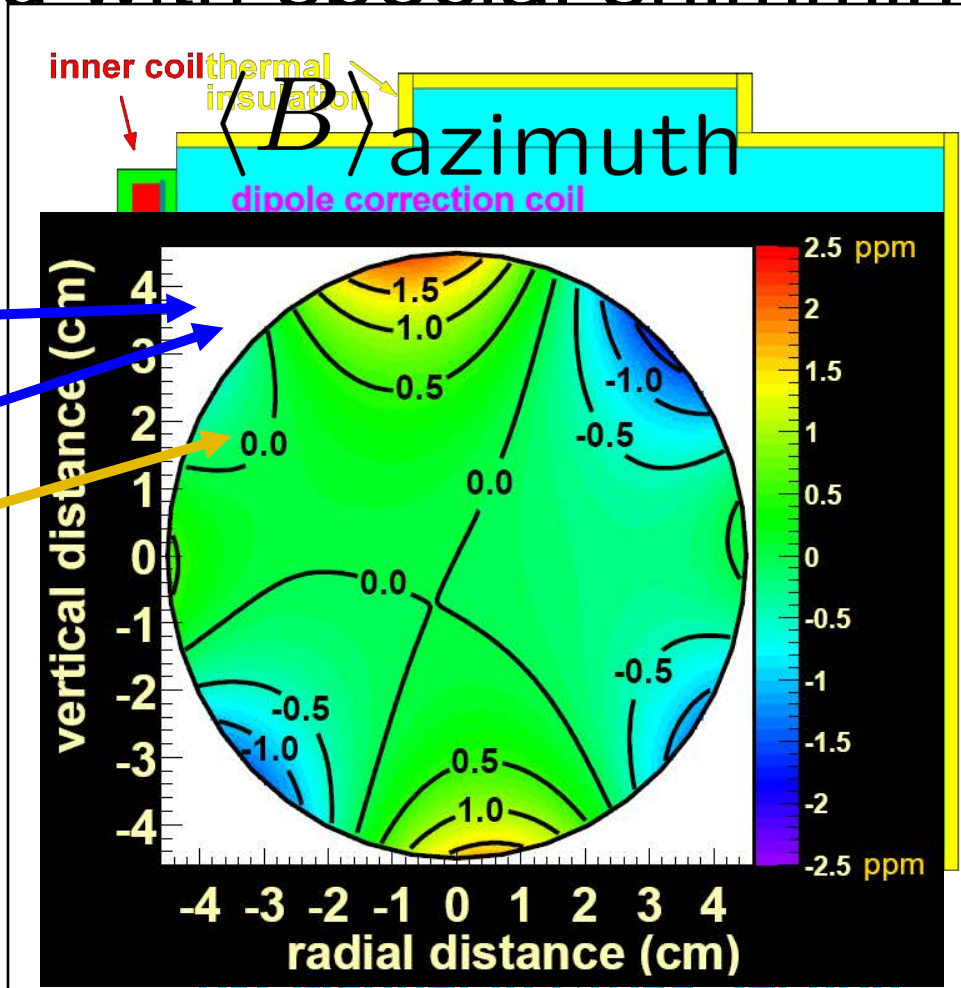
(b) Distribution of NMR probes over a cross section of the trolley

Magnetic field distribution along the muon beam orbit



The ± 1 ppm uniformity in the average field is obtained with special shimming tools.

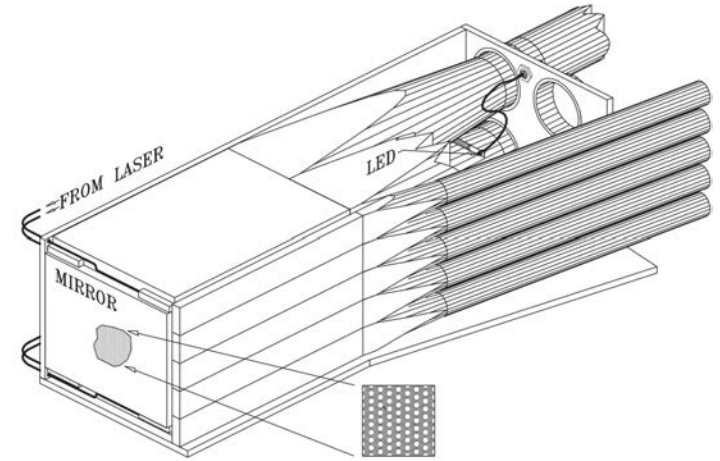
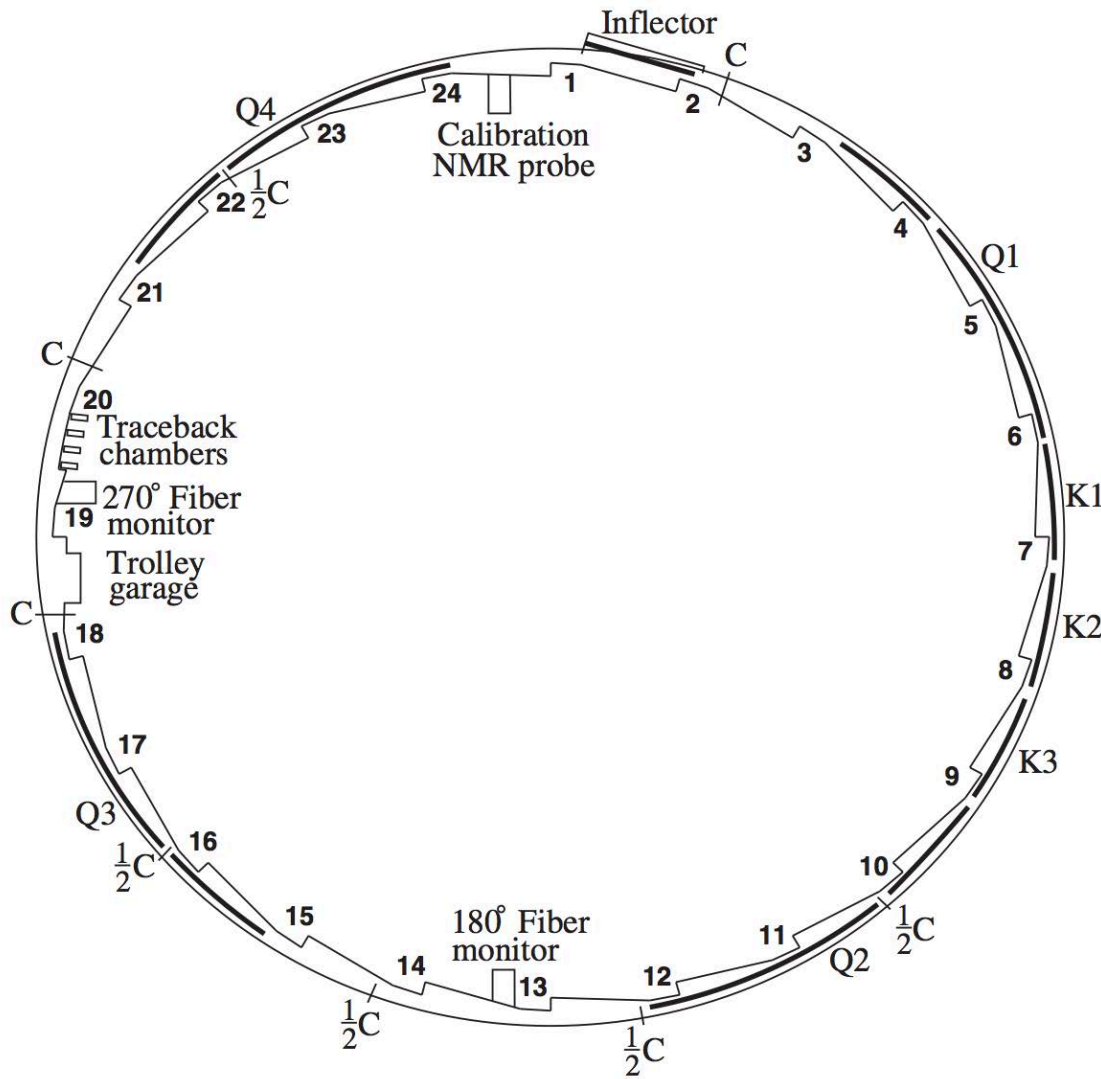
We can shim the
dipole,
quadrupole
sextupole
 independently



0.5 ppm contours

σ_{system} on $\langle B \rangle_{\mu}$ dist = ± 0.03 ppm

Positron detectors



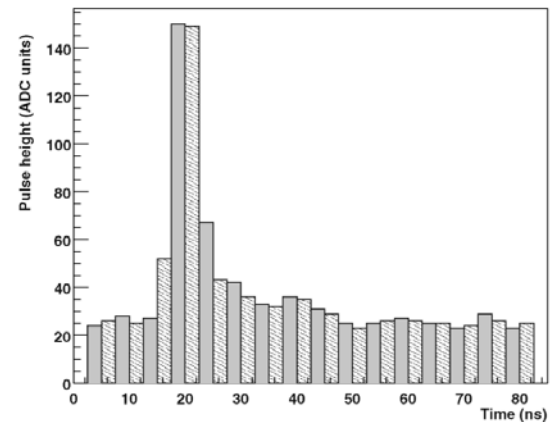
Pb/SciFi calorimeter

Lead alloy (52%)

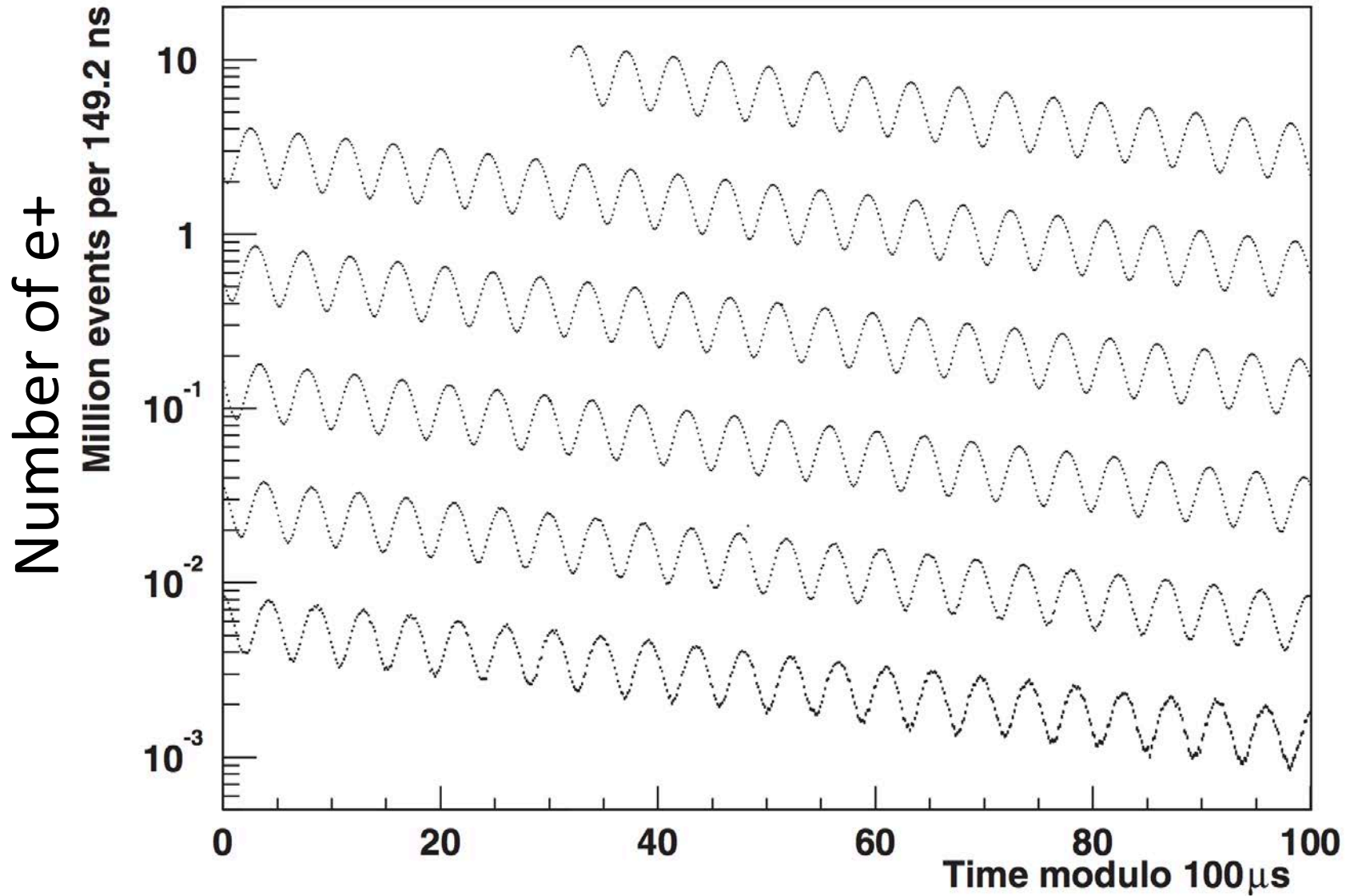
Scintillation fiber (38%)

Epoxy (10%)

Energy resolution 7% at 1.9 GeV



Time distribution of e^+ (BNL E821)



Pitch and E-field corrections

- Corrections to ω_a determined by calorimeter required because:

- (1) Not all muons at magic momentum \Rightarrow not on center orbit \Rightarrow see net electric field
- (2) Vertical betatron motion: muons pitching up/down out of horizontal plane

$$\vec{\omega}_a \approx \vec{\omega}_S - \vec{\omega}_C = \underbrace{-\frac{e}{m} [a_\mu \vec{B}]}_{\text{What we want}} - \underbrace{a_\mu \left(\frac{\gamma}{\gamma + 1} \right) (\vec{\beta} \cdot \vec{B}) \vec{\beta}}_{\text{Pitch Correction}} - \underbrace{\left(a_\mu - \frac{1}{\gamma^2 - 1} \right) \frac{\vec{\beta} \times \vec{E}}{c}}_{\text{E-Field Correction}}$$

+0.27 \pm 0.04 ppm +0.47 \pm 0.05 ppm

Relating measurements to g-2

- muon spin precession

$$\omega_a = \frac{e}{m_\mu} a_\mu B$$

- proton spin precession

$$\omega_p = \mu_p B$$

- muon magnetic moment

$$\mu_\mu = g \frac{e}{2m_\mu} = (1 + a_\mu) \frac{e}{m_\mu}$$

$$a_\mu = \frac{\frac{\omega_a}{\omega_p}}{\frac{\mu_\mu}{\mu_p}}$$

540 ppb (BNL)
 140 ppb
 (Fermilab/J-PARC)

Magnetic moment ratio

LAMPF(1999)

$$\Delta \left(\frac{\mu_\mu}{\mu_p} \right) = 120 \text{ ppb (30 ppb)}$$

direct

using Δv

+ theory

Systematic uncertainties ω_a

TABLE XIV. Systematic errors for ω_a in the R99, R00 and R01 data periods.

| $\sigma_{\text{syst}} \omega_a$ | R99 (ppm) | R00 (ppm) | R01 (ppm) |
|---------------------------------|-----------|-----------|--------------|
| Pileup | 0.13 | 0.13 | 0.08 |
| AGS background | 0.10 | 0.01 | ^a |
| Lost muons | 0.10 | 0.10 | 0.09 |
| Timing shifts | 0.10 | 0.02 | ^a |
| E -field and pitch | 0.08 | 0.03 | ^a |
| Fitting/binning | 0.07 | 0.06 | ^a |
| CBO | 0.05 | 0.21 | 0.07 |
| Gain changes | 0.02 | 0.13 | 0.12 |
| Total for ω_a | 0.3 | 0.31 | 0.21 |

^aIn R01, the AGS background, timing shifts, E field and vertical oscillations, beam debunching/randomization, binning and fitting procedure together equaled 0.11 ppm.

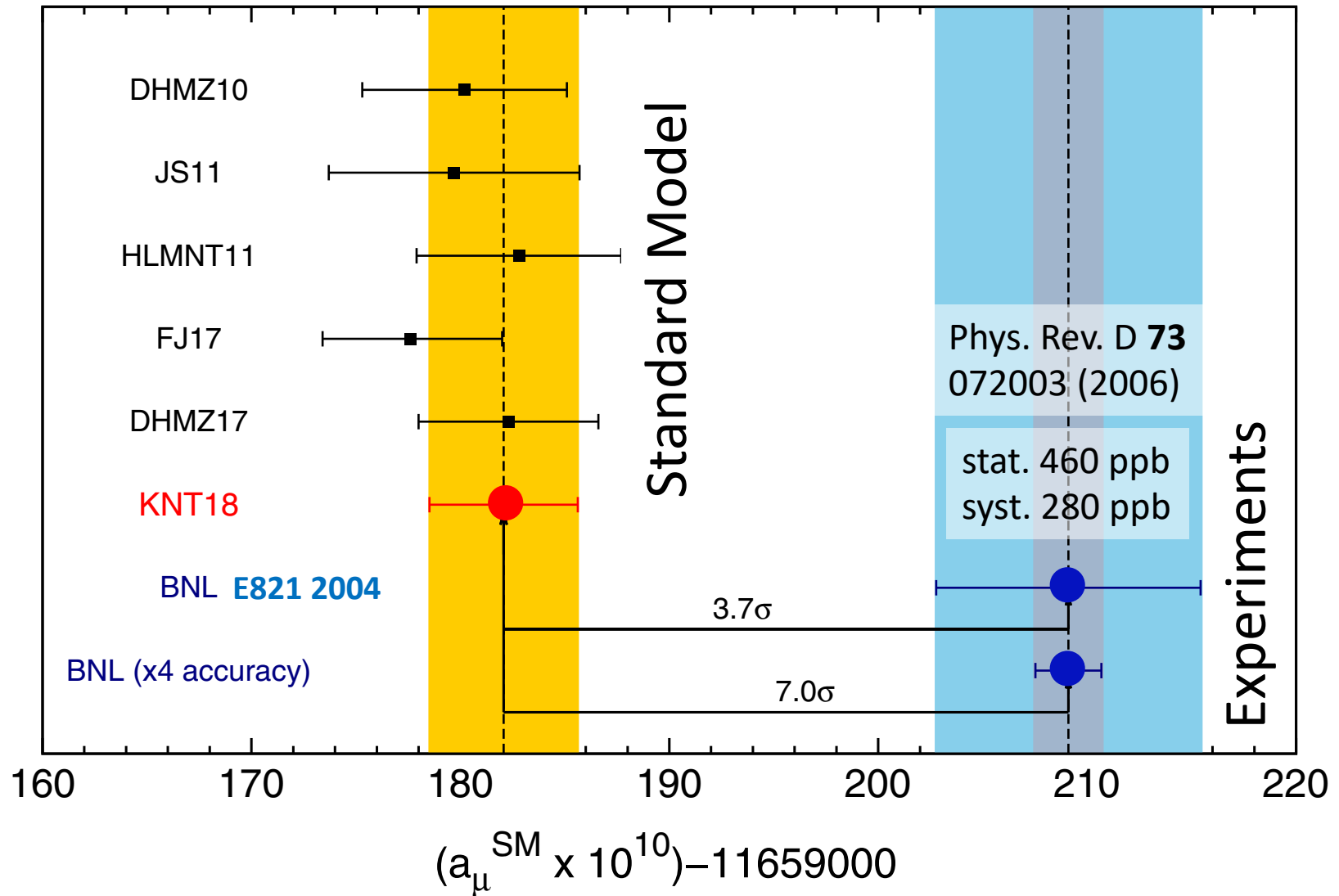
Systematic uncertainties ω_p

TABLE XI. Systematic errors for the magnetic field for the different run periods.

| Source of errors | R99 [ppm] | R00 [ppm] | R01 [ppm] |
|---------------------------------------------------|-----------|-----------|-----------|
| Absolute calibration of standard probe | 0.05 | 0.05 | 0.05 |
| Calibration of trolley probes | 0.20 | 0.15 | 0.09 |
| Trolley measurements of B_0 | 0.10 | 0.10 | 0.05 |
| Interpolation with fixed probes | 0.15 | 0.10 | 0.07 |
| Uncertainty from muon distribution | 0.12 | 0.03 | 0.03 |
| Inflector fringe field uncertainty | 0.20 | — | — |
| Others ^a | 0.15 | 0.10 | 0.10 |
| Total systematic error on ω_p | 0.4 | 0.24 | 0.17 |
| Muon-averaged field [Hz]: $\tilde{\omega}_p/2\pi$ | 61791256 | 61791595 | 61791400 |

^aHigher multipoles, trolley temperature and its power supply voltage response, and eddy currents from the kicker.

Result of BNL E821 experiment



Why Fermilab? Statistics!

⇒ Brookhaven statistics limited:

$$a_{\mu}^{\text{BNL}} = 0.001\,165\,920\,89\,(54)_{\text{stat}}\,(33)_{\text{sys}}$$

- BNL ± 540 ppb uncertainty on a_{μ} , 9×10^9 events

⇒ Fermilab goal 2×10^{11} , factor 21

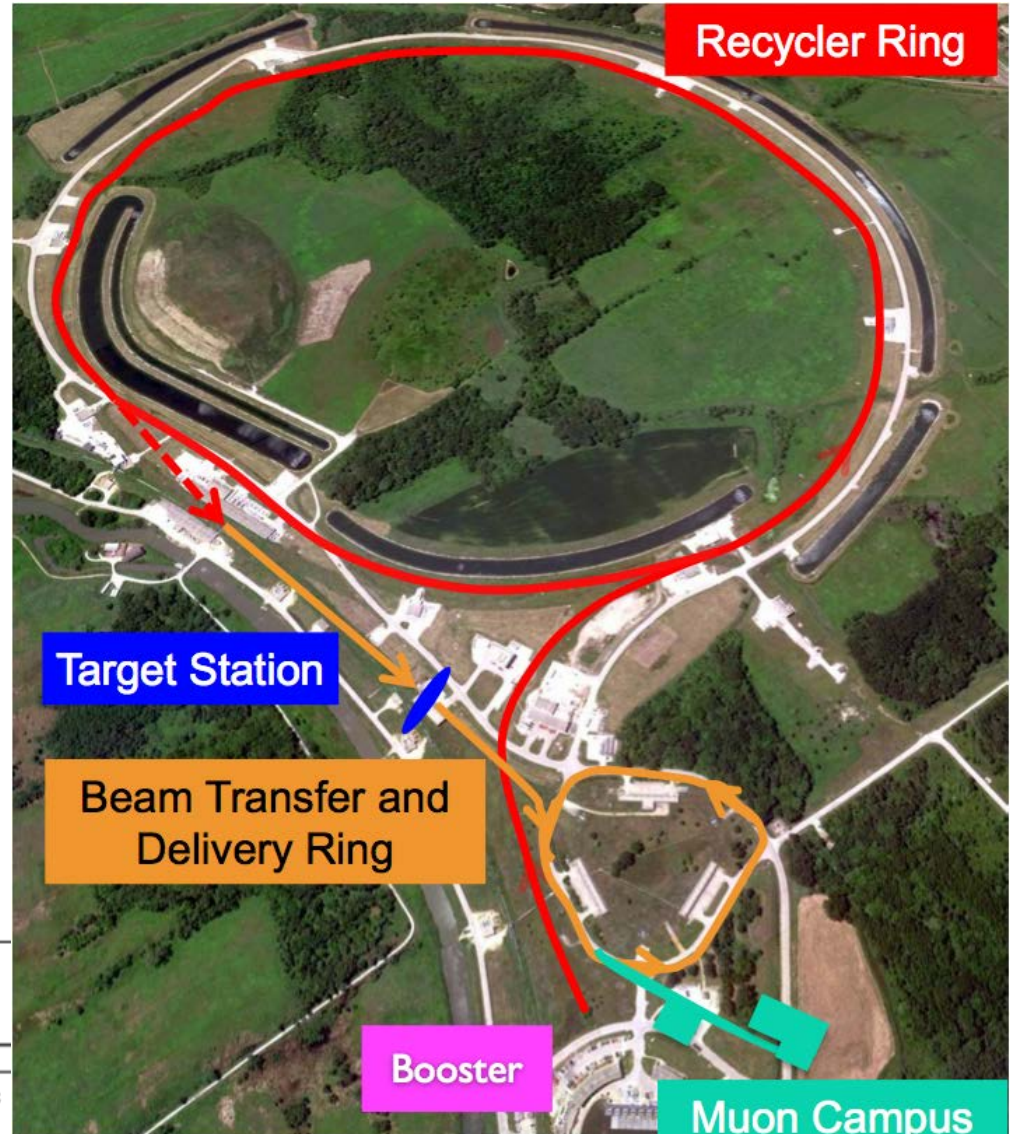
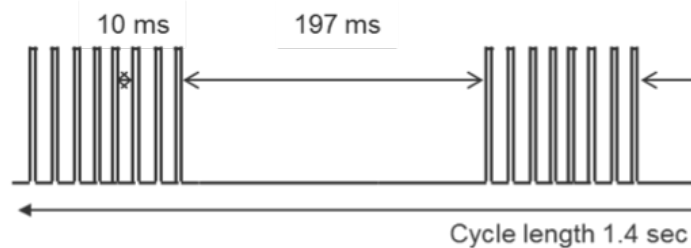
Fermilab Advantages:

- Long decay channel for $\pi \Rightarrow \mu$
- Reduced π and p in ring
- Factor 20 reduction in hadronic flash

⇒ $4\times$ higher fill frequency than BNL

- Muons per fill about the same

⇒ 21 times more detected e^+ , 2×10^{11}











21 times more detected e^+

Estimated systematic uncertainties ω_a

| Category | E821 [ppb] | E989 Improvement Plans | Goal [ppb] |
|---------------|---------------|------------------------------------------------------------------|---------------|
| Gain changes | 120 | Better laser calibration low-energy threshold | 20 |
| Pileup | 80 | Low-energy samples recorded calorimeter segmentation | 40 |
| Lost muons | 90 | Better collimation in ring | 20 |
| CBO | 70 | Higher n value (frequency) Better match of beamline to ring | < 30 |
| E and pitch | 50 | Improved tracker Precise storage ring simulations | 30 |
| Total | 180 | Quadrature sum | 70 |

Estimated systematic uncertainties ω_p

| Source of uncertainty | 1999 | 2000 | 2001 | | E989 |
|-------------------------------------------|------------|------------|------------|-------------------------------------------------------------------------------------|------|
| Systematics of calibration probes | 50 | 50 | 50 |  | 35 |
| Calibration of trolley probes | 200 | 150 | 90 |  | 30 |
| Trolley measurements of B_0 | 100 | 100 | 50 |  | 30 |
| Interpolation with fixed probes | 150 | 100 | 70 |  | 30 |
| Uncertainty from muon distribution | 120 | 30 | 30 |  | 10 |
| Inflector fringe field uncertainty | 200 | – | – | | – |
| Time dependent external B fields | – | – | – |  | 5 |
| Others † | 150 | 100 | 100 |  | 30 |
| Total systematic error on ω_p | 400 | 240 | 170 |  | 70 |
| Muon-averaged field [Hz]: $\omega_p/2\pi$ | 61 791 256 | 61 791 595 | 61 791 400 | | – |

CERN COURIER

VOLUME 54 NUMBER 9 NOVEMBER 2014



**Muon g-2 moves
on to a new life**



CERN60

Celebrations of 60 years of science for peace
p28

CP VIOLATION

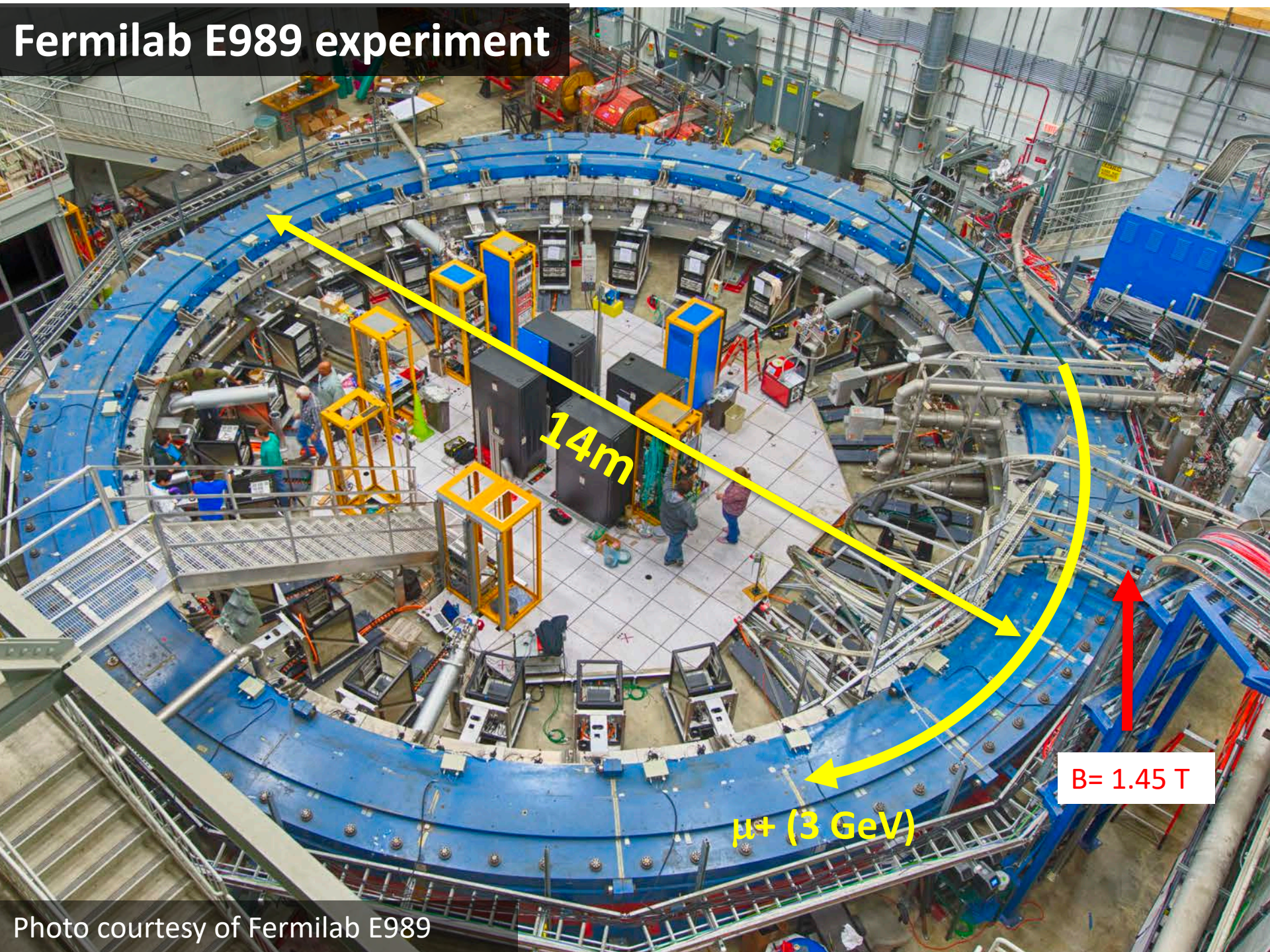
Meeting honours 50 years of a major discovery
p32



NEW RESULTS FROM AMS

Evidence for a new source of positrons
p6

Fermilab E989 experiment



14m

μ^+ (3 GeV)

B= 1.45 T

Muon beam line

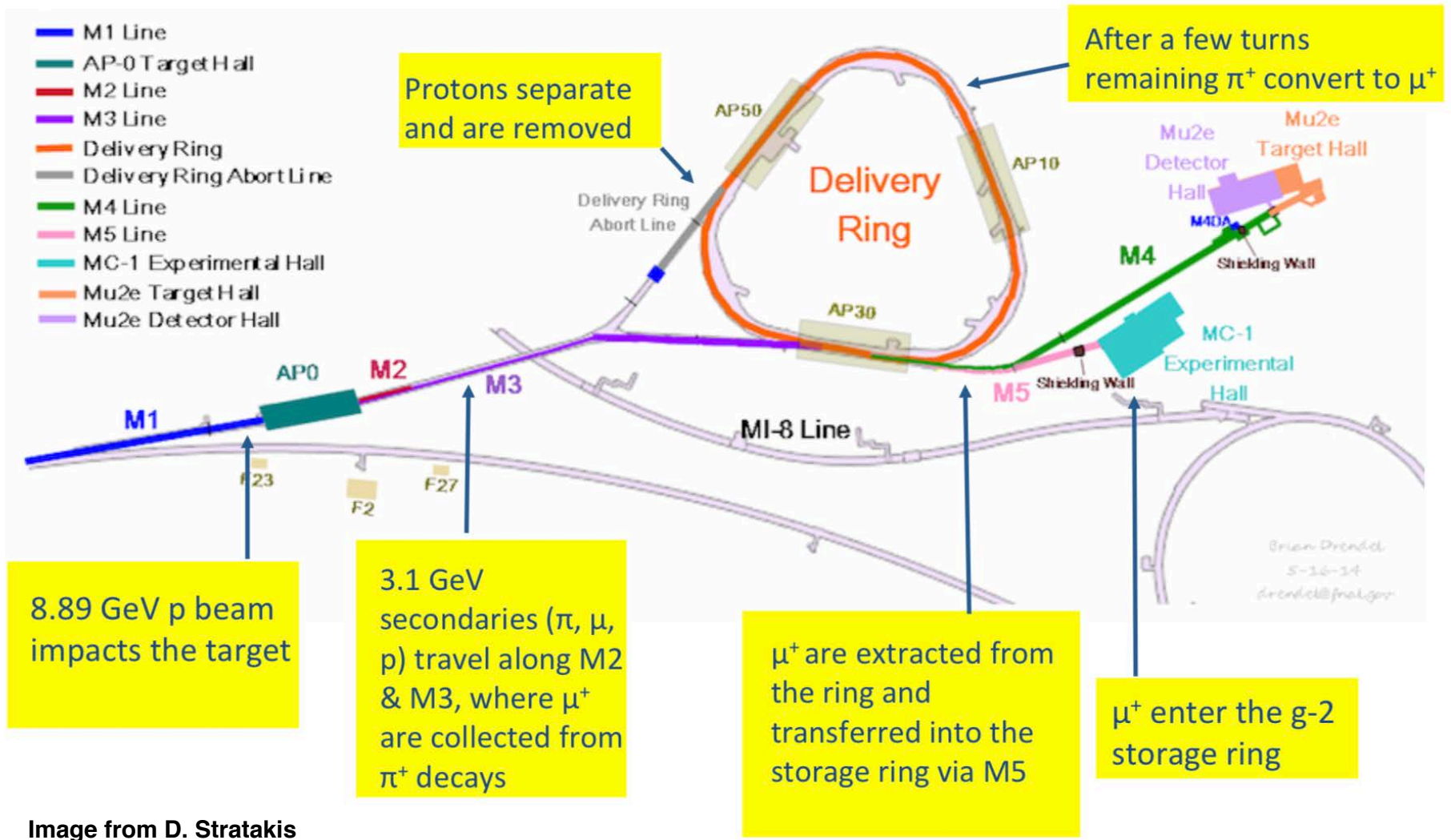
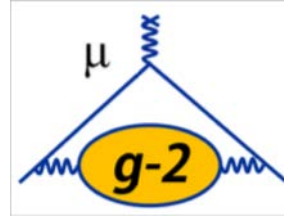


Image from D. Stratakis

History of Fermilab muon g-2 (2009-present)

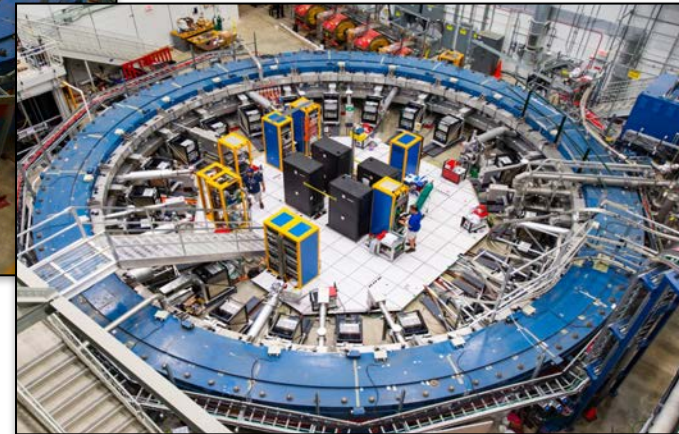
Courtesy of Kim Siang Khaw



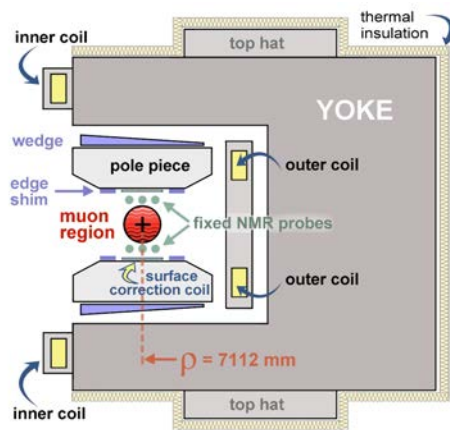
Transportation of magnet to FNAL (2013)



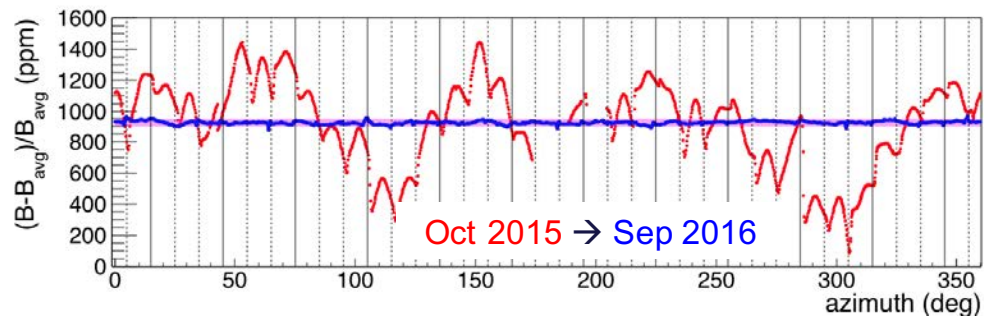
Assembly of the magnet (2014-2015)



Full installation (2017)



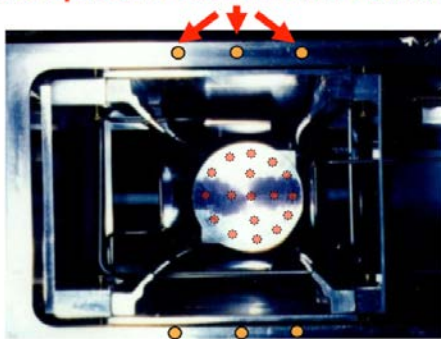
g-2 Magnet in Cross Section



Mapping the magnetic field

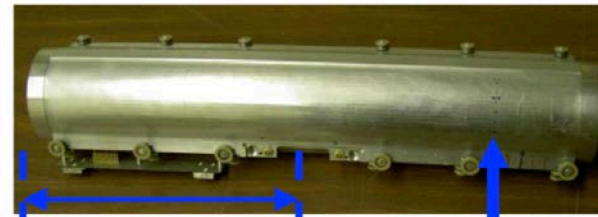
- Map the magnetic field inside the ring every 3 days
- Fixed probes for continuously monitoring

Fixed probes on vacuum chambers



- Measure field while muons are in ring
– 378 probes **outside** storage region

Trolley matrix of 17 NMR probes

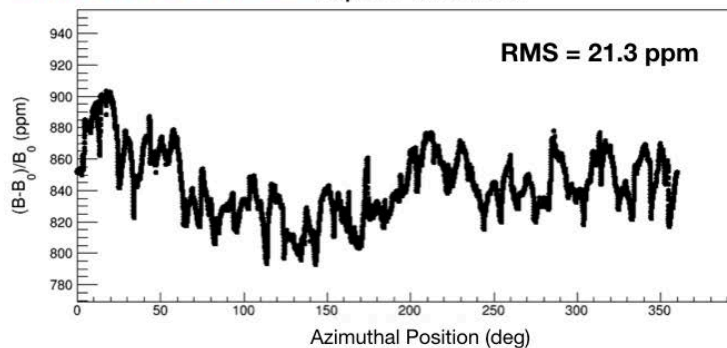


Electronics,
Microcontroller,
Communication

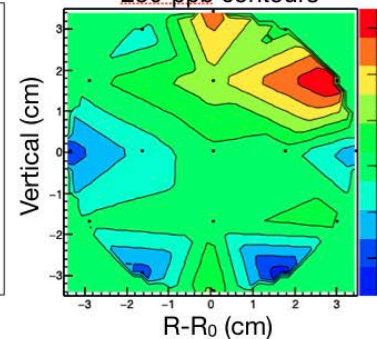
Position of NMR probes

- Measure field in storage region during **specialized runs** when **muons are not being stored**

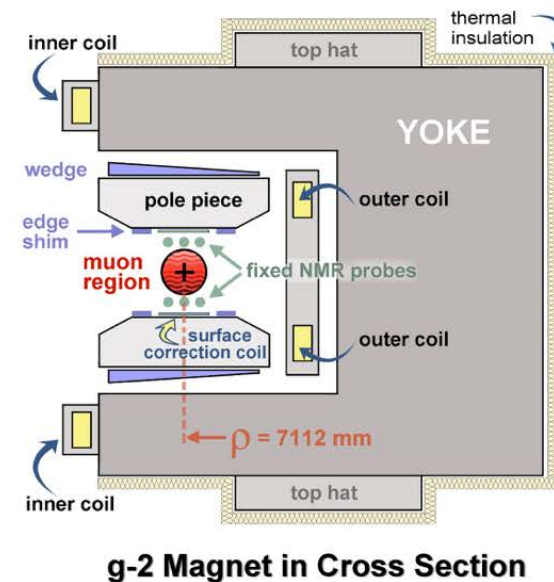
Typical trolley run Dipole Moment



Azimuthal average
250-ppb contours



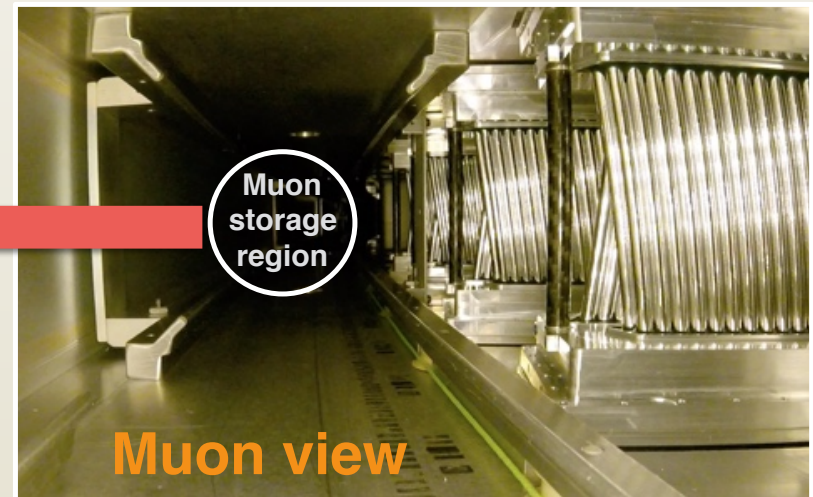
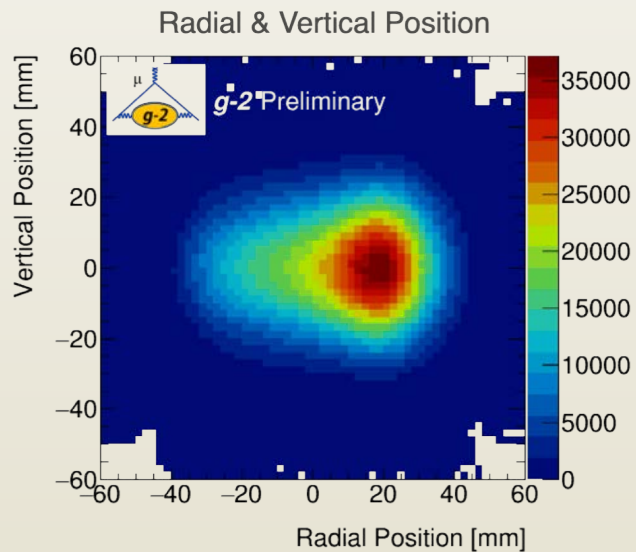
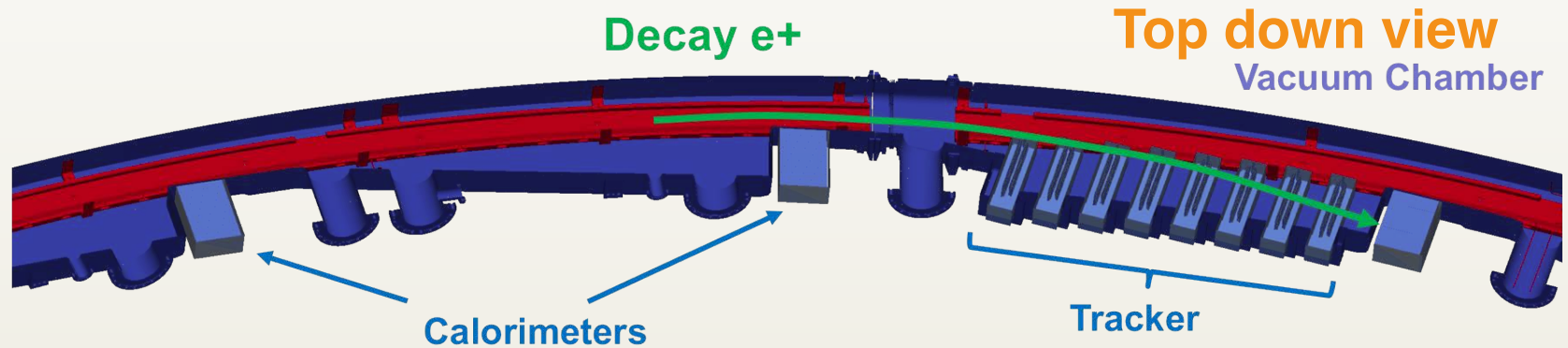
Storage Ring Magnet: Centerpiece of the Experiment



- 682 tons, 4 coils \times 24 windings \times 5200 Amps/winding, 72 poles, $B=1.4513$ T
- $B \times \text{gap} \approx \mu_0 I \Rightarrow 1.45 \text{ T} \times 0.2 \text{ m} \approx 4\pi \times 10^{-7} \times 48 \times 5200 \text{ Amps}$, $\frac{\Delta B}{B} \approx -\frac{\Delta \text{gap}}{\text{gap}}$
- Oct 2015-Aug 2016: adjustments of pole gaps, tilts, 8000+ fine iron laminations
- B uniformity at ± 20 ppm level (RMS) \Leftrightarrow gap uniform at 4 micron level over 45 m

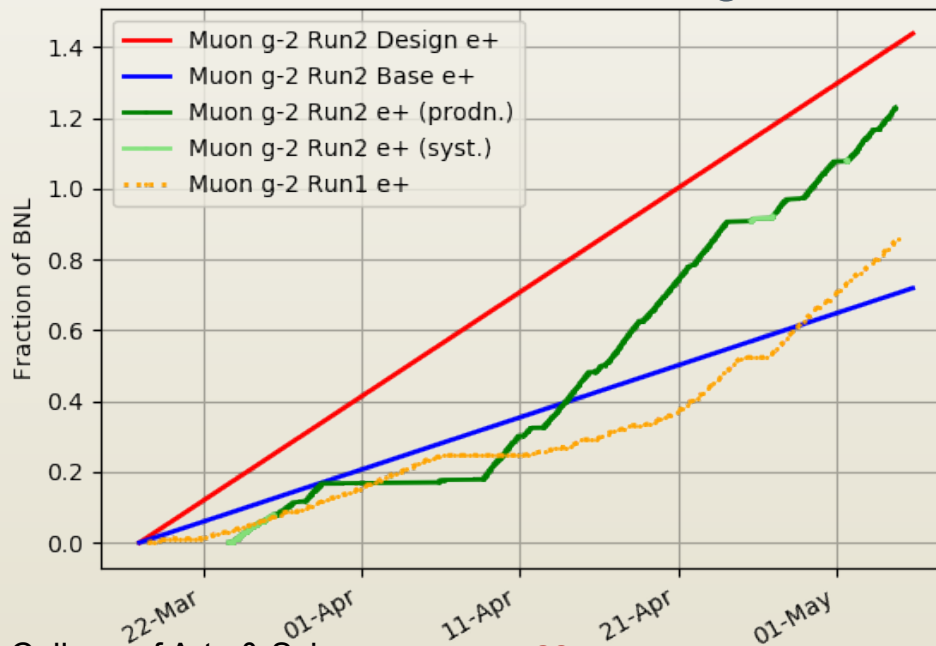
Beam profile measurement

- Two tracker stations for monitoring



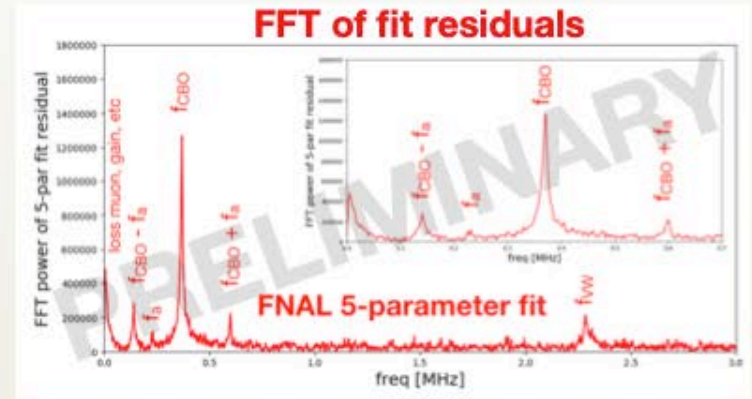
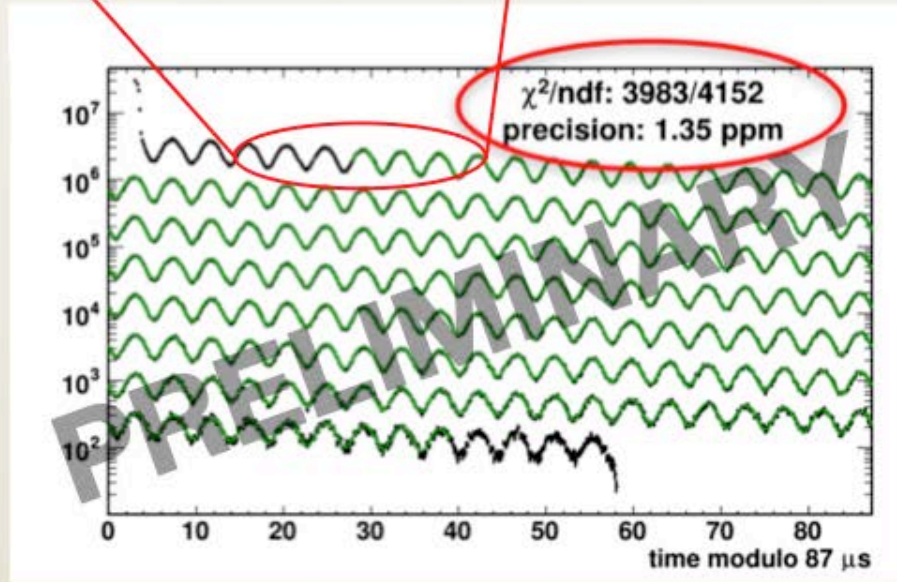
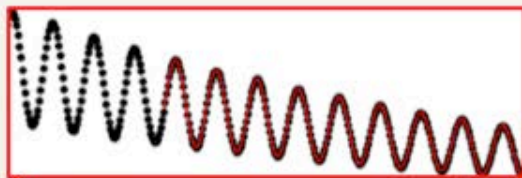
Data taking progress

- Finished first physics run, Run 1, in July 2018
 - Field uniformity 2x better than BNL
 - 1.75×10^{10} positrons collected, $\sim 2x$ BNL stats
 - 1.4x BNL after data quality cut, $\delta\omega_a(\text{stat}) \sim 350$ ppb
 - analysis in progress
- Half way through the Run 2
 - Improvements: muon flux, kicker strength, overall stability, ...

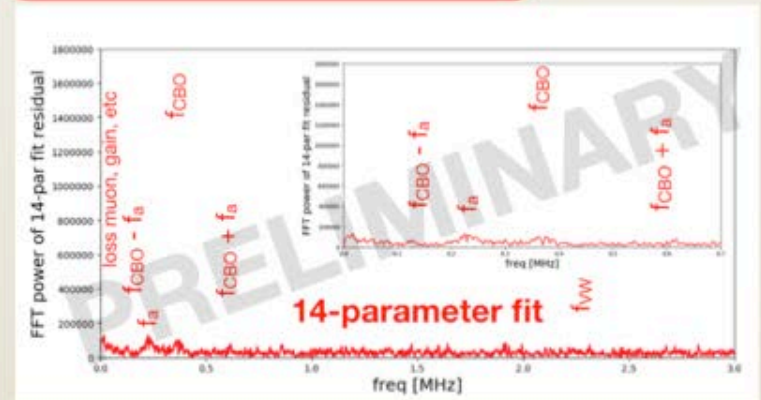


ω_a in Run 1

$$N(t) = N_0 e^{-t/\tau} [1 - A \cos(\omega_a t + \phi)]$$



Big improvements when accounting for CBO, lost muons,...



Systematic uncertainties

- BNL/FNAL major systematics (on ω_a)

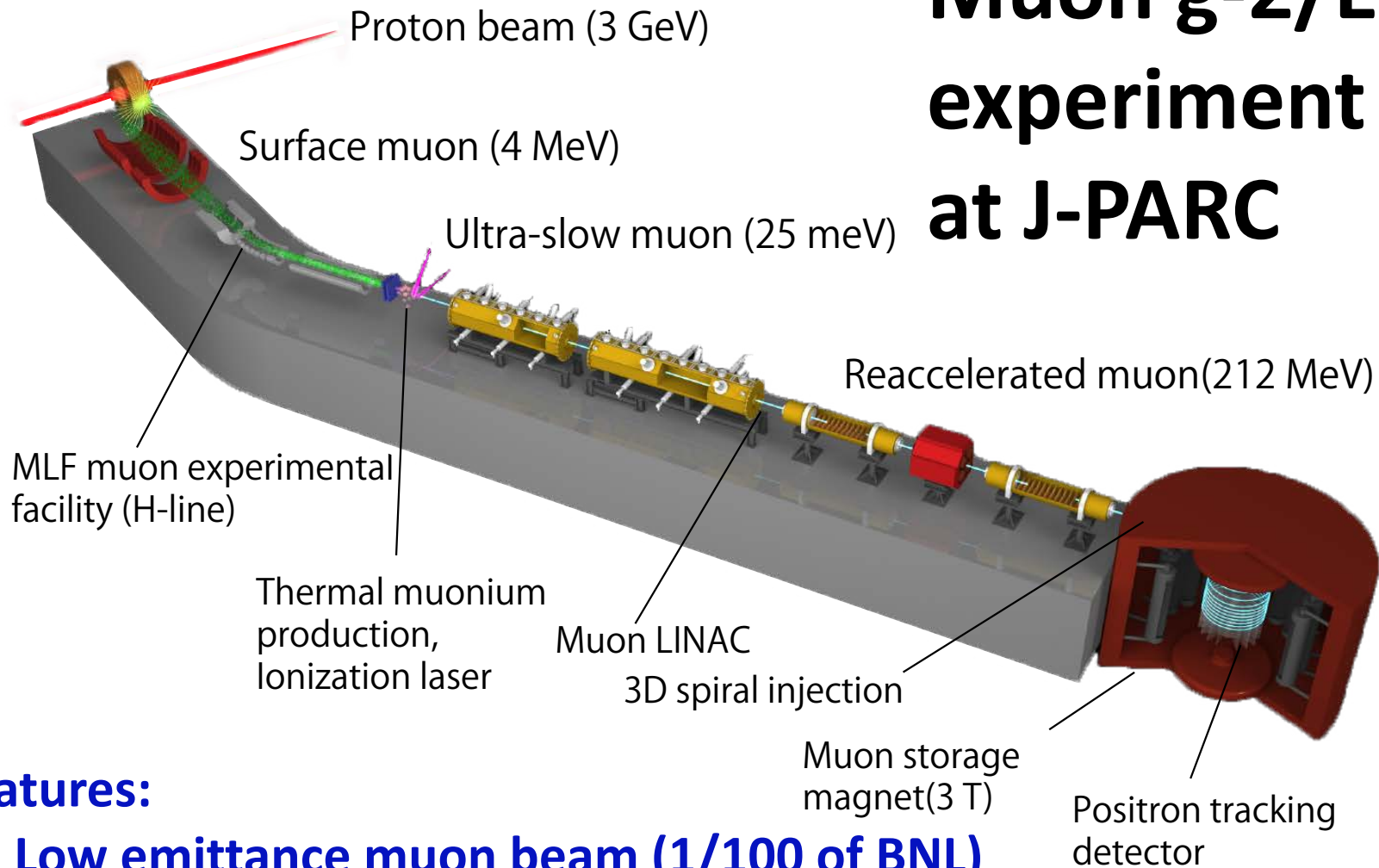
| Source | BNL (ppm) | FNAL goal (ppm) |
|--------------|-------------|-----------------|
| Gain changes | 0.12 | 0.02 |
| Lost muons | 0.09 | 0.02 |
| Pile up | 0.08 | 0.04 |
| CBO | 0.07 | 0.04 |
| E and pitch | 0.05 | 0.03 |
| Total | 0.18 | 0.07 |

All related with **beam quality and characteristics.**



Largely suppressed if **emittance of muon beam is small.**

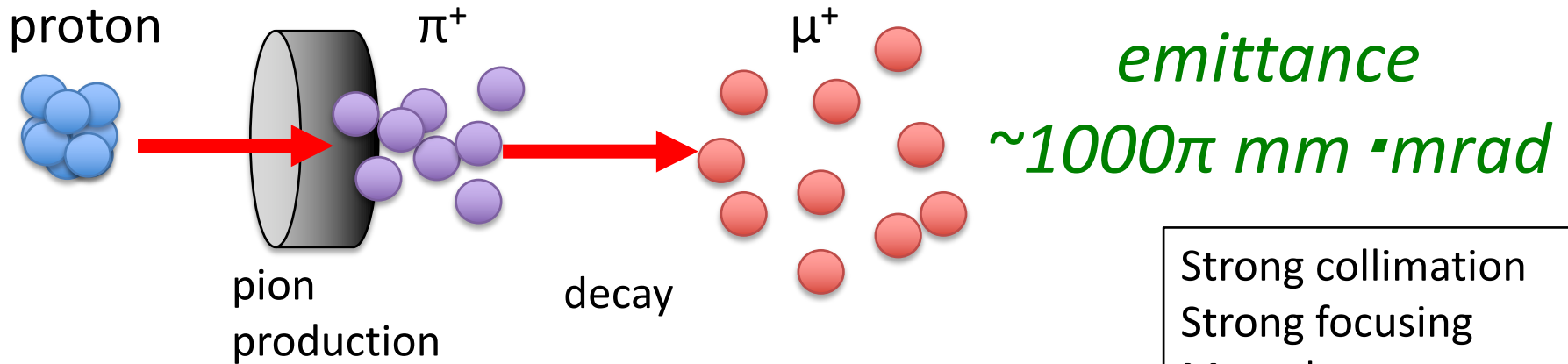
Muon g-2/EDM experiment at J-PARC



Features:

- **Low emittance muon beam (1/100 of BNL)**
- **No strong focusing (1/1000) & good injection eff. (x10)**
- **Compact storage ring (1/20)**
- **Tracking detector with large acceptance**
- **Completely different from BNL/FNAL method**

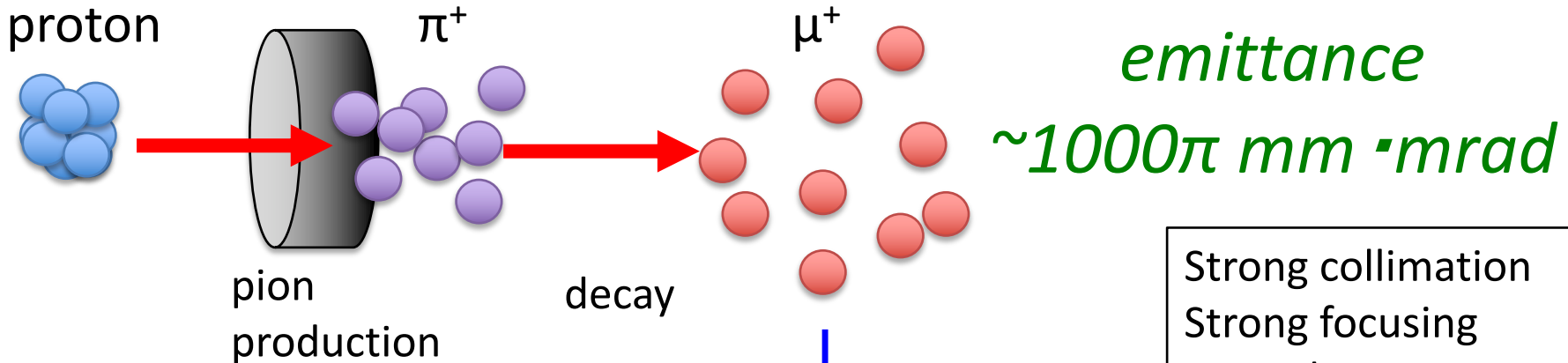
Conventional muon beam



Strong collimation
Strong focusing
Muon loss
BG π contamination

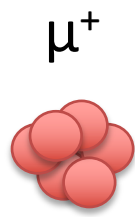


Muon beam at J-PARC



- Strong collimation
- Strong focusing
- Muon loss
- BG π contamination

cooling



Reaccelerated thermal muon

Free from any of these



Re-accelerated thermal muon

surface muon

3.4 MeV

27 MeV/c

0.05

thermal muon

30 meV

2.3 keV/c

0.4

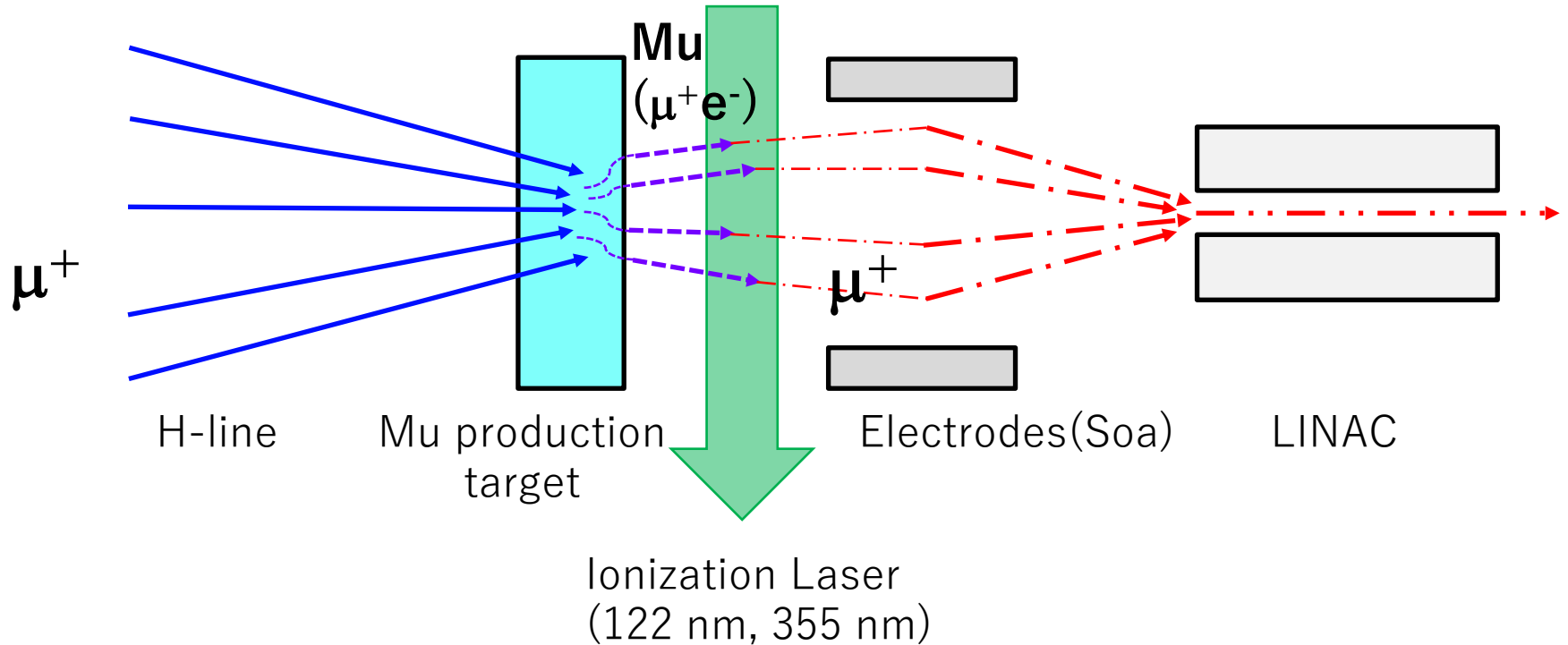
accelerated muon

212 MeV

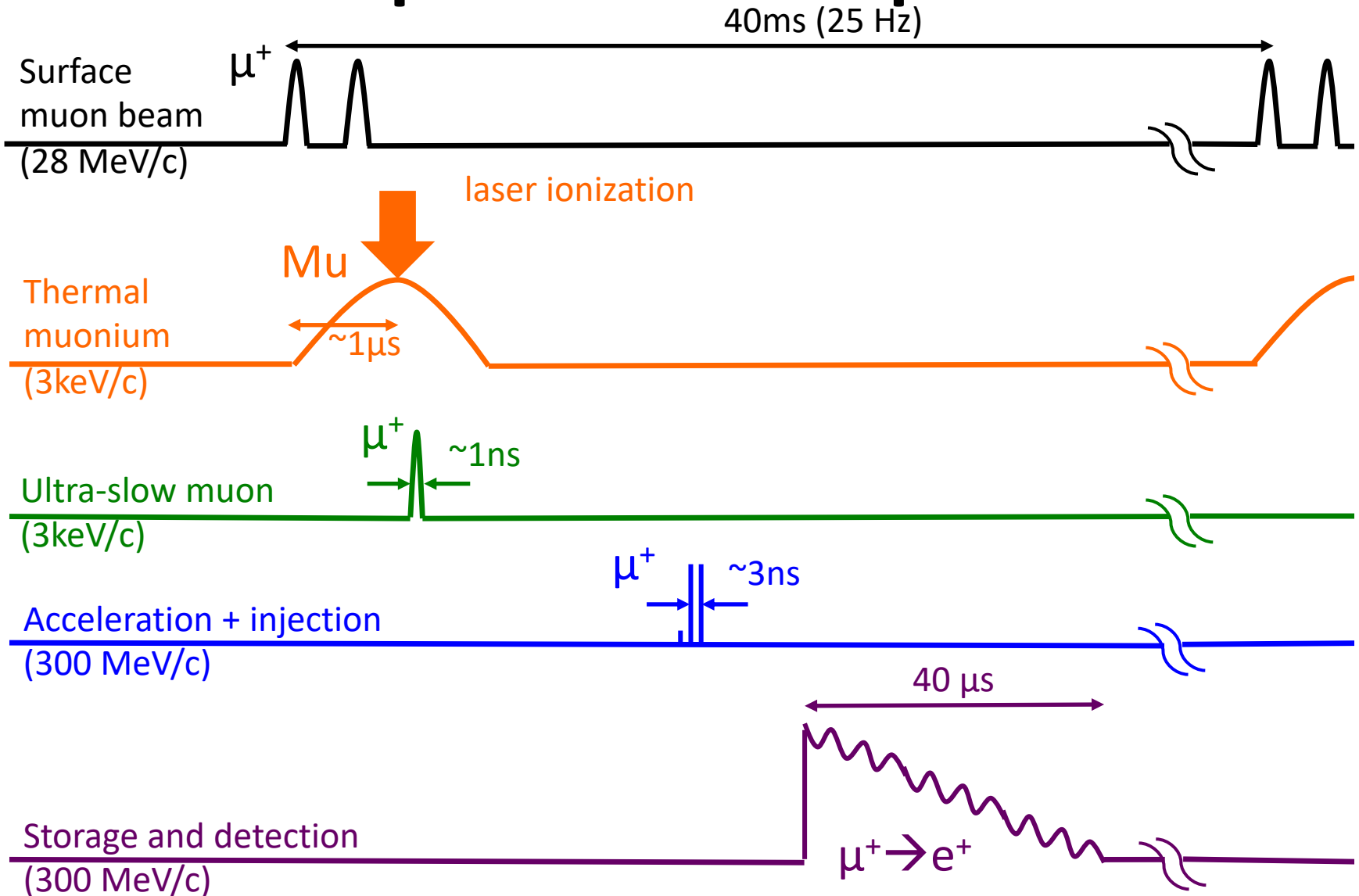
300 MeV/c

4×10^{-4}

E
p
 $\Delta p/p$

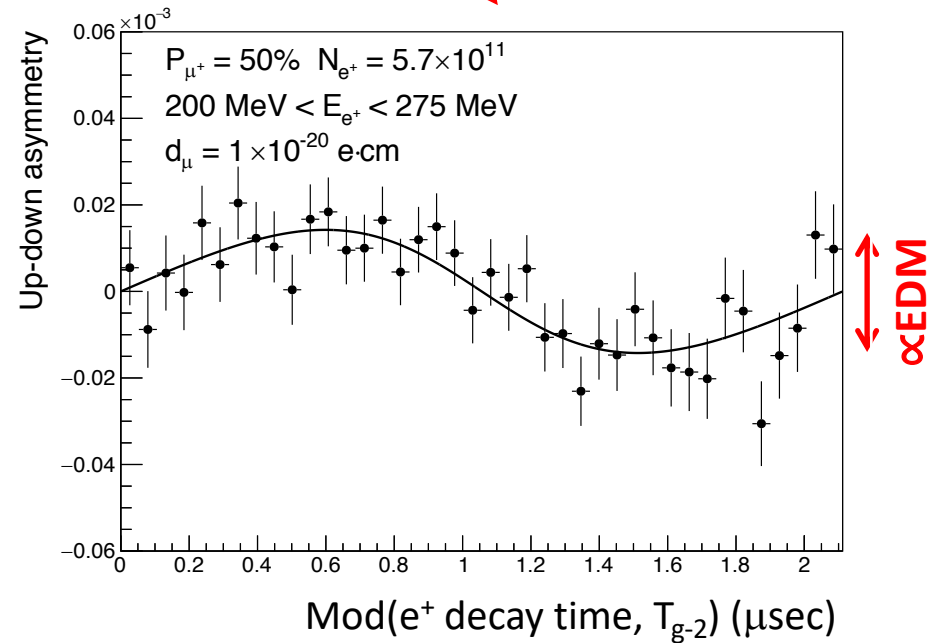
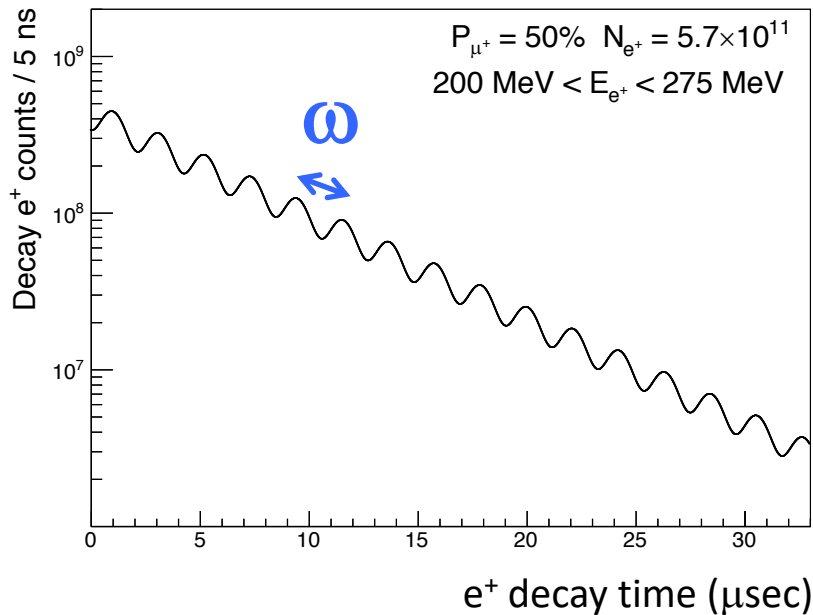


Experimental sequence



Expected time spectrum of e^+ in $\mu \rightarrow e^+ \nu \nu$ decay

$$\vec{\omega} = -\frac{e}{m} \left[a_\mu \vec{B} + \frac{\eta}{2} (\vec{\beta} \times \vec{B}) \right]$$



Comparison of experiments

| | BNL-E821 | Fermilab-E989 | Our experiment |
|---------------------------|-------------------------------------------|----------------------|--------------------------------------------|
| Muon momentum | | 3.09 GeV/ c | 300 MeV/ c |
| Lorentz γ | | 29.3 | 3 |
| Polarization | | 100% | 50% |
| Storage field | | $B = 1.45$ T | $B = 3.0$ T |
| Focusing field | | Electric quadrupole | Very weak magnetic |
| Cyclotron period | | 149 ns | 7.4 ns |
| Spin precession period | | 4.37 μ s | 2.11 μ s |
| Number of detected e^+ | 5.0×10^9 | 1.6×10^{11} | 5.7×10^{11} |
| Number of detected e^- | 3.6×10^9 | – | – |
| a_μ precision (stat.) | 460 ppb | 100 ppb | 450 ppb |
| (syst.) | 280 ppb | 100 ppb | <70 ppb |
| EDM precision (stat.) | 0.2×10^{-19} $e \cdot \text{cm}$ | – | 1.5×10^{-21} $e \cdot \text{cm}$ |
| (syst.) | 0.9×10^{-19} $e \cdot \text{cm}$ | – | 0.36×10^{-21} $e \cdot \text{cm}$ |

Expected uncertainties

Table 5. Summary of statistics and uncertainties.

| | Estimation |
|-------------------------------------------------------------------------|----------------------|
| Total number of muons in the storage magnet | 5.2×10^{12} |
| Total number of reconstructed e^+ in the energy window [200, 275 MeV] | 5.7×10^{11} |
| Effective analyzing power | 0.42 |
| Statistical uncertainty on ω_a [ppb] | 450 |
| Uncertainties on a_μ [ppb] | 450 (stat.) |
| | < 70 (syst.) |
| Uncertainties on EDM [10^{-21} e·cm] | 1.5 (stat.) |
| | 0.36 (syst.) |

Table 6. Estimated systmatic uncertainties on a_μ .

| Anomalous spin precession (ω_a) | | Magnetic field (ω_p) | |
|------------------------------------------|------------------|-------------------------------|------------------|
| Source | Estimation (ppb) | Source | Estimation (ppb) |
| Timing shift | < 36 | Absolute calibration | 25 |
| Pitch effect | 13 | Calibration of mapping probe | 20 |
| Electric field | 10 | Position of mapping probe | 45 |
| Delayed positrons | 0.8 | Field decay | < 10 |
| Differential decay | 1.5 | Eddy current from kicker | 0.1 |
| Quadratic sum | < 40 | Quadratic sum | 56 |

J-PARC Facility
(KEK/JAEA)

LINAC

3 GeV
Synchrotron

Neutrino Beam
To Kamioka

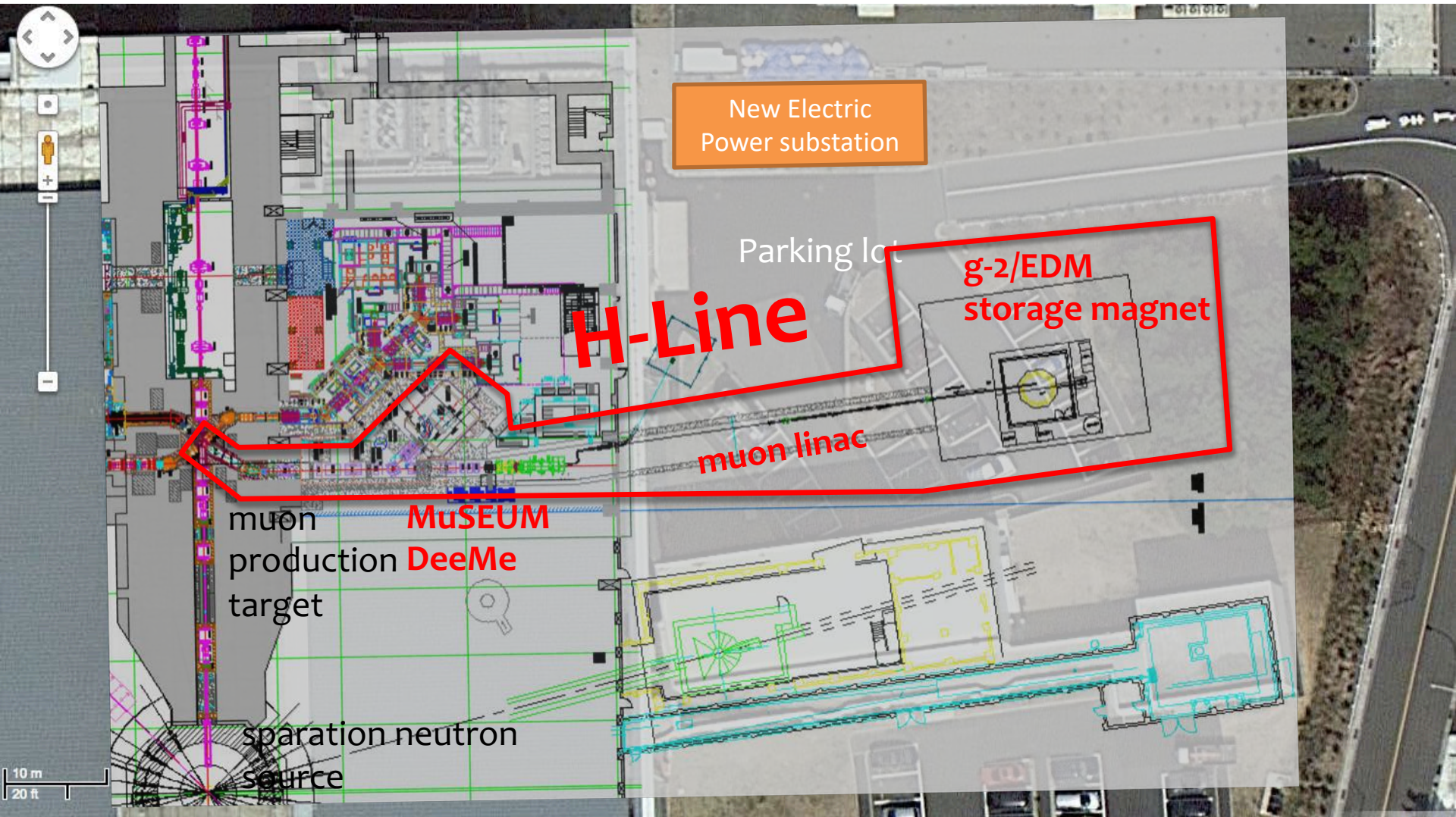
Material and Life Science
Facility

Main Ring
(30 GeV)

Hadron Hall

Proposed experimental site

Material and Life science Facility in J-PARC



H-line being constructed!

Photo by T. Yamazaki

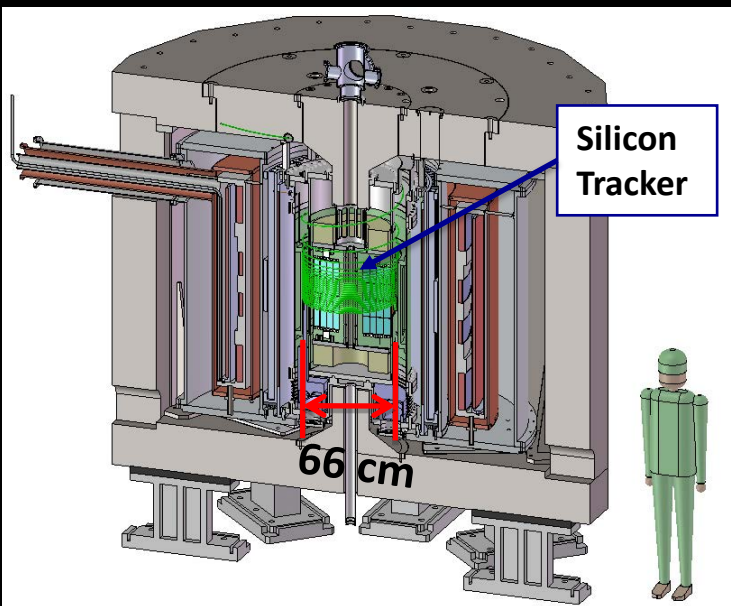
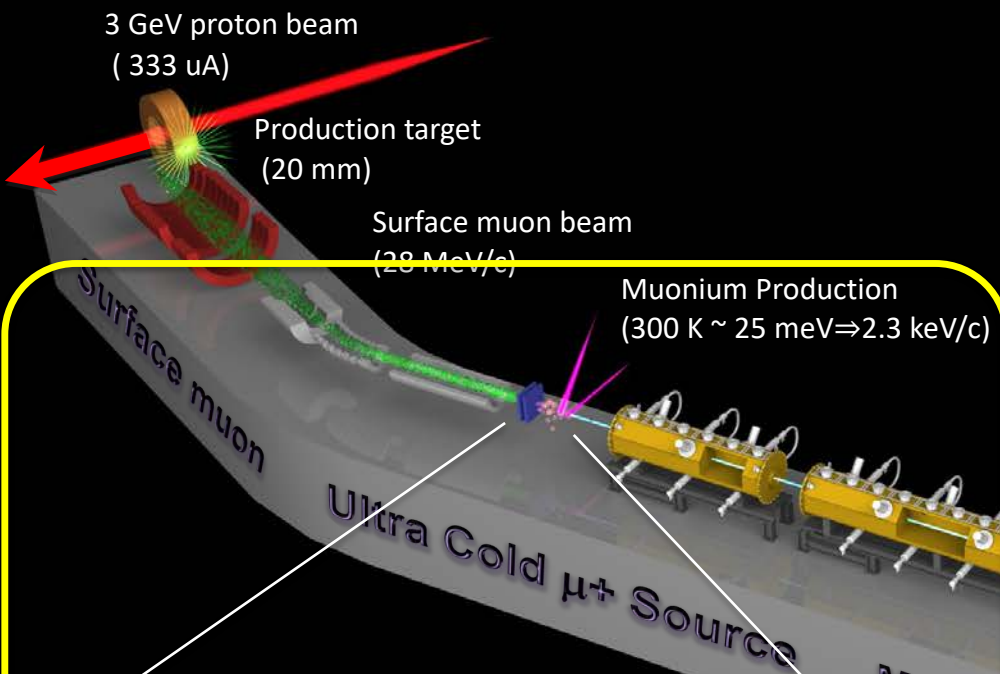
DeeMe
MuSEUM (Mu-HFS)
Mu 1S-2S

To g-2/EDM

Photo by T. Yamazaki

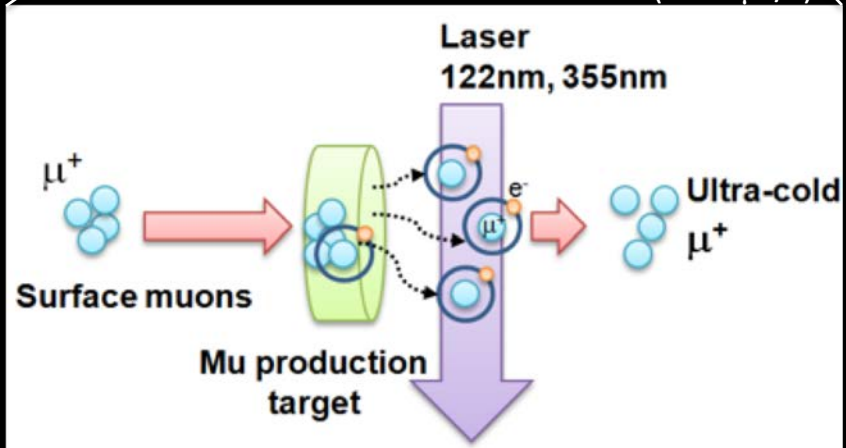
H-line being constructed!





Super Precision Storage Magnet
(3T, ~1ppm local precision)

Resonant Laser Ionization of Muonium ($\sim 10^6 \mu^+/s$)



$$\Delta(g-2) = 0.1 \text{ ppm}$$

$$\Delta EDM = 10^{-21} \text{ e} \cdot \text{cm}$$

Production of thermal energy muonium

Silica aerogel
(SiO₂, 30 mg/cc)

Laser-ablated holes

Muonium
(μ^+e^-)

Efficiency (measured)

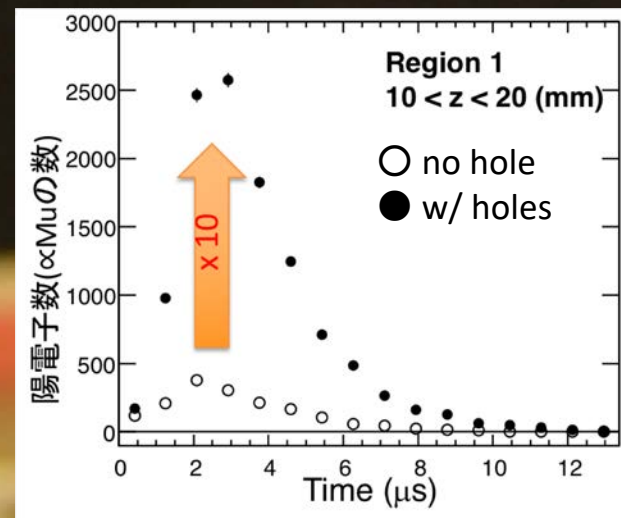
$$3 \times 10^{-3} / \mu$$

(laser region 5mm x 50mm)

surface
muon beam

8 mm

Data taken at TRIUMF

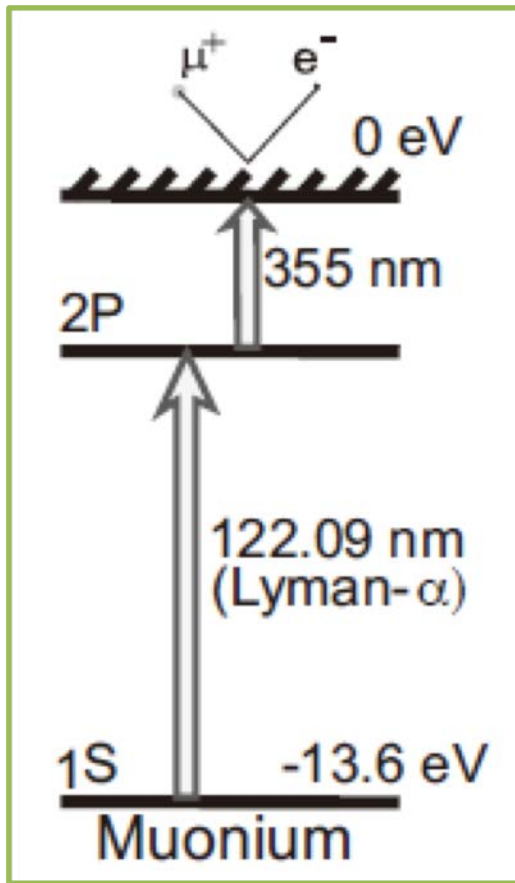


P. Bakule et al., PTEP 103C0 (2013)

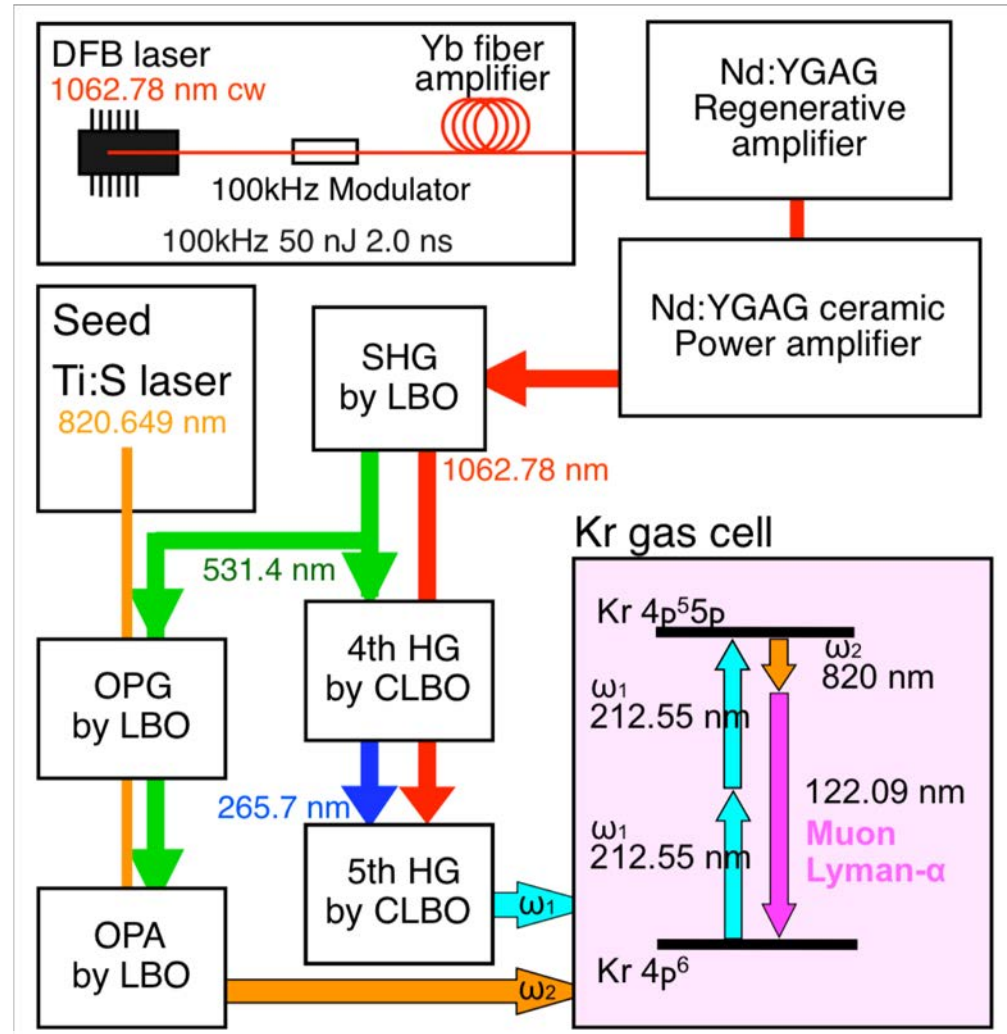
G. Beer et al., PTEP 091C01 (2014)

Laser ionization of muonium

1S → 2P → unbound



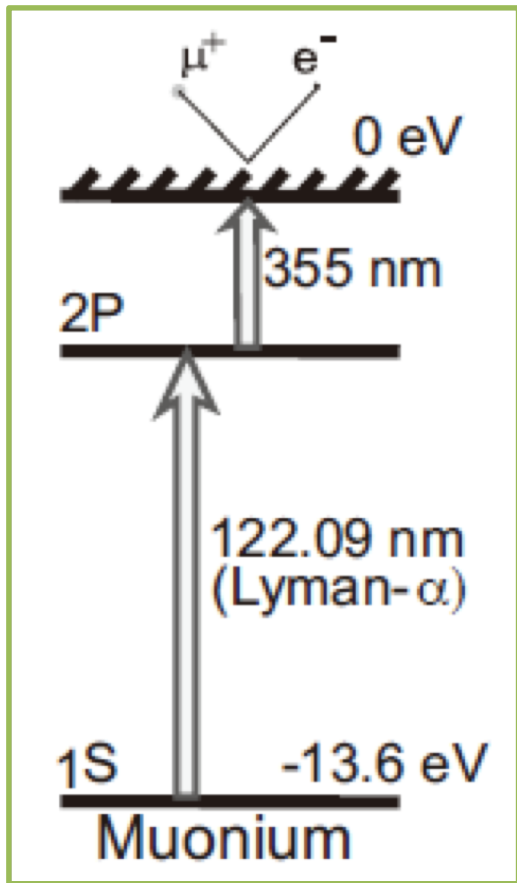
J-PARC MLF U-line laser system (RIKEN+KEK)



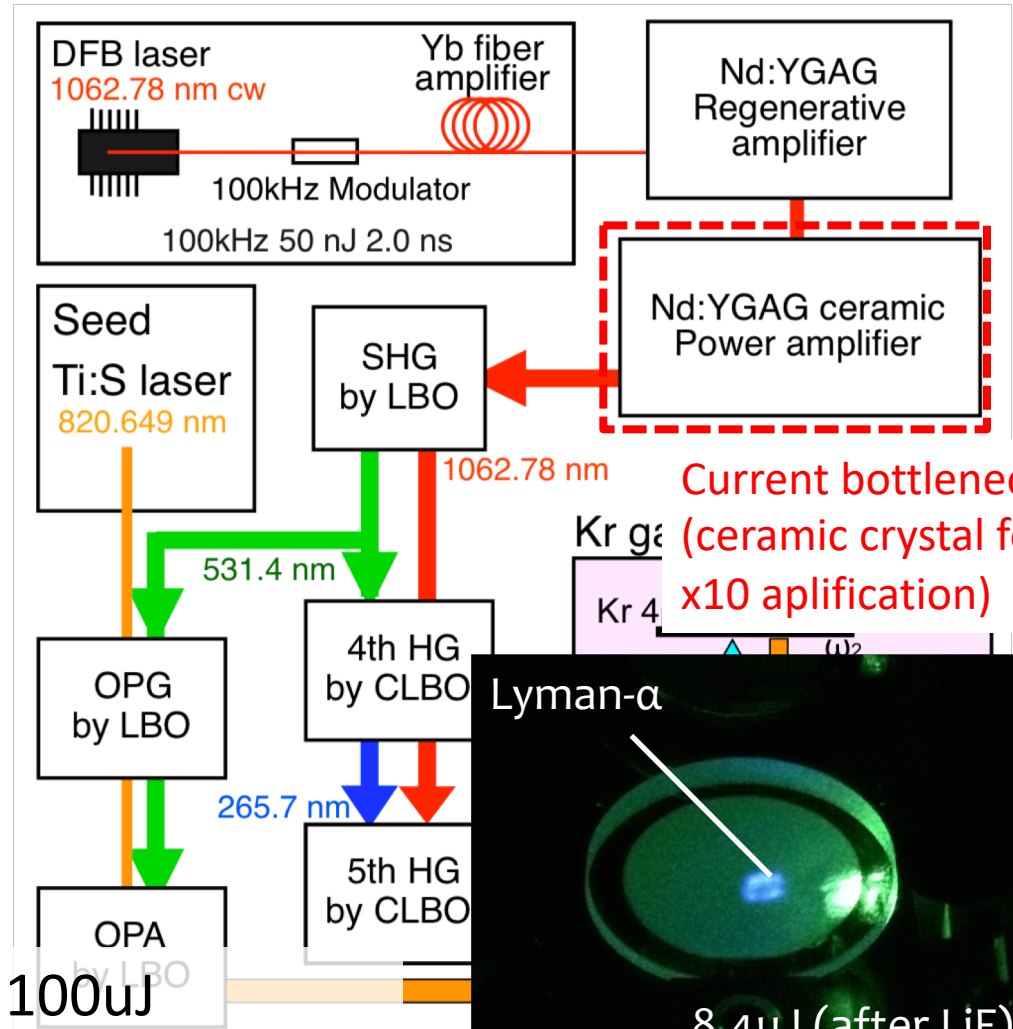
efficiency (calculated) 73% @100uJ

Laser ionization of muonium

1S → 2P → unbound



J-PARC MLF U-line laser system (RIKEN+KEK)

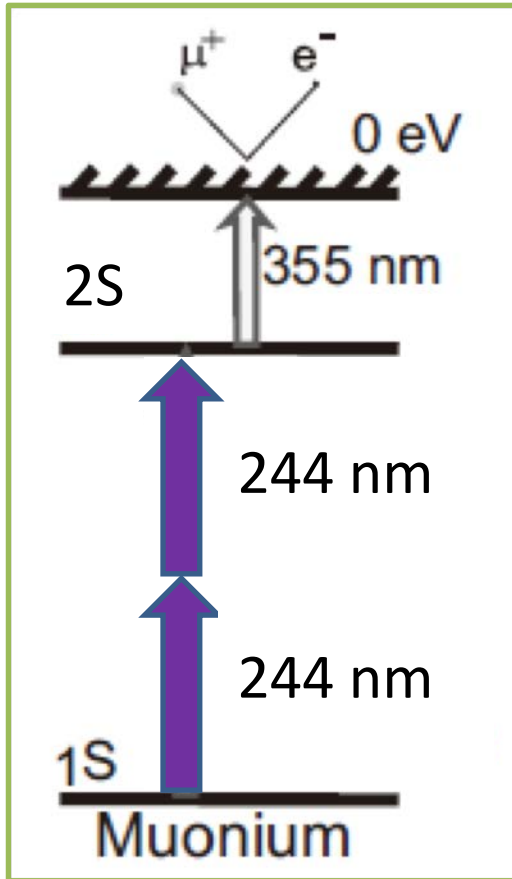


efficiency (calculated) 73% @100 μ J

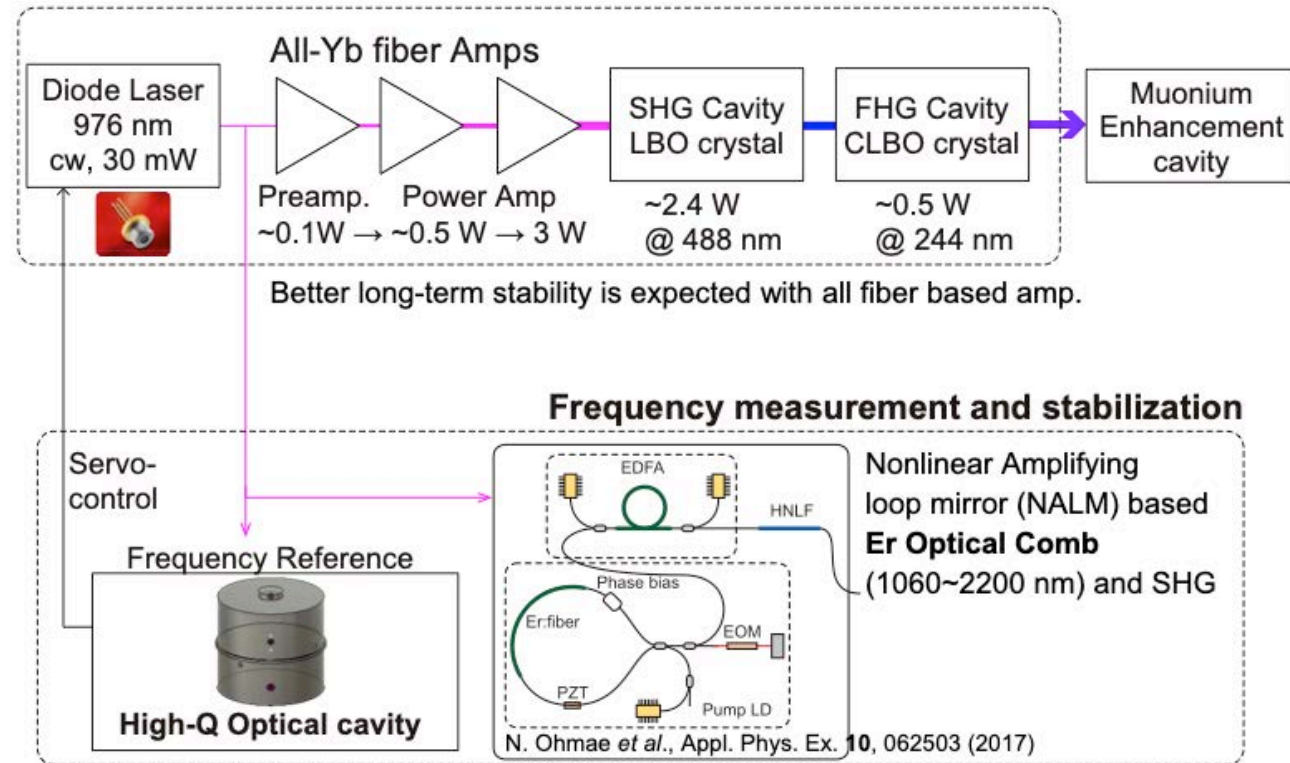
~20% @10 μ J (Current)

Laser ionization of muonium (Plan B)

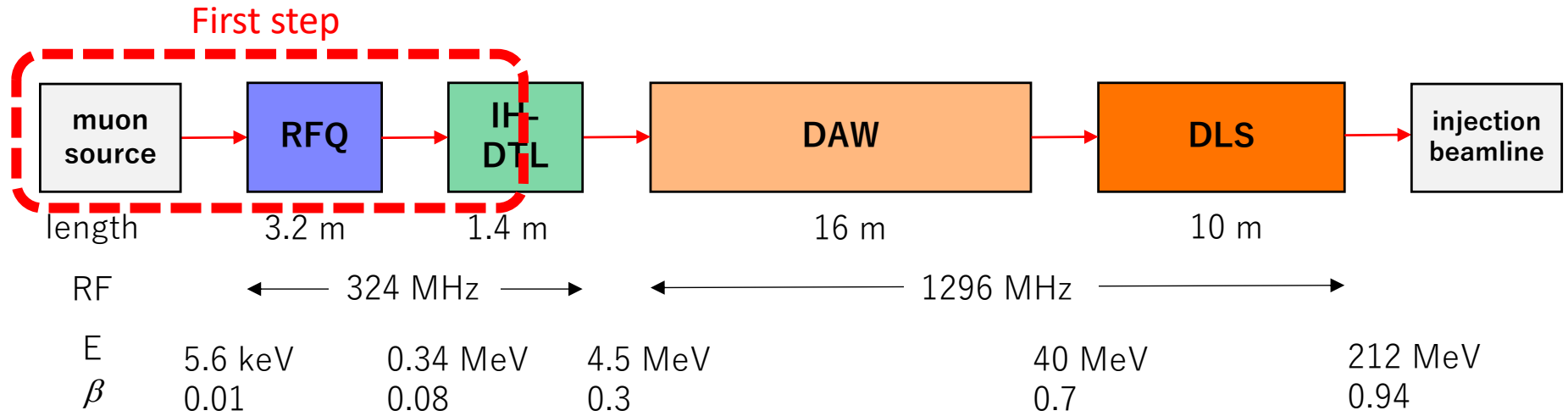
Slide by S. Uetake (Muonium WS in Osaka, Dec. 2018)



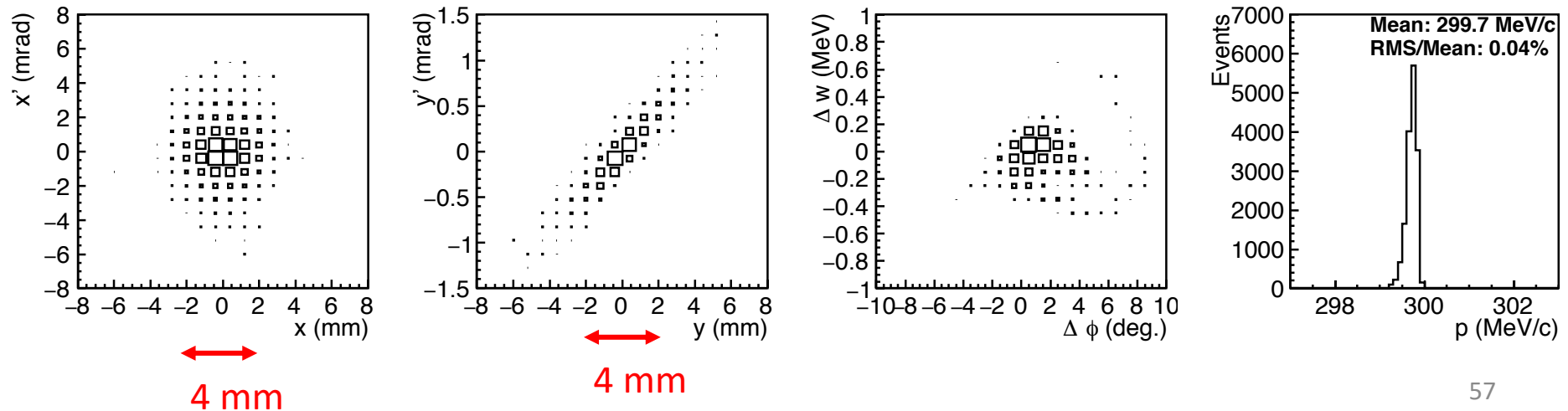
Design of Laser for 1S-2S Spectroscopy @J-PARC



Muon LINAC



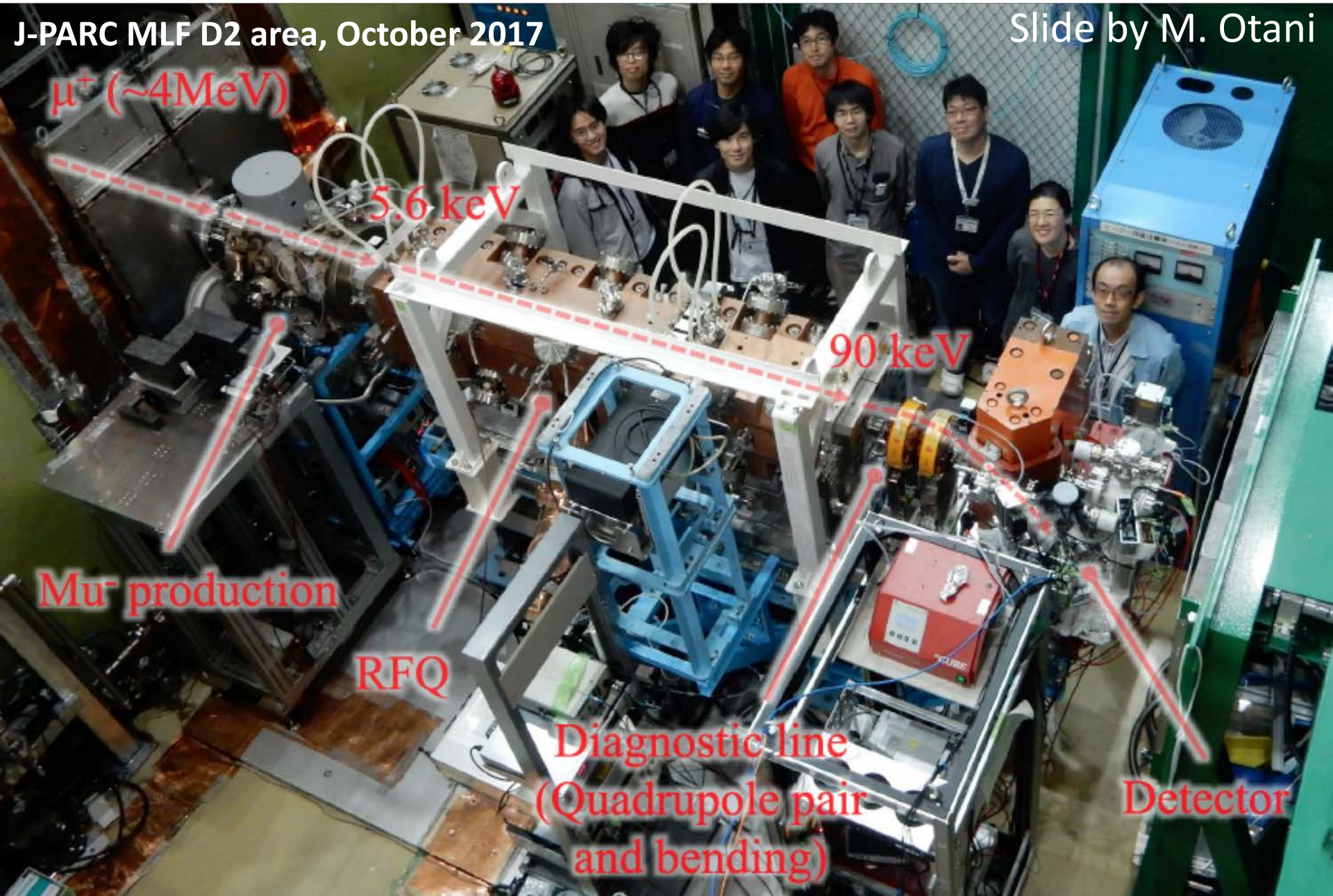
Phase space distributions after muon LINAC (simulation)



RF acceleration of Mu^- for the first time!

J-PARC MLF D2 area, October 2017

Slide by M. Otani



RF acceleration of Mu^- for the first time!

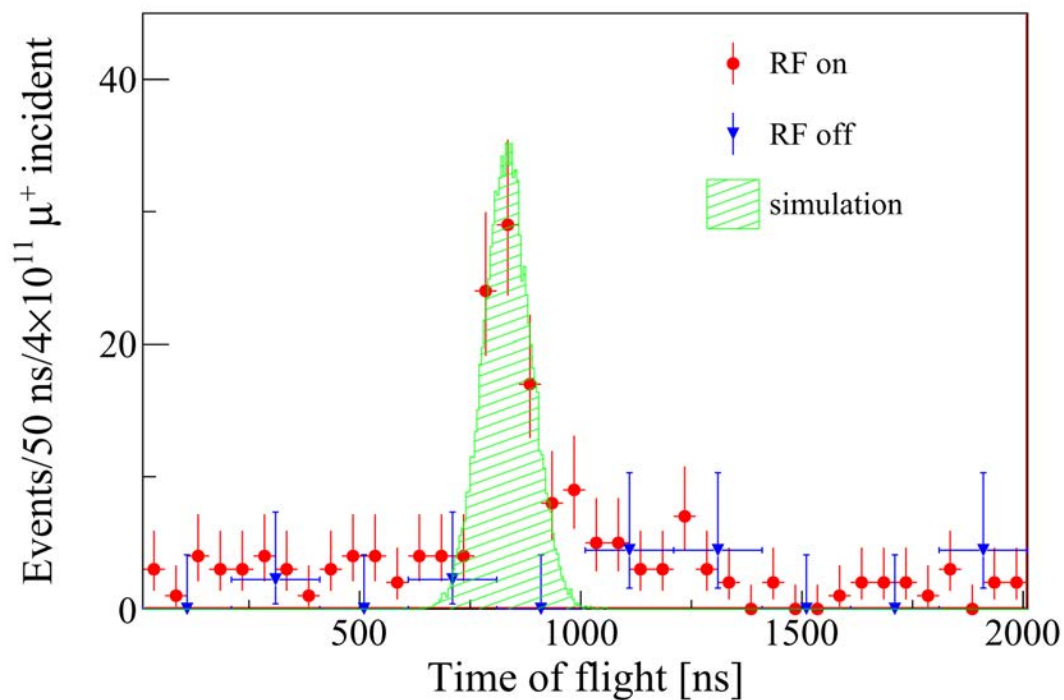
J-PARC MLF D2 area, October 2017

Slide by M. Otani

μ^+ (~4MeV)

5.6 keV

90 keV



line pair

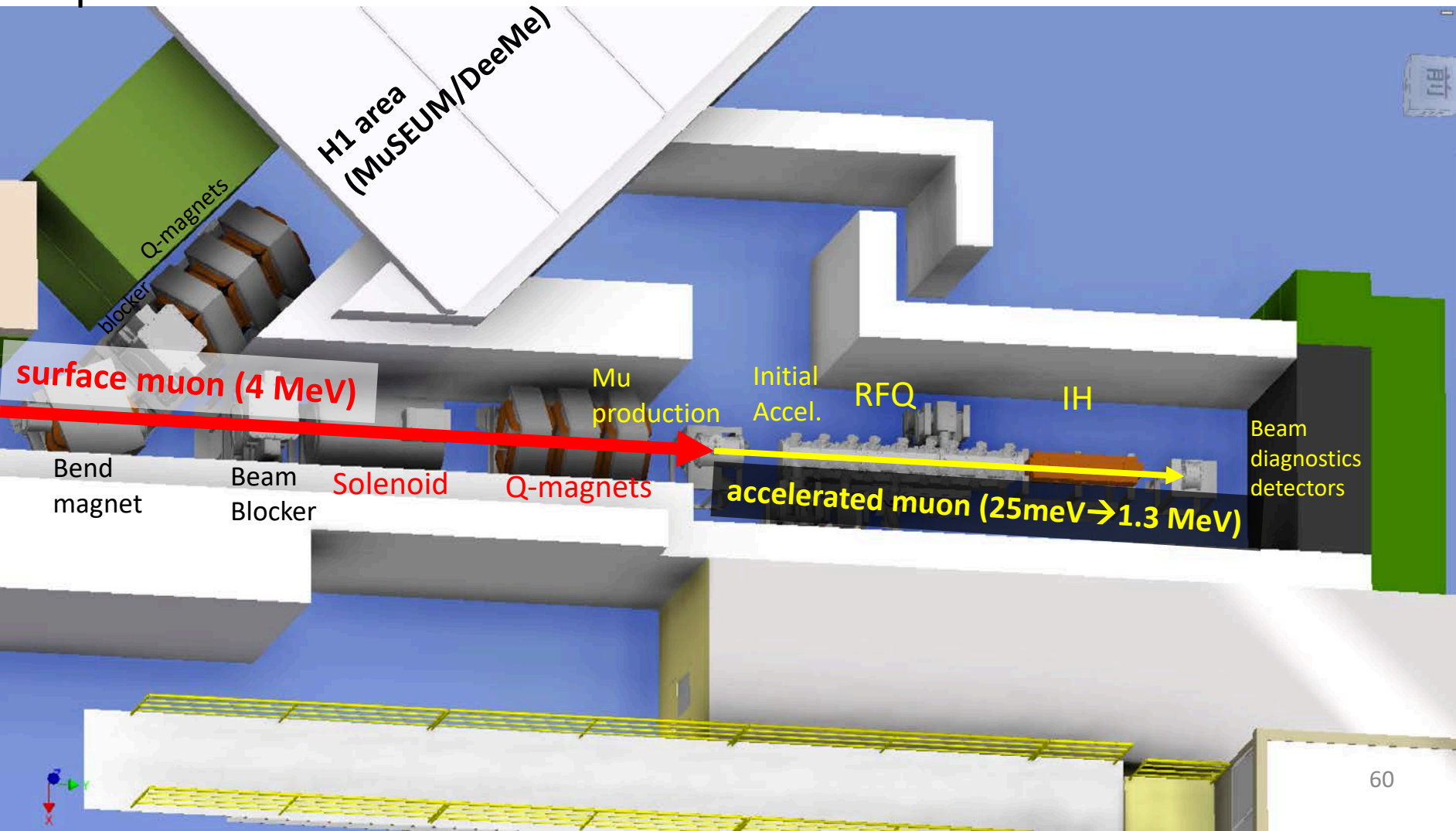
Detector

S. Bae et al., Phys. Rev. AB 21, 050101 (2018).

Next step: re-acceleration to 1 MeV

J-PARC MLF

Experimental Hall



First measurement of beam bunch structure of accelerated Mu-

2018A beam test
November 2nd - 8th

MLF D2 area

Mu- 5.6 keV

Soa lens

25 Hz

RFQ

$f_{RF}=324$ MHz

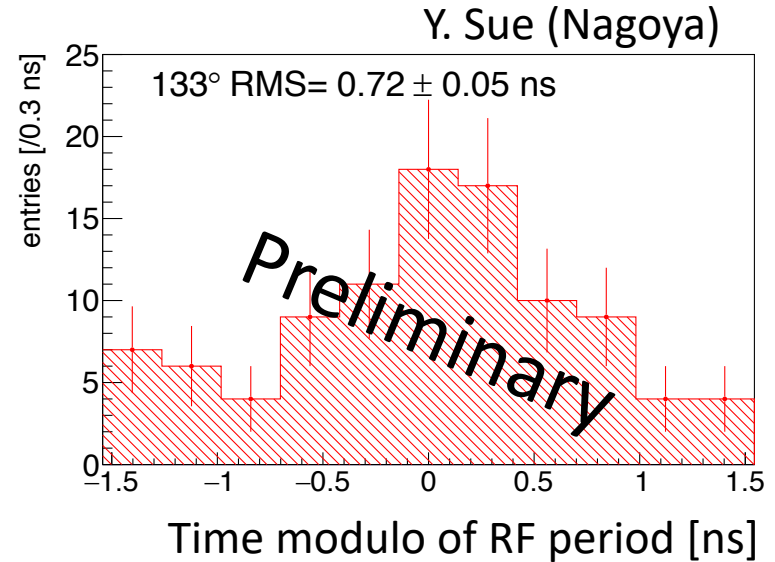
Buncher

90 keV

Q1
Q2

Bend

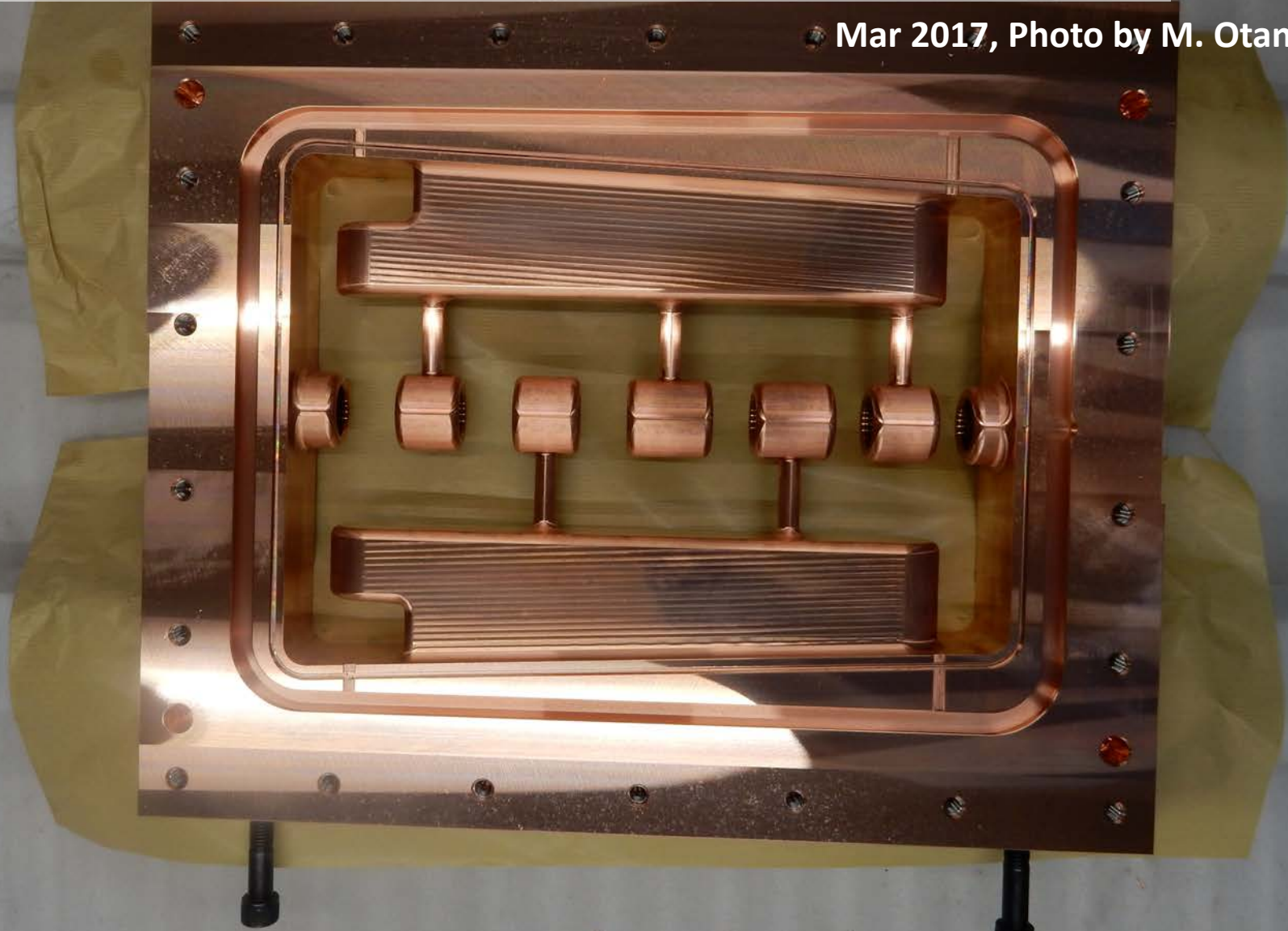
MCP
Detector



Nagoya, KEK,
JAEA, Ibaraki,
Tokyo

An accelerating structure (IH-DTL cavity) to 1.3 MeV

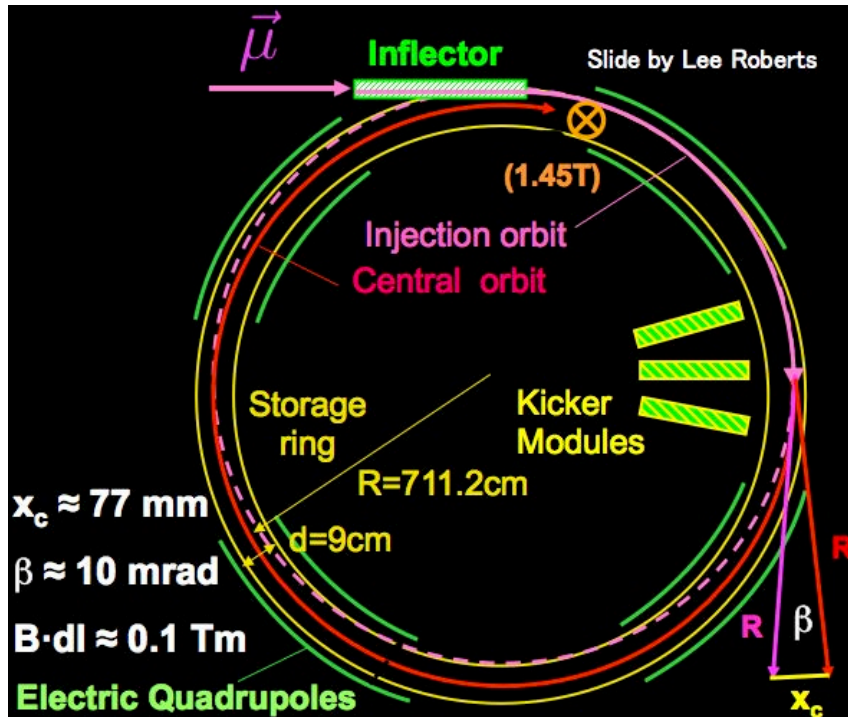
Mar 2017, Photo by M. Otani



Design: M. Otani et al., Phys. Rev. AB 19, 040101 (2016)

Muon beam injection and storage

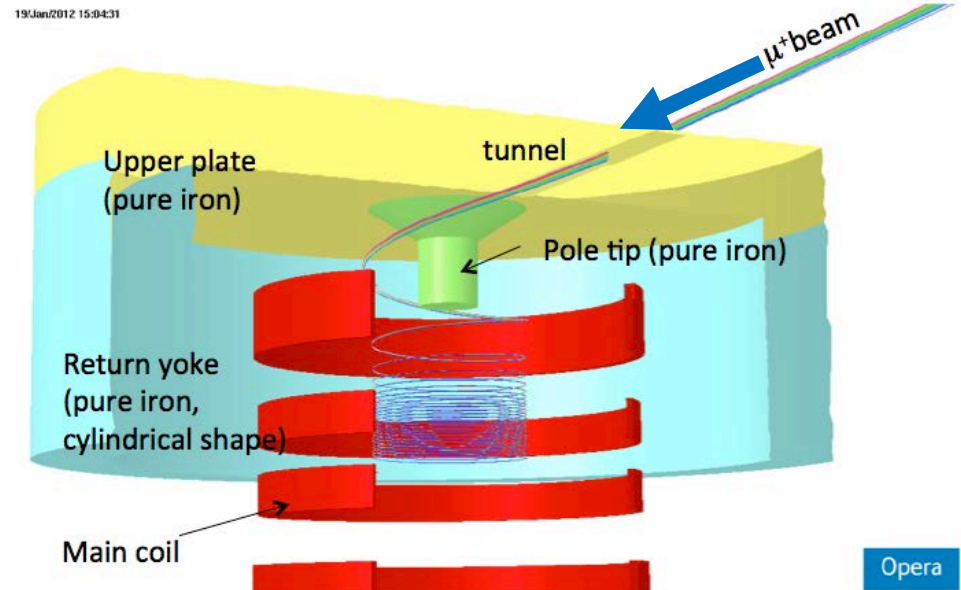
Horizontal injection + kicker
(BNL E821, FNAL E989)



Injection efficiency : 3-5%(*)

(*) PRD73,072003 (2006)

3D spiral injection + kicker
(J-PARC E34)

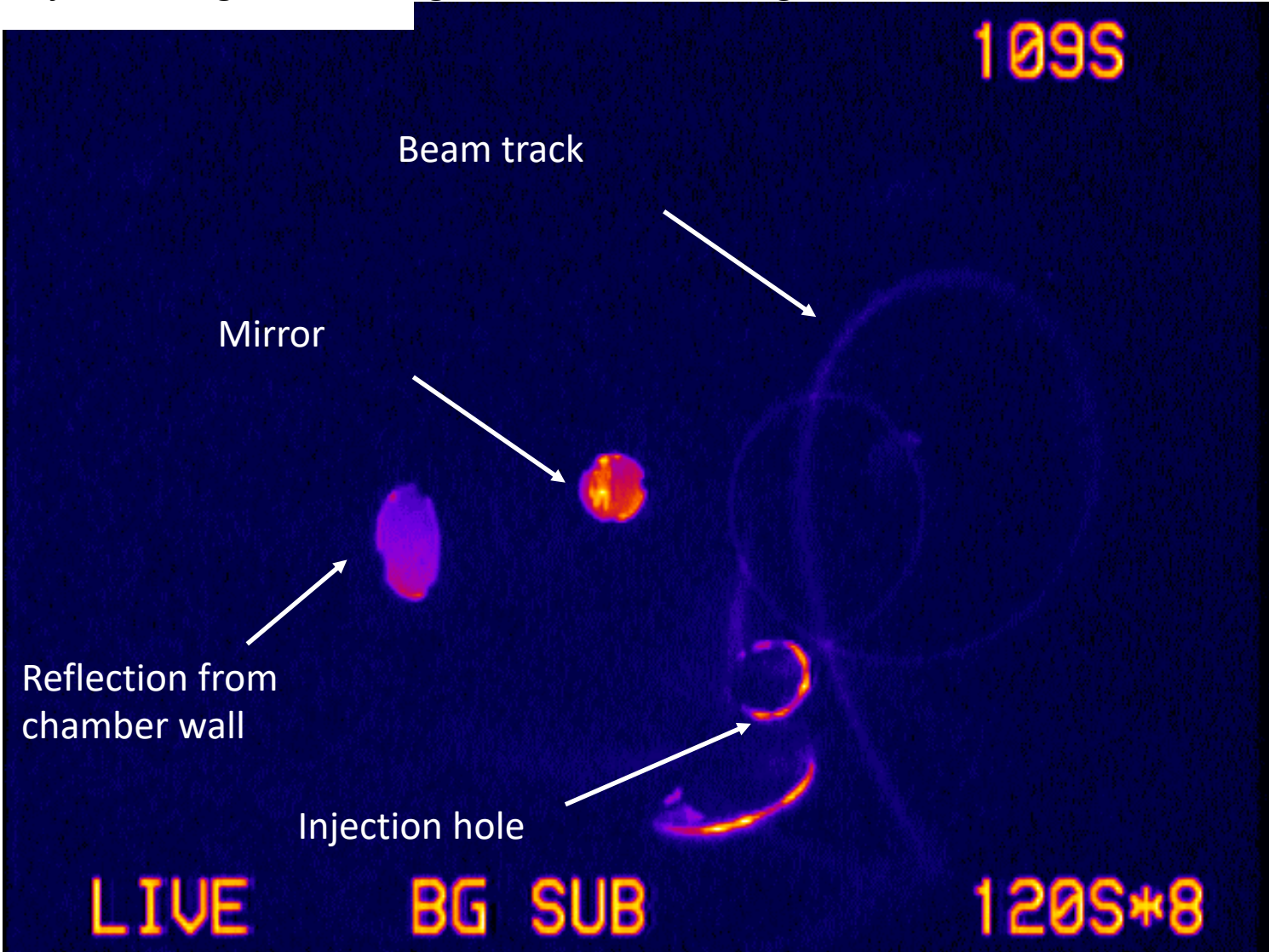


Injection efficiency : ~85%

H. Inuma et al., Nucl. Instr. And Methods. A 832, 51 (2016)

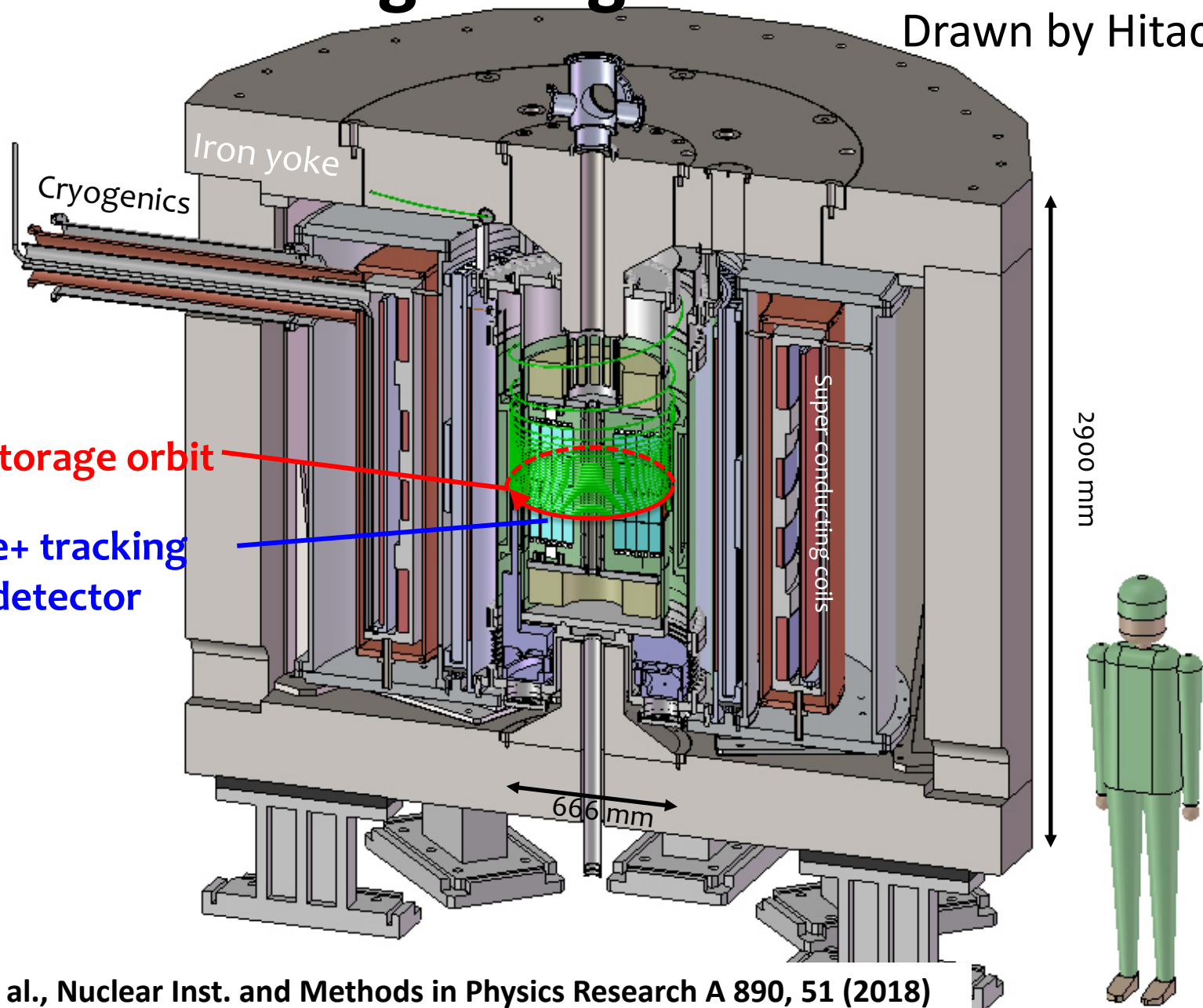
Testing spiral injection with electron beam

Injection angle was changed from 47 to 44 deg.

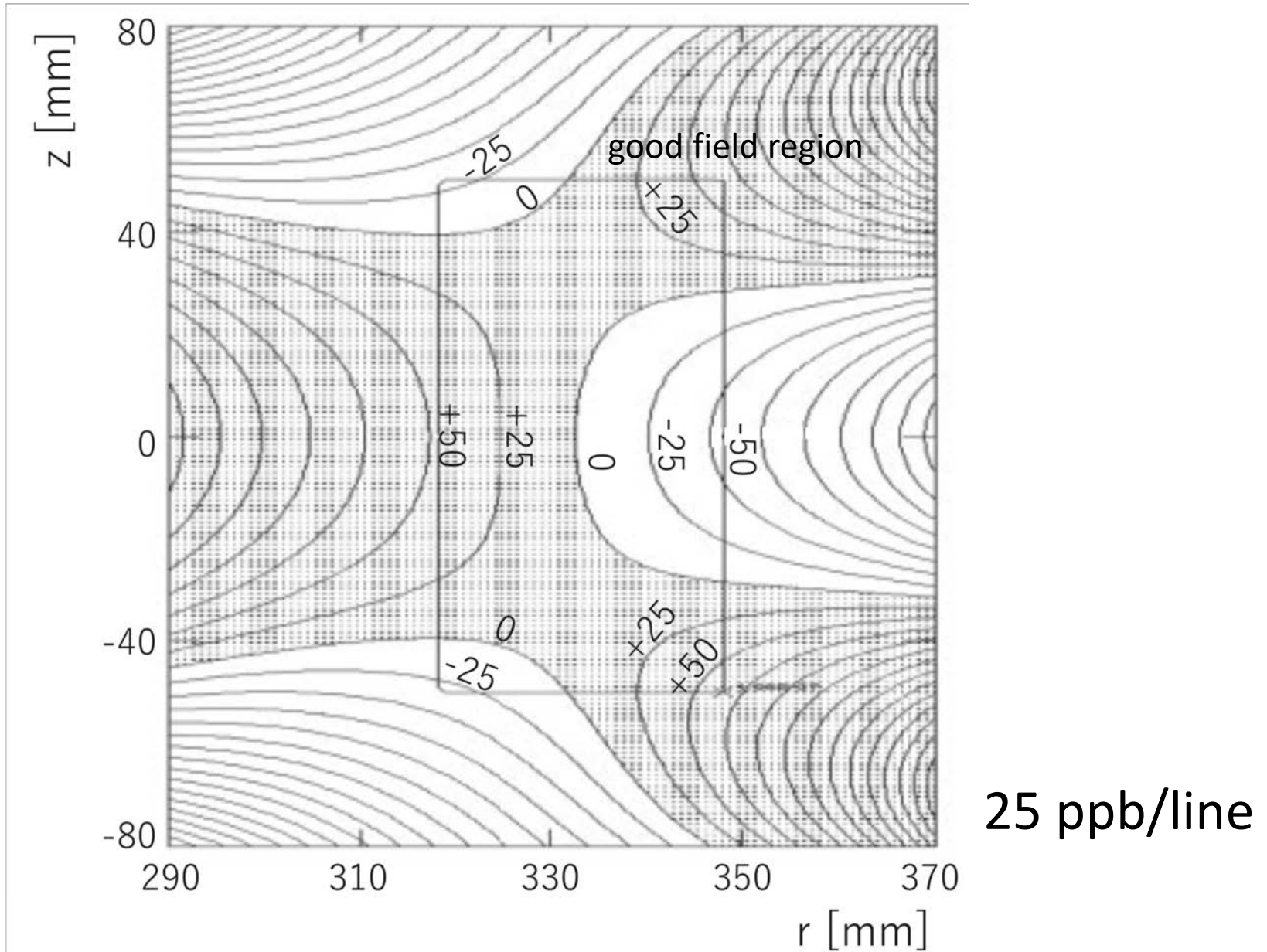


Muon storage magnet and detector

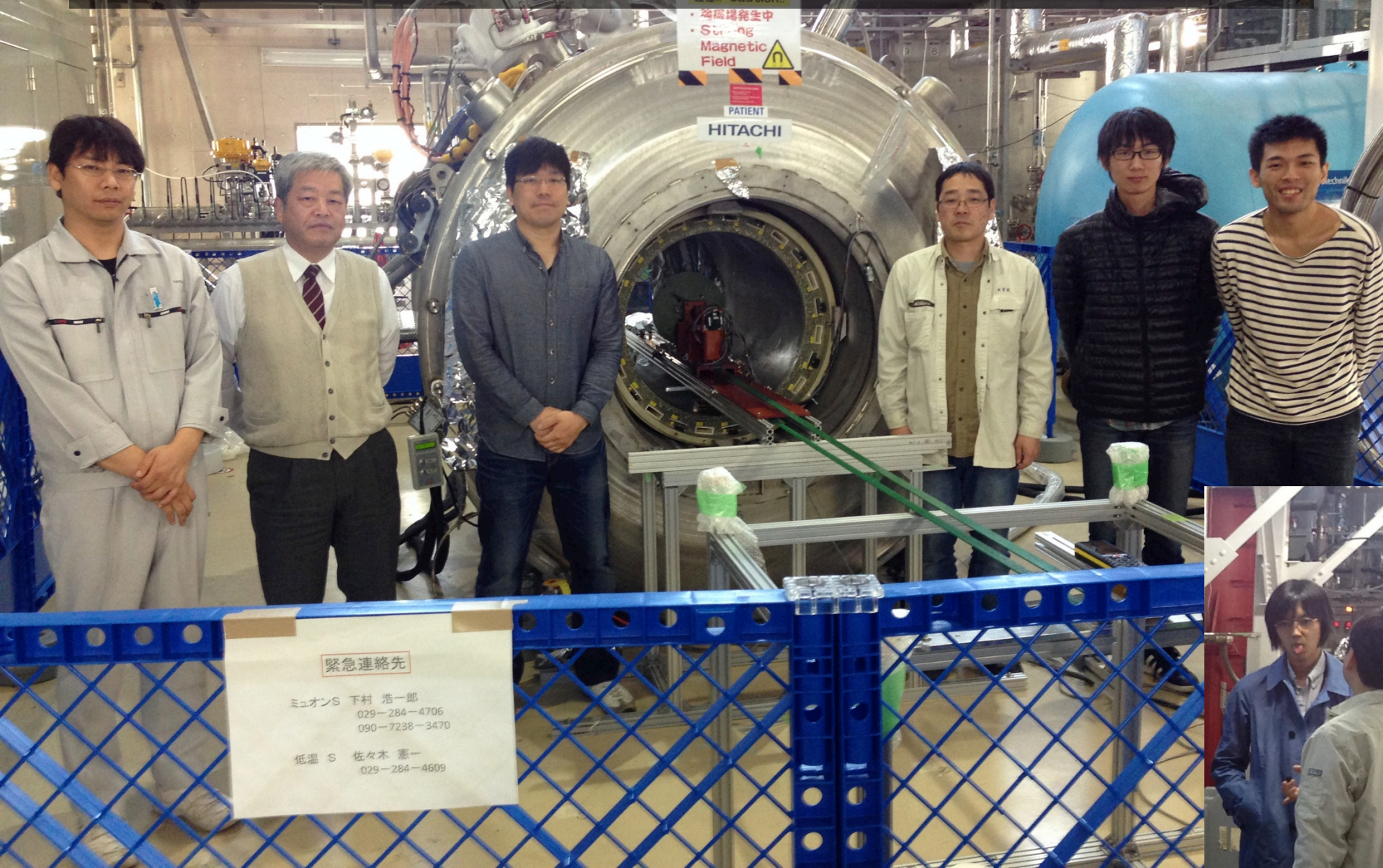
Drawn by Hitachi Co.



Average magnetic field



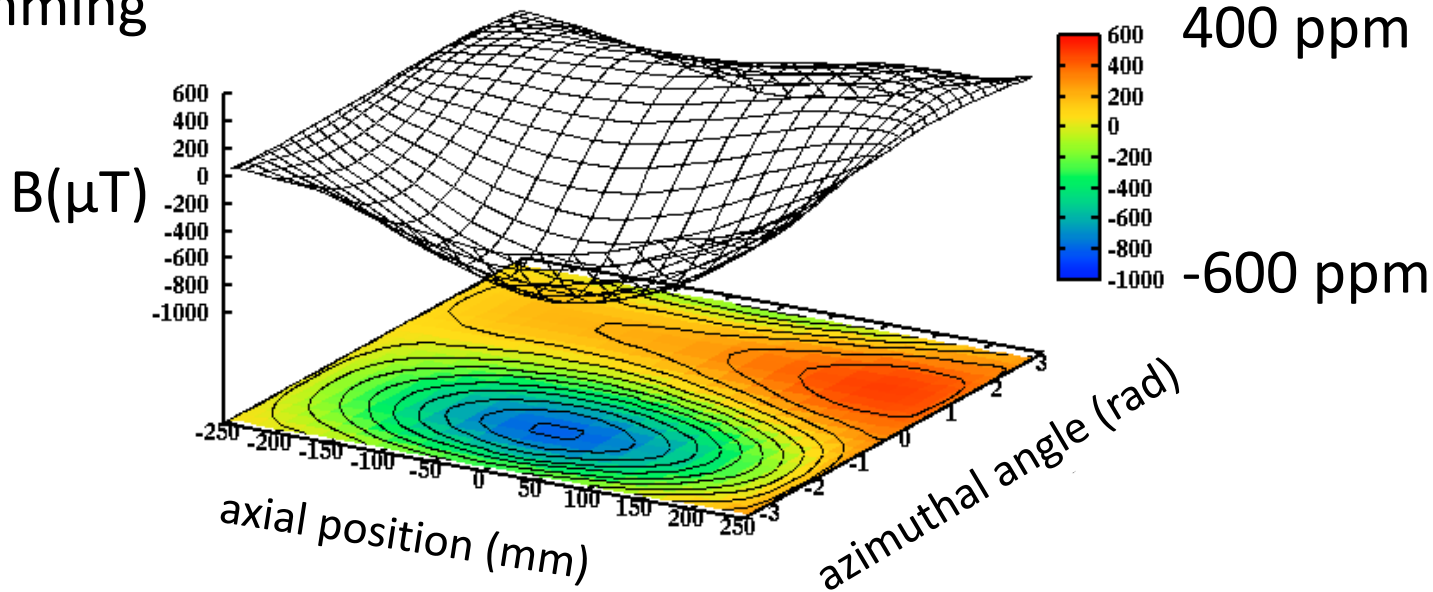
B-field shimming test with the MuSEUM magnet (1.7 T) at J-PARC



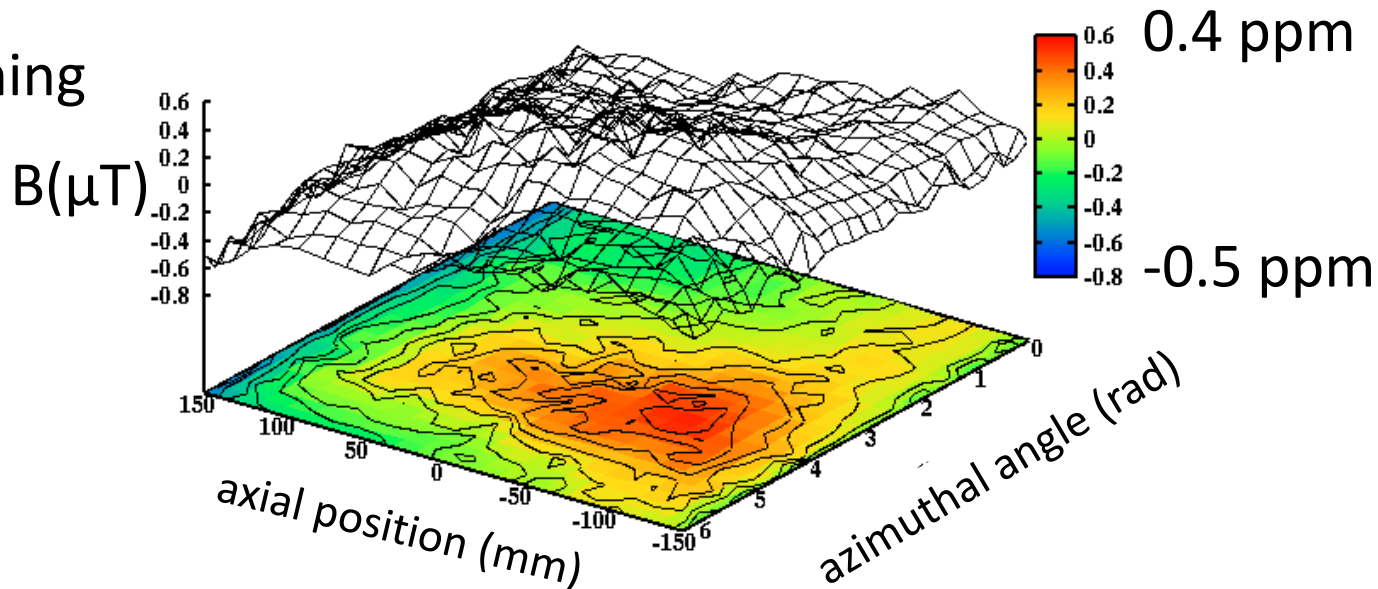
Field shimming by iron arrays

Plots by K. Sasaki

Before shimming

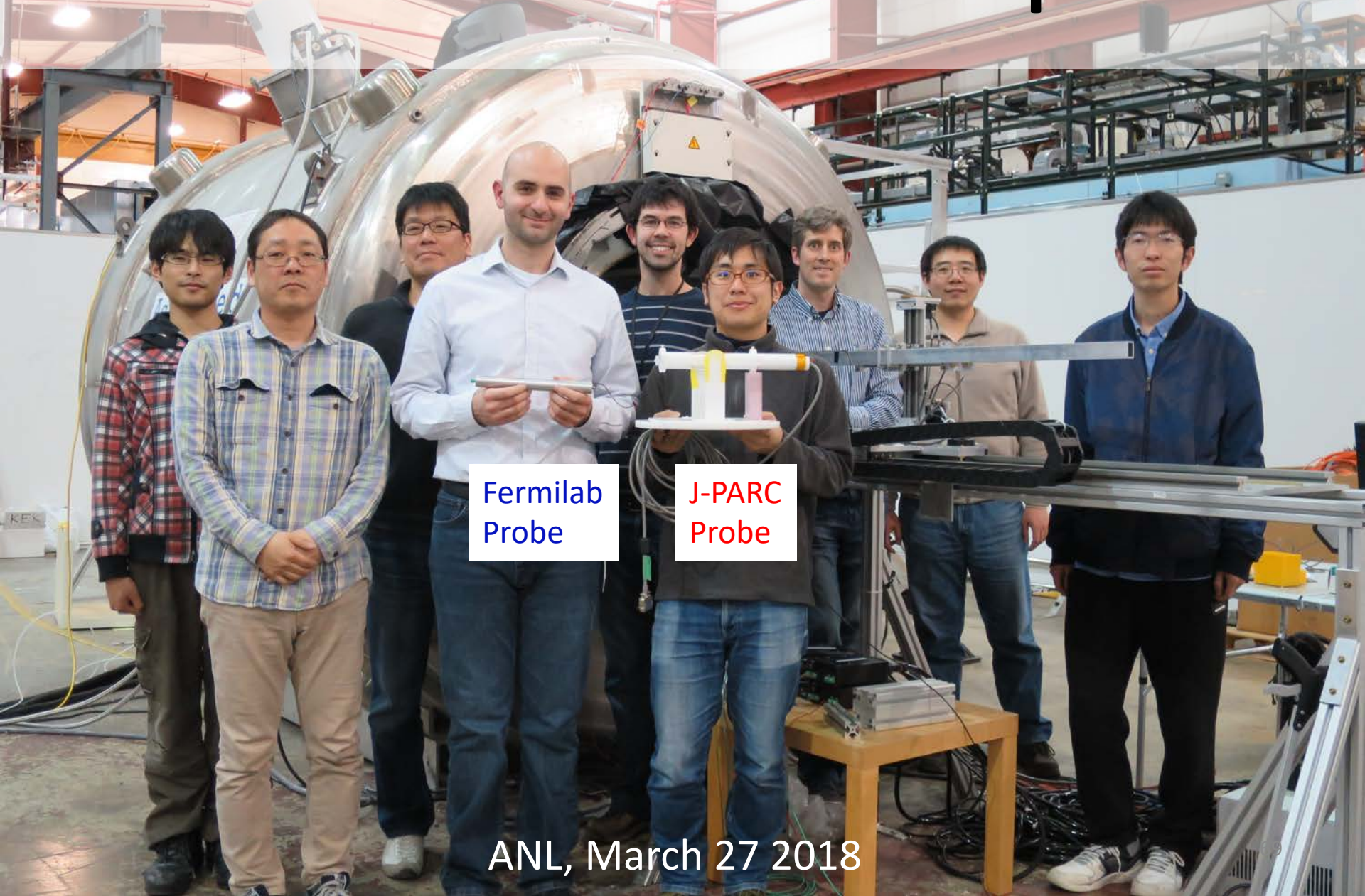


After shimming



$r = 140 \text{ mm}$

Cross calibration of B-field probes

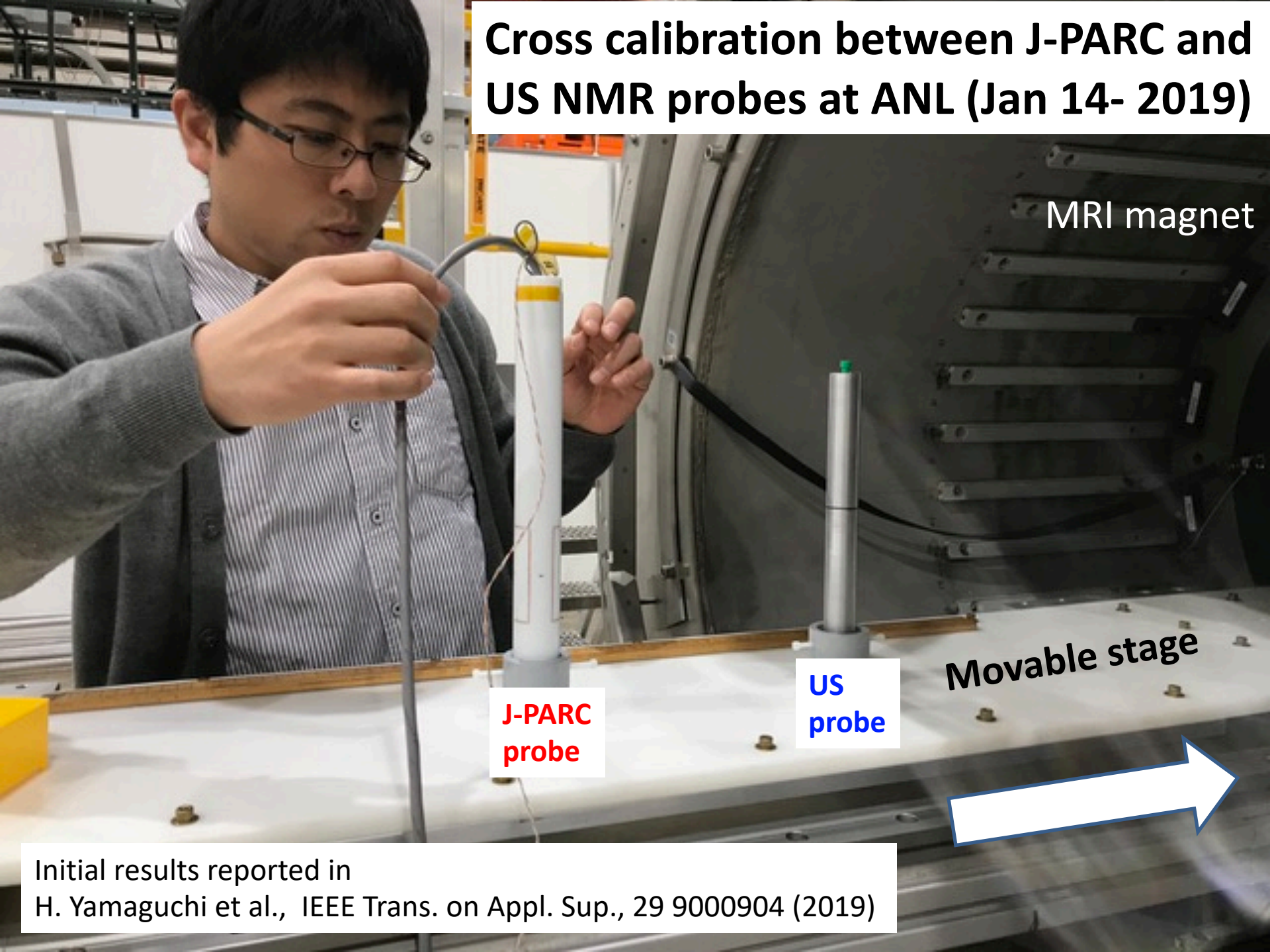


Fermilab
Probe

J-PARC
Probe

ANL, March 27 2018

Cross calibration between J-PARC and US NMR probes at ANL (Jan 14- 2019)



MRI magnet

Movable stage

J-PARC
probe

US
probe

Initial results reported in
H. Yamaguchi et al., IEEE Trans. on Appl. Sup., 29 9000904 (2019)

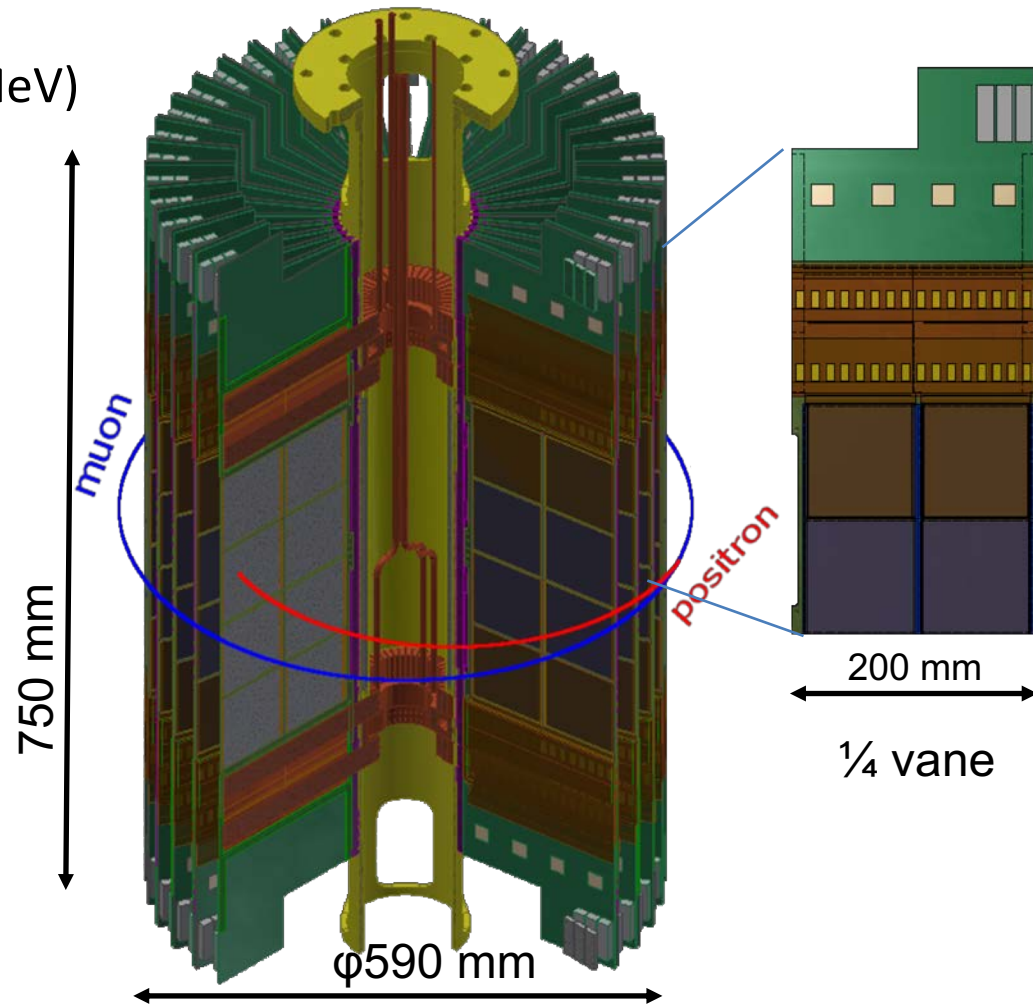
Positron tracking detector

- Requirements

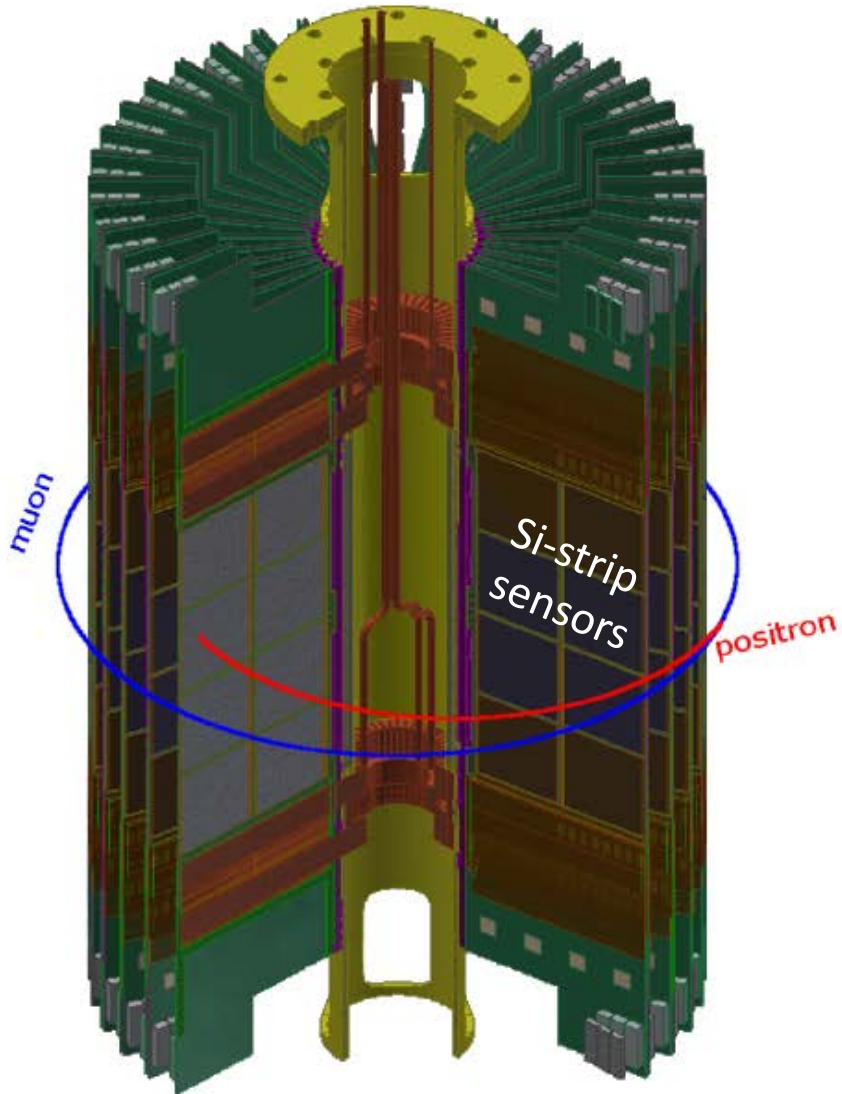
- Detection of e^+ ($100 < E < 300$ MeV)
- Reconstruction of momentum vector
- Stability over rate changes (1.4 MHz \rightarrow 14 kHz)

- Specifications

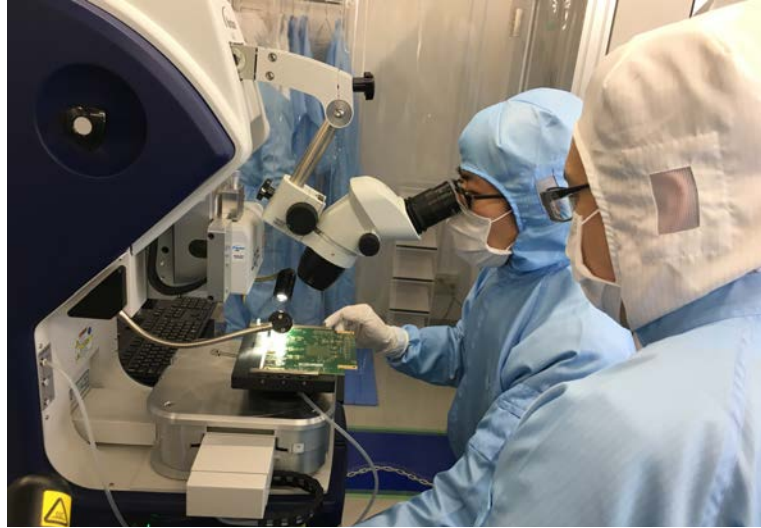
- Sensor: p-on-n single-sided strip
- Number of vanes: 40
- Number of sensors : 640
- Number of strips : 655,360
- Area of sensors : 6.24 m²



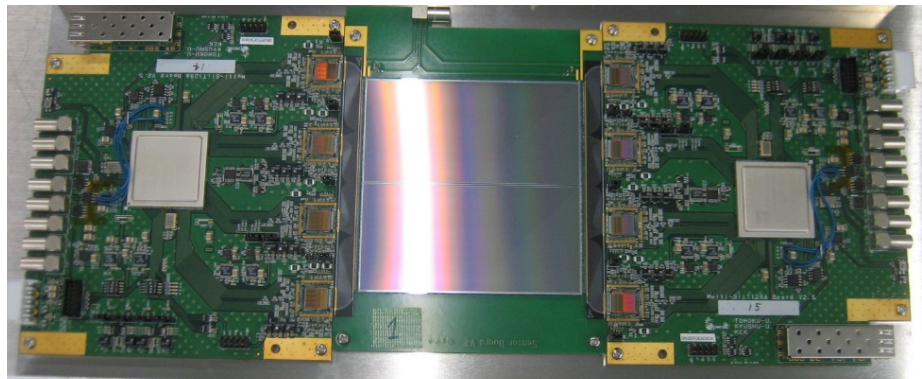
Positron tracking detector



Assembly (Kyushu + KEK)

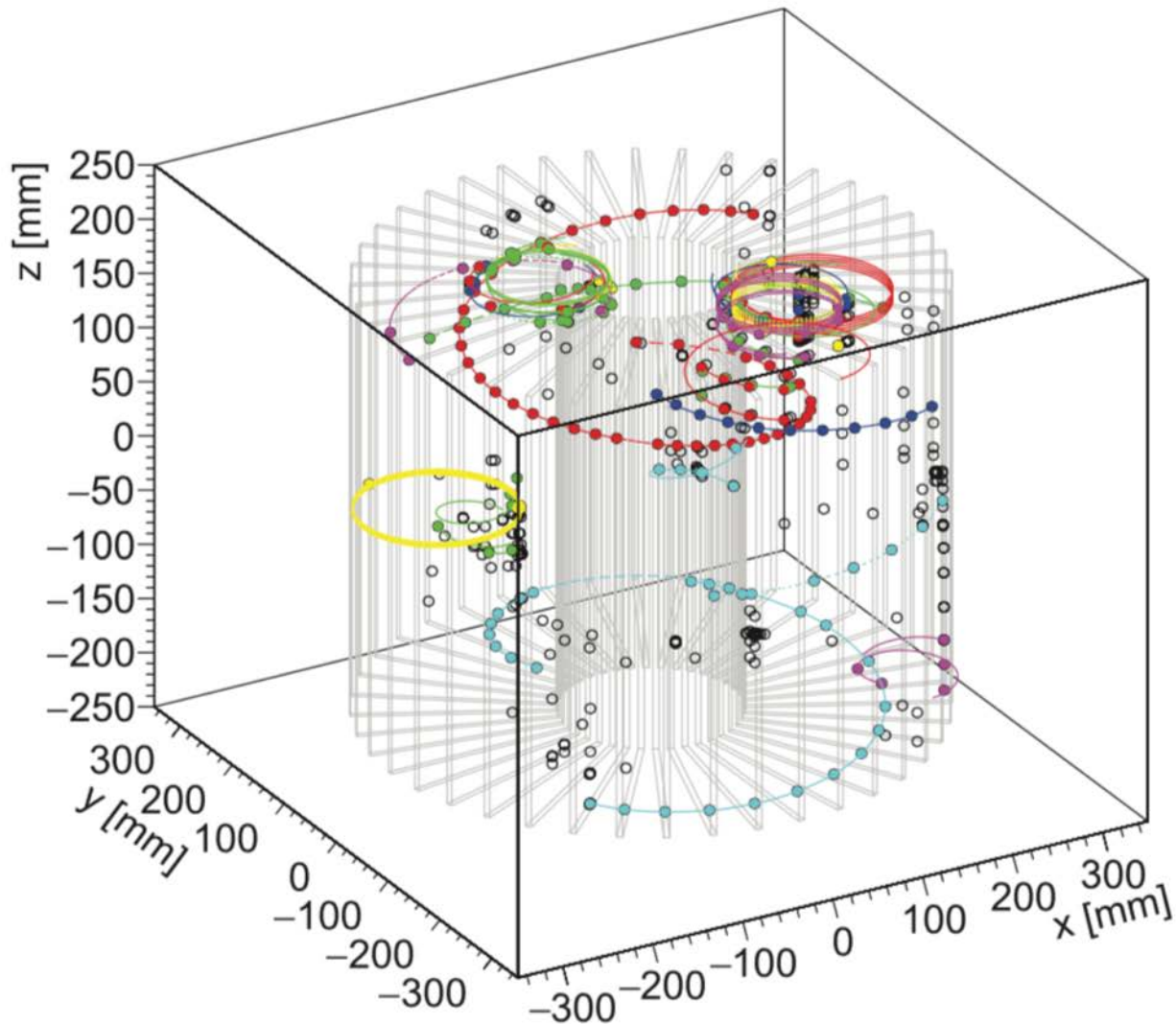


Test module (Kyushu + KEK)



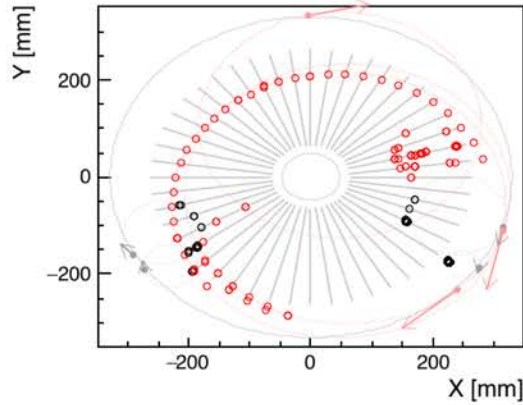
Great help from ATLAS and Belle II group at KEK ⁷²

Typical event positron track in a 5 ns time window

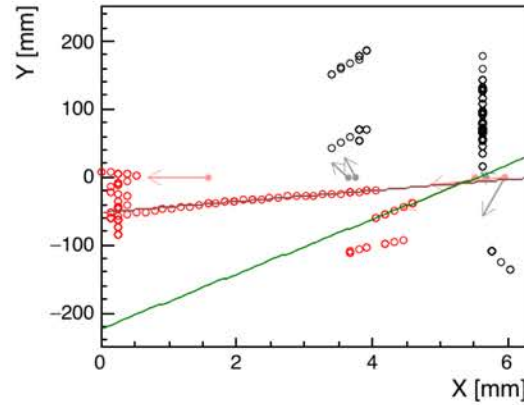


Track finding at low rate (0.6 track/ns)

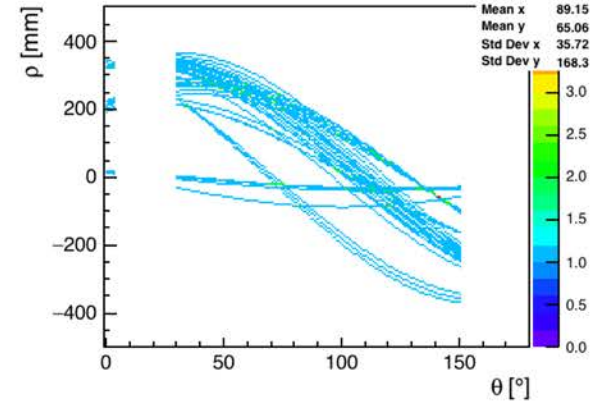
EvtNo:0, T = 80 ~ 90



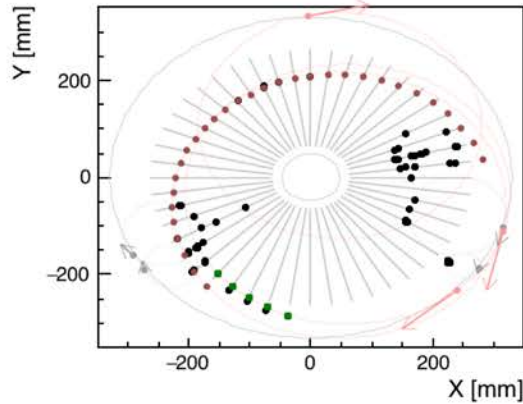
EvtNo:0, T = 80 ~ 90



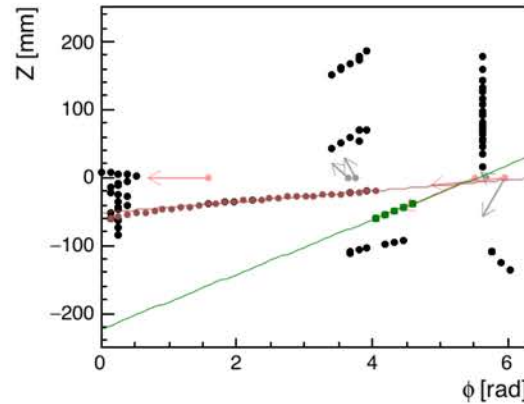
Hough3($\phi \rightarrow Z \rightarrow \theta - \rho$), $(\theta, \rho) = (141.0, -56.5)$



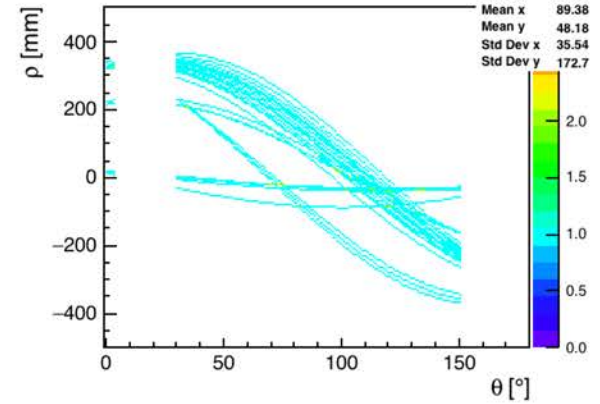
EvtNo:0, E(e+)=104.0 MeV, P(e+) = (-19.4, -102.0, -5.6), Clustered Hits



EvtNo:0, E(e+)=104.0 MeV, P(e+) = (-19.4, -102.0, -5.6), Clustered Hits



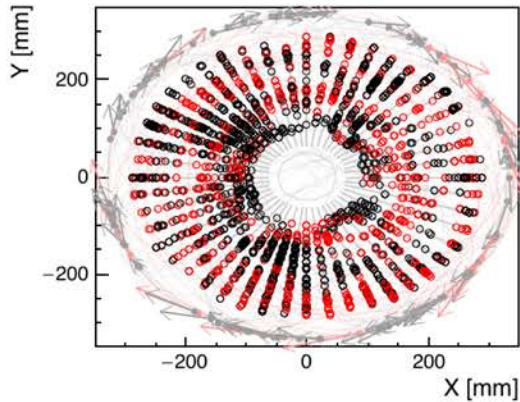
Hough4($\phi \rightarrow Z \rightarrow \theta - \rho$), $(\theta, \rho) = (30.0, 230.5)$



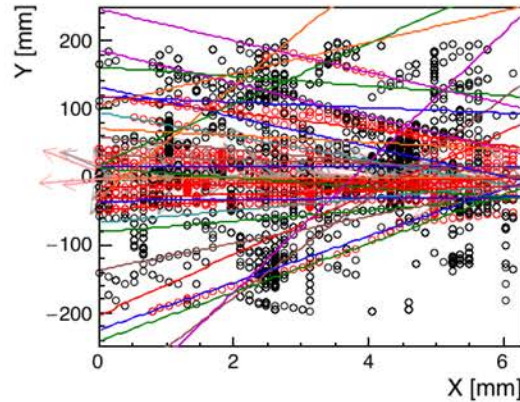
Y. Sato

Track finding at high rate (6 track/ns)

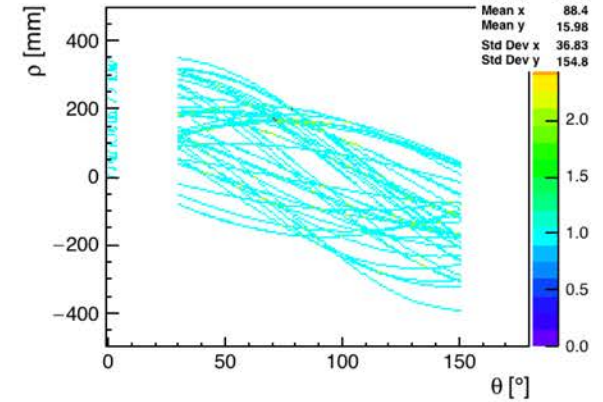
EvtNo:0, T = 50 ~ 60



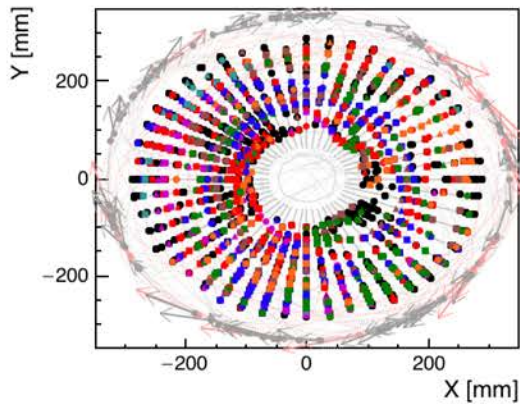
EvtNo:0, T = 50 ~ 60



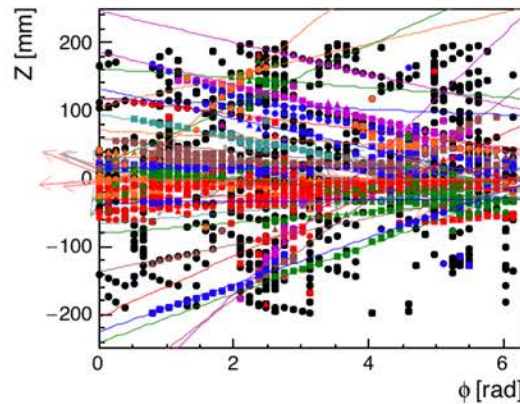
Hough27($\phi \rightarrow \theta - \rho$), $(\theta, \rho) = (91.0, 134.5)$



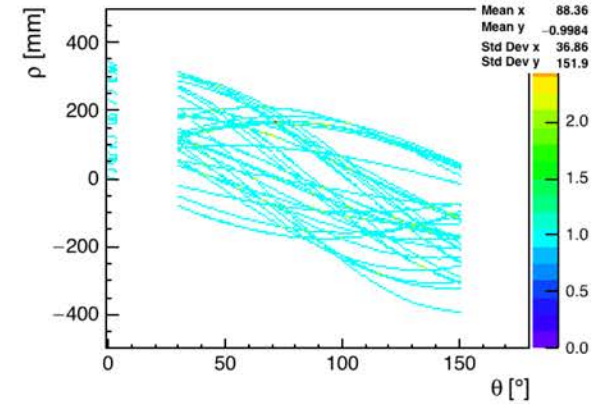
EvtNo:0, E(e+)=104.0 MeV, P(e+) = (-19.4, -102.0, -5.6), Clustered Hits



EvtNo:0, E(e+)=104.0 MeV, P(e+) = (-19.4, -102.0, -5.6), Clustered Hits



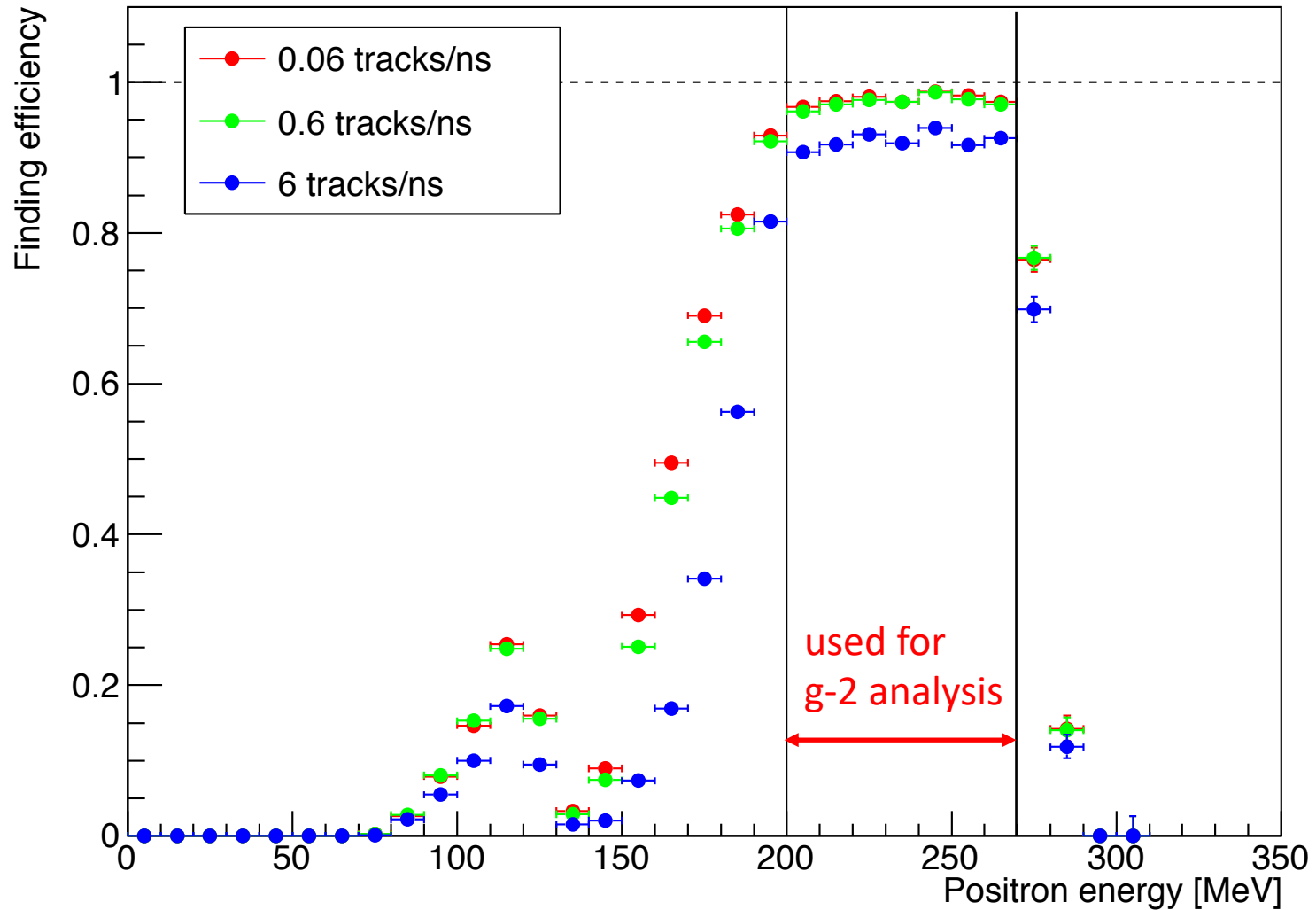
Hough28($\phi \rightarrow \theta - \rho$), $(\theta, \rho) = (41.0, 140.5)$



Y. Sato

Reconstruction efficiency

Yamanaka + Sato



Status of R&D and remaining milestones

| Level of R&D achievements (%) | 0 | 10 | 20 | 30 | 40 | 50 | 60 | 70 | 80 | 90 | 100 | Status Remaining milestones |
|-------------------------------|------------------|----|----|----|----|----|----|----|----|----|-----|-------------------------------------------------|
| Beamline & Facility | 100% (Green bar) | | | | | | | | | | | Done Under construction |
| Muon Source | 80% (Green bar) | | | | | | | | | | | (1) Hi-power laser (2) ionization test |
| Accelerator | 90% (Green bar) | | | | | | | | | | | (3) Demonstration of low emittance acceleration |
| High Precision Magnet | 100% (Green bar) | | | | | | | | | | | Done |
| Beam Transport | 100% (Green bar) | | | | | | | | | | | Done |
| Detector | 100% (Green bar) | | | | | | | | | | | Done Under construction |

Technically-driven schedule and cost

Assumption : Major construction fund becomes available in JFY201X

component production
 assembly
 installation
 comissioning
 physics run

| Calendar Year | CY2020 | | | | CY2021 | | | | CY2022 | | | | CY2023 | | | | CY2024 | | | | CY2025 | | | | | |
|--------------------------------------------|---------|----|----|----|---------|----|----|----|---------|----|----|----|---------|----|----|----|---------|----|----|----|---------|----|----|----|--|--|
| Japanese Fiscal Year | JFY2020 | | | | JFY2021 | | | | JFY2022 | | | | JFY2023 | | | | JFY2024 | | | | JFY2025 | | | | | |
| Month | F1 | F2 | F3 | F4 | F1 | F2 | F3 | F4 | F1 | F2 | F3 | F4 | F1 | F2 | F3 | F4 | F1 | F2 | F3 | F4 | F1 | F2 | F3 | F4 | | |
| Beamline & Facility 12.7 Oku | | | | | | | | | | | | | | | | | | | | | | | | | | |
| Muon Source 3.3 Oku | | | | | | | | | | | | | | | | | | | | | | | | | | |
| Accelerator 7.9 Oku | | | | | | | | | | | | | | | | | | | | | | | | | | |
| High Precision Magnet 17.0 Oku | | | | | | | | | | | | | | | | | | | | | | | | | | |
| Beam Transport 1.0 Oku | | | | | | | | | | | | | | | | | | | | | | | | | | |
| Detector 4.3 Oku | | | | | | | | | | | | | | | | | | | | | | | | | | |
| Data taking (3.8 Oku) | | | | | | | | | | | | | | | | | | | | | | | | | | |

Relating measurements to g-2

- **muon spin precession** $\omega_a = \frac{e}{m_\mu} a_\mu B$
- **proton spin precession** $\omega_p = \mu_p B$
- **muon magnetic moment** $\mu_\mu = g \frac{e}{2m_\mu} = (1 + a_\mu) \frac{e}{m_\mu}$

$$a_\mu = \frac{\frac{\omega_a}{\omega_p}}{\frac{\mu_\mu}{\mu_p}}$$

540 ppb (BNL)
 140 ppb
 (Fermilab/J-PARC)

Magnetic moment ratio

LAMPF(1999)

$$\Delta \left(\frac{\mu_\mu}{\mu_p} \right) = 120 \text{ ppb (direct)} \quad (30 \text{ ppb using } \Delta v + \text{theory})$$

Relating measurements to $g-2$

- **muon spin precession**

$$\omega_a = \frac{e}{m_\mu} a_\mu B$$

- **proton spin precession**

$$\omega_p = \mu_p B$$

- muon magnetic moment

$$\mu_e = g_e \frac{e}{2m_e}$$

$$a_\mu = \frac{\omega_a}{\omega_p} \frac{\mu_p}{\mu_e} \frac{m_\mu}{m_e} \frac{g_e}{2}$$

540 ppb (BNL)
 140 ppb
 (Fermilab/J-PARC)

8 ppb

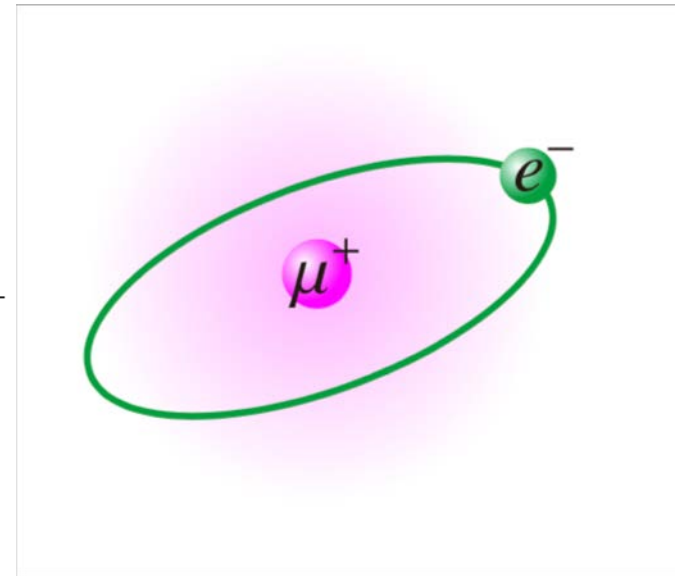
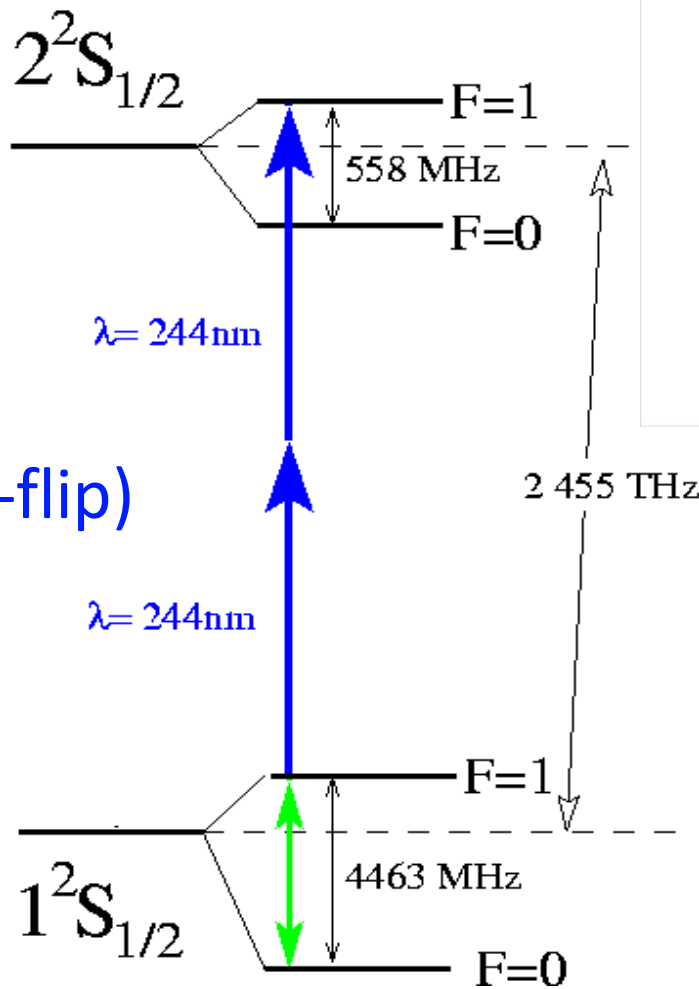
0.3 ppt

120 ppb (using μ_μ/μ_p)
 22 ppb (using Δv + theory)

Energy spectrum of muonium

From K. Jungmann

1S-2S
(spin non-flip)



HFS (spin flip transition)

Muon g-2 and muonium spectroscopy experiments

inspired by
K. Jungmann

g-2

$$a_\mu = \frac{\frac{\omega_a}{\omega_p}}{\frac{\omega_a}{\omega_p} - \frac{\mu_\mu}{\mu_p}}$$

$$a_\mu = \frac{\omega_a}{\omega_p} \frac{\mu_p}{\mu_e} \frac{m_\mu}{m_e} \frac{g_e}{2}$$

μ_μ

m_μ

Mu HFS

Mu 1S-2S

m_μ

$$\Delta\nu_{1S\text{-HFS}} \simeq \frac{16}{3} \alpha^2 R_\infty \frac{\mu_\mu}{\mu_B} \left(1 + \frac{m_e}{m_\mu}\right)^{-3}$$

$$\nu_{34} - \nu_{12} \propto \frac{\mu_\mu}{\mu_p}$$

$$\Delta\nu_{1S2S} \simeq \frac{3\alpha^2}{8h} m_e c^2 \left(1 + \frac{m_e}{m_\mu}\right)^{-1}$$

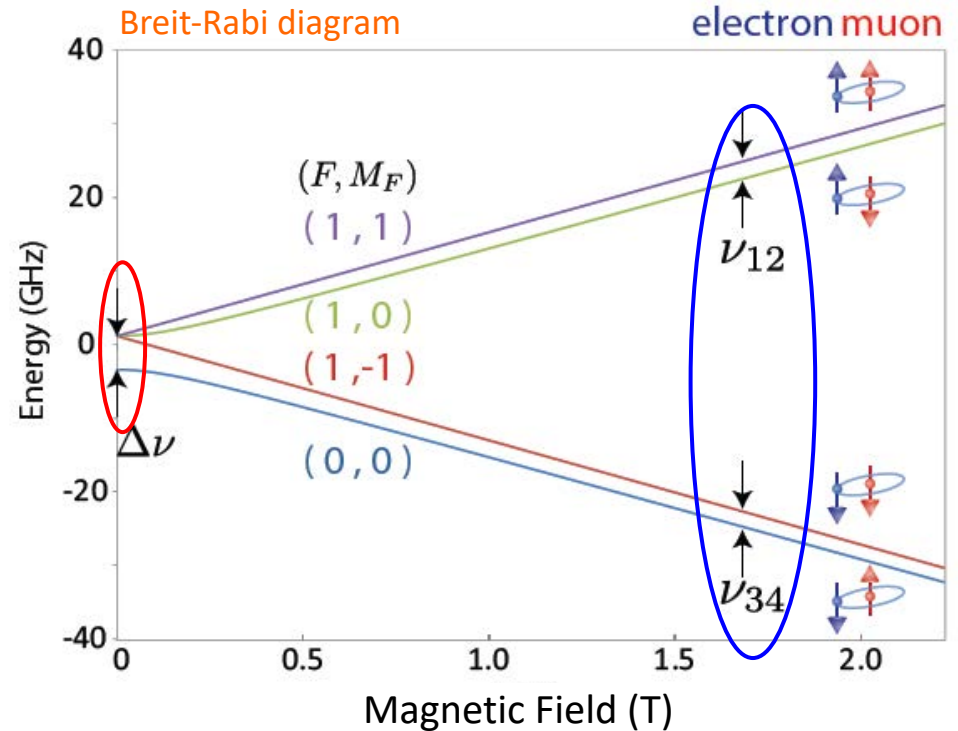
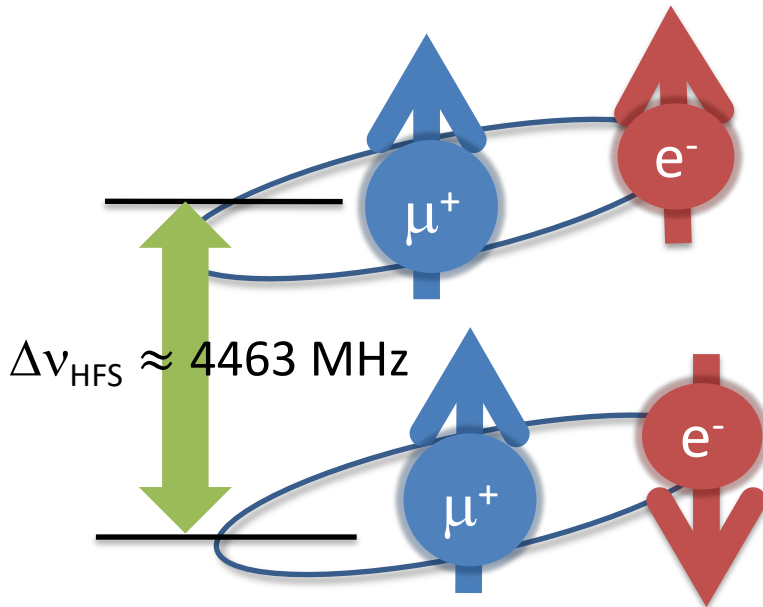
Muonium Hyperfine Structure

K. Shimomura

$$\mathcal{H} = h\Delta\nu \mathbf{I}_\mu \cdot \mathbf{J} - \mu_B^\mu g'_\mu \mathbf{I}_\mu \cdot \mathbf{H} + \mu_B^e g_J \mathbf{J} \cdot \mathbf{H}$$

$\Delta\nu_{\text{HFS}}$: Mu Hyperfine Structure

Zeeman Splitting



$$\nu_{12} + \nu_{34} = \Delta\nu_{\text{HFS}}$$

$$\nu_{12} - \nu_{34} \propto \mu_\mu / \mu_p \propto m_\mu / m_p$$

Most Precise Test of Bound State QED

Experiment:

LAMPF Experiment (1999)

| | | |
|--------------------------------|------------------------------------|----------|
| $\nu_{\text{HFS}}(\text{exp})$ | 4463.302 765 (53) MHz | [12 ppb] |
| | $\mu_{\mu}/\mu_p = 3.18334524(37)$ | [120ppb] |
| | $m_{\mu}/m_e = 206.768277(24)$ | [120ppb] |

Theory:

| | | |
|--------------------------------------|--------------------------------------|----------|
| $\nu_{\text{HFS}}(\text{theory})$ | 4463.302 868 (271) MHz | [61 ppb] |
| $\nu_{\text{HFS}}(\text{QED})$ | 4463.302 720 (253) (98) (3) MHz | |
| | (m_{μ}/m_e) (QED) (α) | |
| $\nu_{\text{HFS}}(\text{weak})$ | -65 Hz | |
| $\nu_{\text{HFS}}(\text{had. v.p.})$ | 232 (1) Hz | |
| $\nu_{\text{HFS}}(\text{had. h.o.})$ | 5 (2) Hz | |

QED calculation: Effort for 10 Hz accuracy in progress (by Eides et al.)

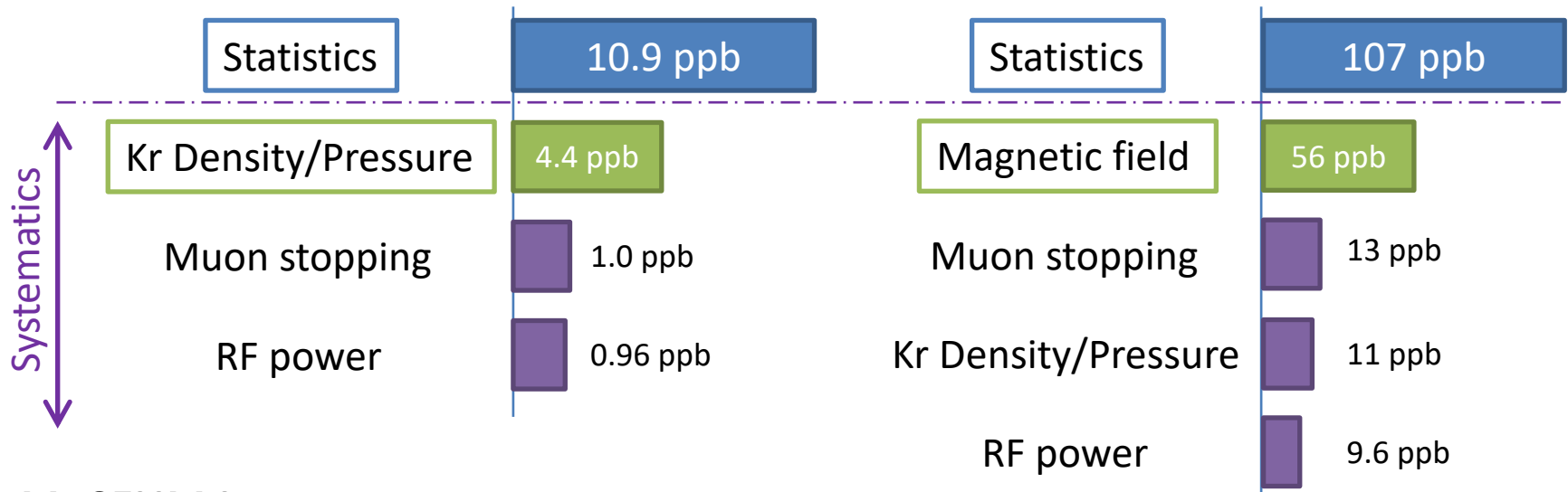
Progress: PRA 86 (2012) 024501, PRL 112 (2014) 173004, PRD 89 (2014) 014034

Improvement of statistics at J-PARC

LAMPF Experiment

$\delta(\Delta v)$

$\delta(\mu_\mu/\mu_p)$



MuSEUM Improvements:

Statistics:

LAMPF: DC $10^7/s$
total 10^{13}

x200

J-PARC/MUSE: **Pulsed $1 \times 10^8/s$**
H-Line
total 2×10^{15}

Systematics:

- magnetic field accuracy & uniformity
- pressure dependence (longer cavity lower pressure)
- muon stopping distribution measurement
- RF power stability

MRI Magnet for High-Field Experiment

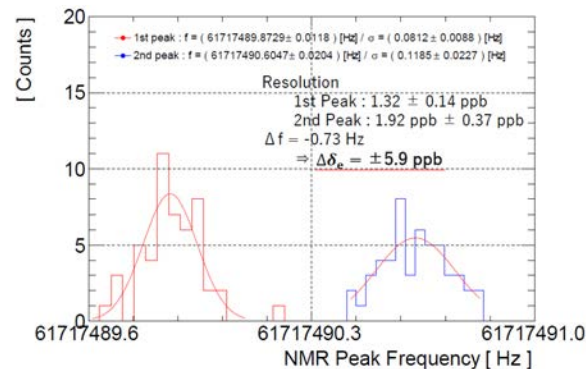
Sasaki, Yamaguchi, T. Tanaka

Second-hand 2.9 T MRI magnet

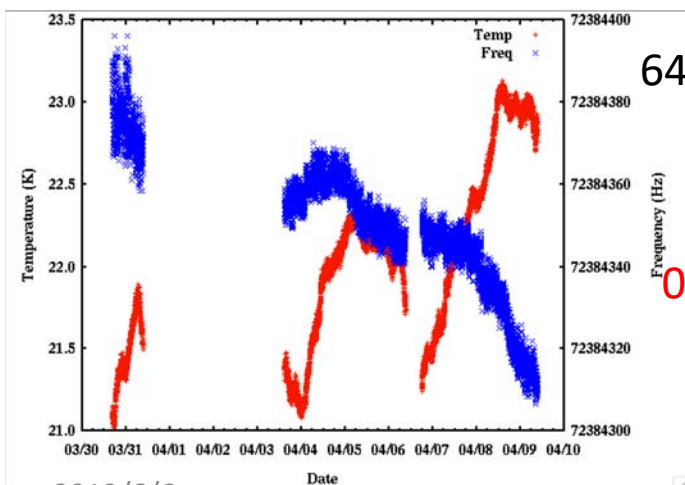


CW-NMR Field Monitoring System

18 ppb → 5.9 ppb (2017 → 2018)



Long Term Stability



64 Hz / 9.7 days

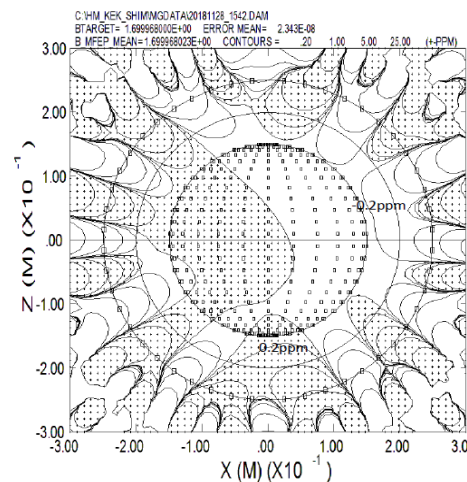


0.003 ppm / h

Field Homogeneity (after shimming)

Spheroid : $r=100$ mm, $z=300$ mm

1.4 ppm p-p → 0.27 ppm p-p (2017 → 2018)



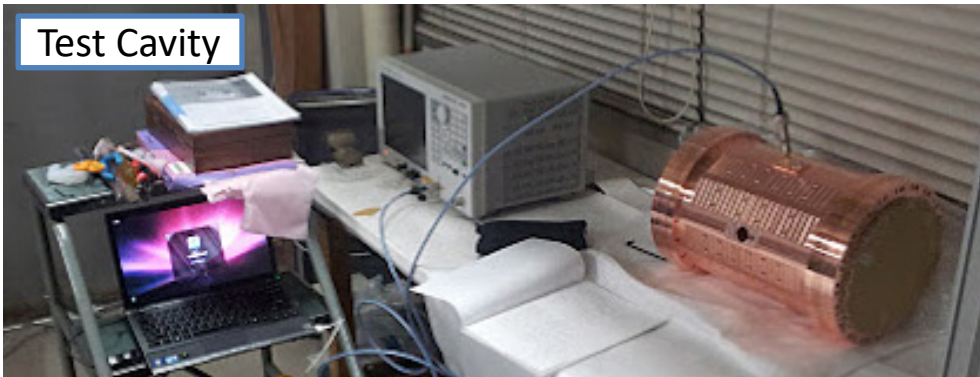
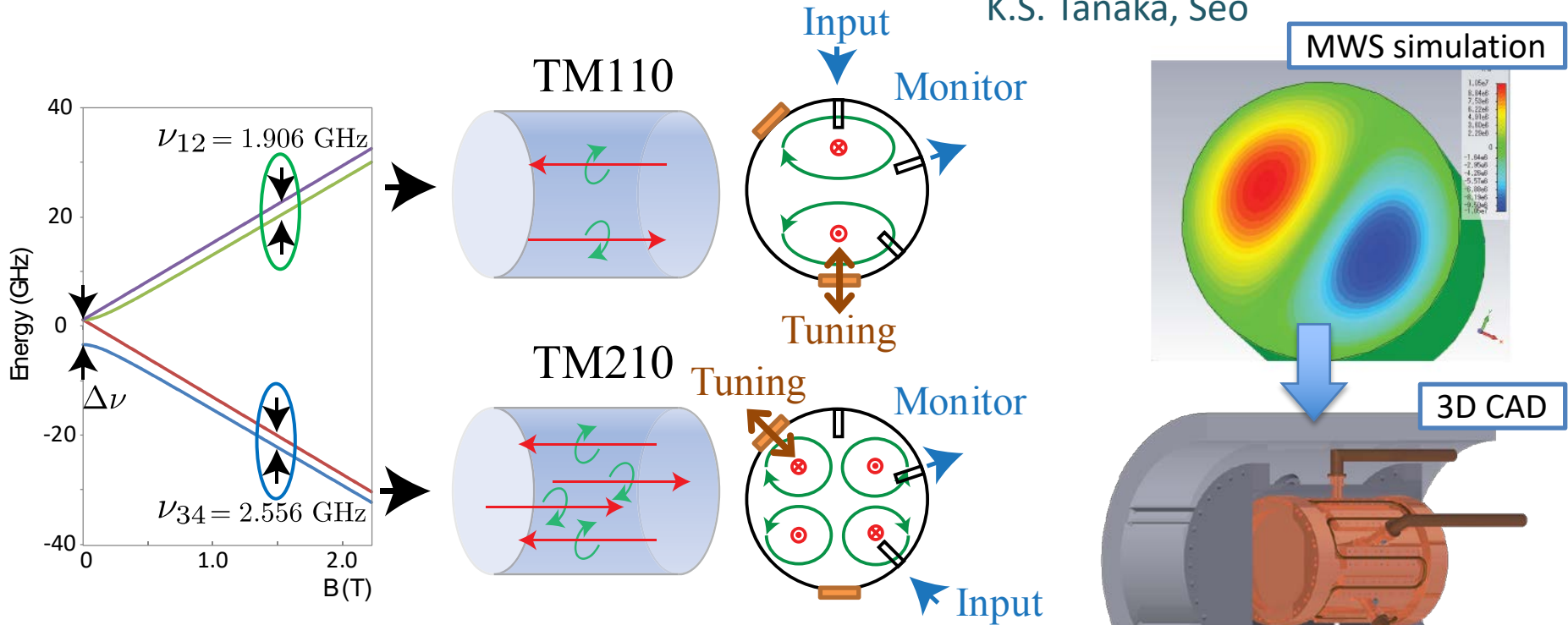
2019/6/6

Muonium WS Osaka

86

RF Cavity for High Field Experiment

K.S. Tanaka, Seo



Q Value

| Modes | Q (measured) | Q (simulation) |
|-------|--------------|----------------|
| TM110 | 11,300 | 29,700 |
| TM210 | 8,050 | 28,900 |

Mu 1S-2S (Mu-MASS@PSI)

Mu-MASS vs RAL(1999) - New essential developments

| | RAL (1999) | Mu-MASS Phase1 | Mu-MASS Phase2 |
|---------------------------------|-----------------------------|------------------------------------|-------------------------|
| μ^+ beam intensity | $3500 \times 50 \text{ Hz}$ | 5000 s^{-1} | $> 9000 \text{ s}^{-1}$ |
| μ^+ beam energy | 4 MeV | 5 keV | 5 keV |
| Temperature M atoms | 300 K | 100 K | 100 K |
| Total number of 2S events | 99 | 1900 (10 d) | > 7000 (40 d) |
| Spectroscopy | Pulsed laser | CW (25 W) | CW (50 W) |
| Experimental linewidth | 20 MHz | 750 kHz | 300 kHz |
| Laser chirping | 10 MHz | 0 kHz | 0 kHz |
| Residual Doppler shift uncert. | 3.4 MHz | 0 kHz | 0 kHz |
| 2nd-order Doppler shift uncert. | 44 kHz | 15 kHz | 1 kHz (corrected) |
| Frequency calibration uncert. | 0.8 MHz | $< 1 \text{ kHz}$ | $< 1 \text{ kHz}$ |
| Background events | 2.8 events/day | 1.6 events/day | 1.6 events/day |
| Statistical uncertainty | 9.1 MHz | $< 100 \text{ kHz}$ | 10 kHz |
| Total uncertainty | 9.8 MHz | $< 100 \text{ kHz}$ (linewidth/10) | 10 kHz (linewidth/30) |

Improved muonium source (higher yield + lower temperature)

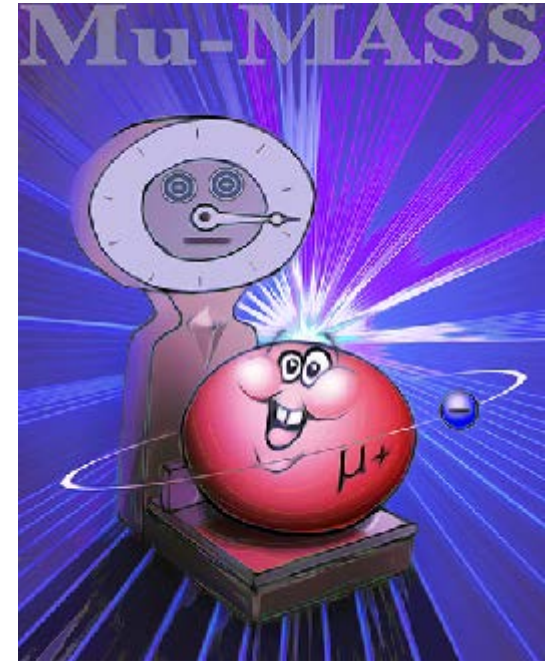
Continuous wave laser spectroscopy vs pulsed



Mu 1S-2S (Mu-MASS@PSI)

Summary

- Mu-MASS aims at improving 3 orders of magnitude on our current knowledge of the 1S-2S of Muonium
- Feasibility builds on expertise acquired during the last decade: Ps CW laser spectroscopy, cryogenic muonium production, high precision detectors development.
- Project funded by European Research Council: start beginning of 2019.
- First results expected in 2020-2021.



Mu 1S-2S at J-PARC

Proposal in preparation

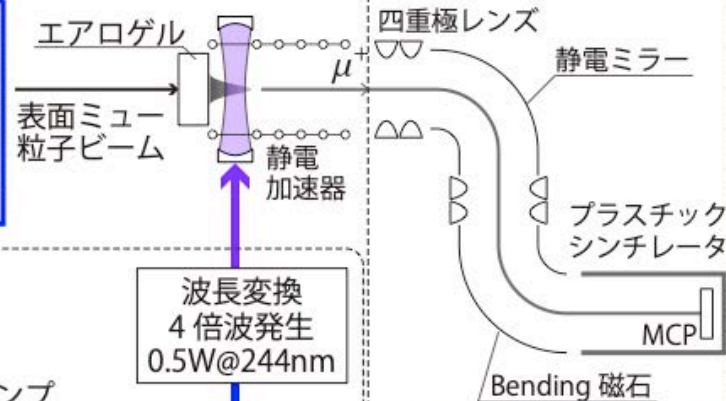
実験セットアップ (1S-2S レーザー分光)

05



2S 励起検出システム

244 nm 光共振器



狭線幅レーザーシステム 波長 244nm

半導体レーザー
976 nm
cw, 30 mW

ファイバ光アンプ

Preamp. Power Amp
 $\sim 0.1\text{ W} \rightarrow \sim 0.5\text{ W} \rightarrow 3\text{ W}$

波長変換
4倍波発生
0.5W@244nm

波長変換
2倍波発生
2.4W@488nm

周波数安定化 & 周波数測定システム

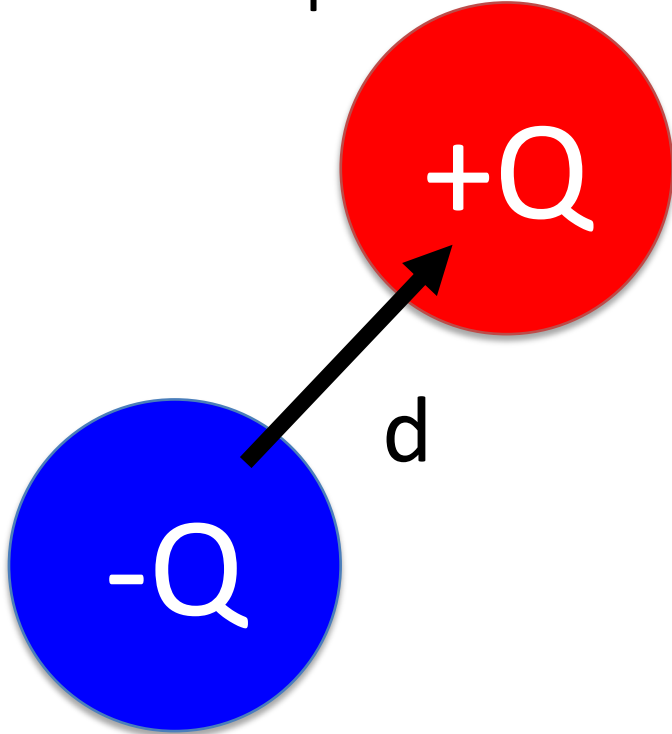


ELECTRIC DIPOLE MOMENT

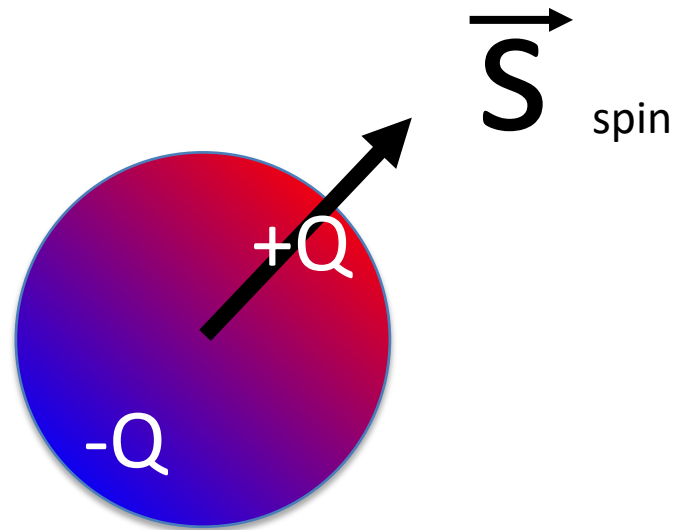
Dipole moments

- A pair of spatially separated (electric, magnetic) charges

Electric dipole moment

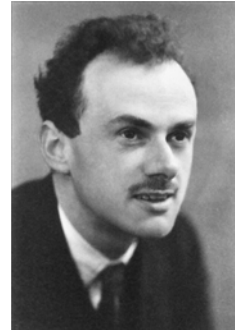


Particle's electric dipole moment



Quantum theory of the electron (1928)

Proceedings of the Royal Society A: Mathematical, Physical and Engineering Sciences 117 (778): 610.



This differs from (1) by the two extra terms

$$\frac{eh}{c} (\boldsymbol{\sigma}, \mathbf{H}) + \frac{ieh}{c} \rho_1 (\boldsymbol{\sigma}, \mathbf{E})$$

in F. These two terms, when divided by the factor $2m$, can be regarded as the additional potential energy of the electron due to its new degree of freedom. The electron will therefore behave as though it has a magnetic moment $eh/2mc \cdot \boldsymbol{\sigma}$ and an electric moment $ieh/2mc \cdot \rho_1 \boldsymbol{\sigma}$. This magnetic moment is just that assumed in the spinning electron model. The electric moment, being a pure imaginary, we should not expect to appear in the model. It is doubtful whether the electric moment has any physical meaning, since the Hamiltonian in (14) that we started from is real, and the imaginary part only appeared when we multiplied it up in an artificial way in order to make it resemble the Hamiltonian of previous theories.

Purcell and Ramsey's letter (1950)

E.M. Purcell and N.F. Ramsey Phys. Rev. 78 (1950)

On the Possibility of Electric Dipole Moments for Elementary Particles and Nuclei

E. M. PURCELL AND N. F. RAMSEY

Department of Physics, Harvard University, Cambridge, Massachusetts

April 27, 1950

IT is generally assumed on the basis of some suggestive theoretical symmetry arguments¹ that nuclei and elementary particles can have no electric dipole moments. It is the purpose of this note to point out that although these theoretical arguments are valid when applied to molecular and atomic moments whose electromagnetic origin is well understood, their extension to nuclei and elementary particles rests on assumptions not yet tested.

One form of the argument against the possibility of an electric dipole moment of a nucleon or similar particle is that the dipole's orientation must be completely specified by the orientation of the angular momentum which, however, is an axial vector specifying a direction of circulation, not a direction of displacement as would be required to obtain an electric dipole moment from electrical charges. On the other hand, if the nucleon should spend part of its time asymmetrically dissociated into opposite magnetic poles of the type that Dirac² has shown to be theoretically possible, a circulation of these magnetic poles could give rise to an electric dipole moment. To forestall a possible objection we may remark that this electric dipole would be a polar vector, being the product of the angular momentum (an axial vector) and the magnetic pole strength, which is a pseudoscalar in conformity with the usual convention that electric charge is a simple scalar.

The argument against electric dipoles, in another form, raises directly the question of parity. A nucleon with an electric dipole moment would show an asymmetry between left and right



- EDM not yet tested
- Ignored due to parity violation (Wu's P-violation experiment was in 1956)
- Possible existence is purely an experimental matter

Ramsey Prize of \$5,000 for the first person, or group to discover non zero EDM of any particle.



"I am personally interested in the EDM tests, since I first proposed them and began looking for them 56 years ago, as tests of P, then T, and then CP. Originally I wanted to be the first person to discover an EDM, but now I at least want to know the answer. I have therefore personally established the time limited " Ramsey Prize of \$5000 for the first person, or group, during my lifetime to announce the convincing discovery of a non zero electric dipole moment for any elementary particle or atomic nucleus." Since I am now 91 years old, please hurry. "

Norman Ramsey

International Conference on Atomic Physics, 2006, Innsbruck

Norman Ramsey先生は2011年11月に永眠されました。

After 60 years of original proposal...



Workshop photo, Lepton Moments 2010, Capecod, MA

Particle dipole moments

$$\mathcal{H} = -\vec{\mu} \cdot \vec{B} - \vec{d} \cdot \vec{E}$$

P,C,T-even

P,T-odd (CP-odd)

Magnetic Dipole Moment

$$\vec{\mu} = g \left(\frac{q}{2m} \right) \vec{s}$$

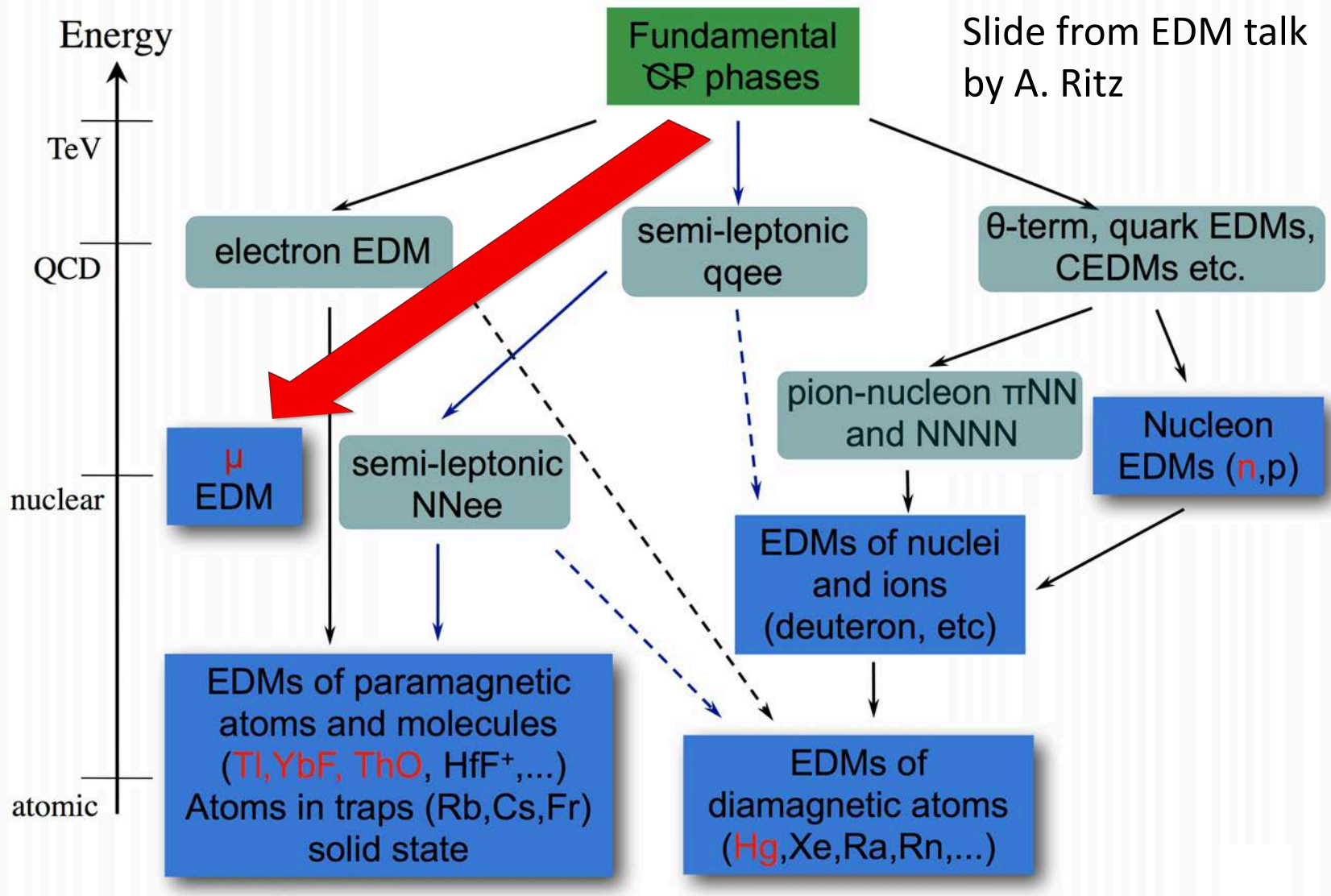
Electric Dipole Moment

$$\vec{d} = \eta \left(\frac{q}{2mc} \right) \vec{s}$$

| | \vec{E} | \vec{B} | $\vec{\mu}$ or \vec{d} |
|-----|-----------|-----------|--------------------------|
| P | - | + | + |
| C | - | - | - |
| T | + | - | - |

Scales of CPV sources and EDM

Slide from EDM talk
by A. Ritz



Spin precession in E and B field

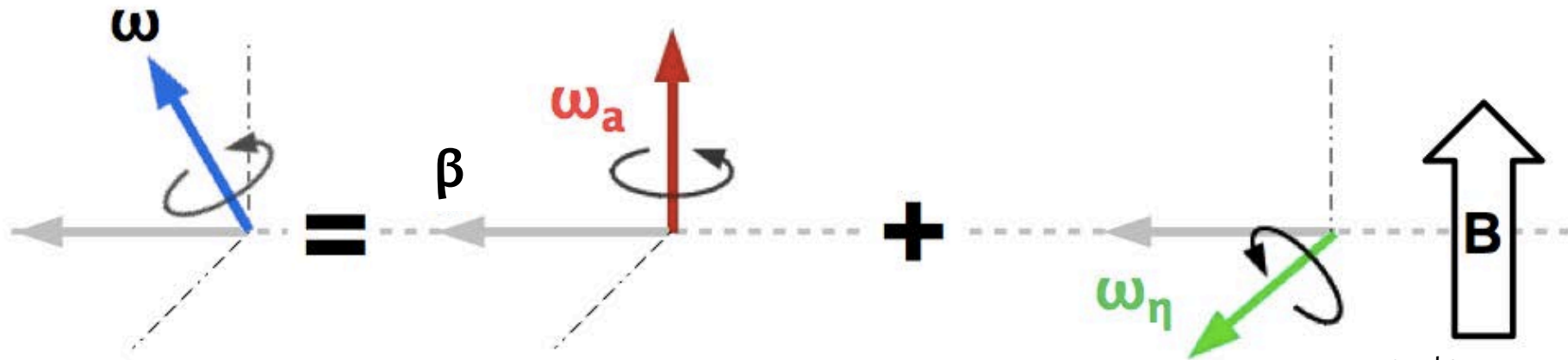
Spin precession vector in static E and B fields ($\vec{\beta} \cdot \vec{B} = 0, \vec{\beta} \cdot \vec{E} = 0$) Fukuyama, Silenko,
arXiv:1308.1580
(reference therein)

$a_\mu = (g-2)/2$

$$\vec{\omega} = -\frac{e}{m} \left[\underbrace{a_\mu \vec{B} - \left(a_\mu - \frac{1}{\gamma^2 - 1} \right) \frac{\vec{\beta} \times \vec{E}}{c}}_{\text{Anomalous magnetic moment}} + \underbrace{\frac{\eta}{2} \left(\vec{\beta} \times \vec{B} + \frac{\vec{E}}{c} \right)}_{\text{EDM}} \right]$$

Anomalous magnetic moment

EDM



courtesy
G. Onderwater

EDM introduces vertical component in spin precession

Spin precession in E and B field

Spin precession vector in static E and B fields ($\vec{\beta} \cdot \vec{B} = 0, \vec{\beta} \cdot \vec{E} = 0$)

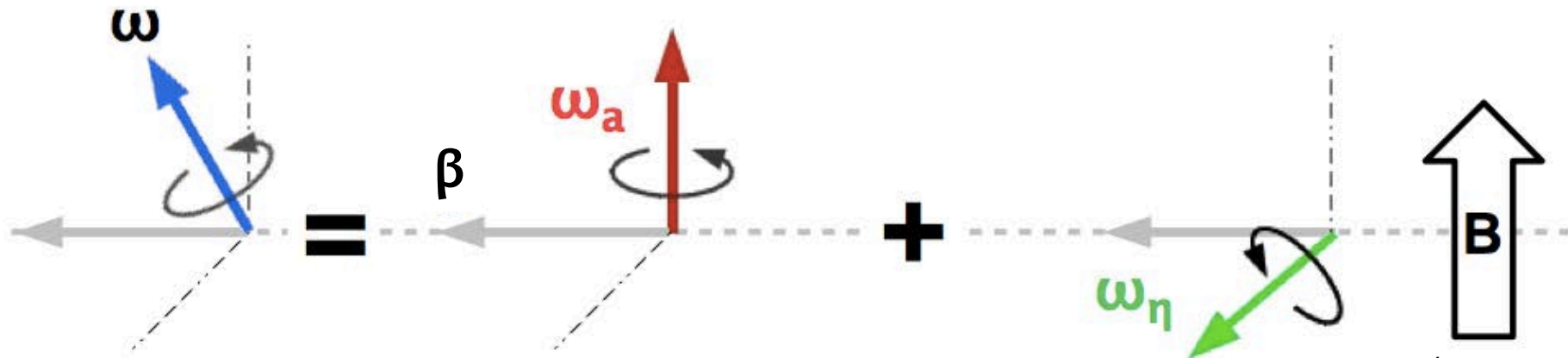
Fukuyama, Silenko,
arXiv:1308.1580
(reference therein)

$$a_\mu = (g-2)/2$$

$$\vec{\omega} = -\frac{e}{m} \left[\underbrace{a_\mu \vec{B} - \left(a_\mu - \frac{1}{\gamma^2 - 1} \right) \frac{\vec{\beta} \times \vec{E}}{c}}_{\text{Anomalous magnetic moment}} + \underbrace{\frac{\eta}{2} \left(\vec{\beta} \times \vec{B} + \frac{\vec{E}}{c} \right)}_{\text{EDM}} \right]$$

Anomalous magnetic moment

EDM



But, it is a tiny : $\omega_\eta / \omega_a \sim (\eta\beta / 2a_\mu) < \sim 10^{-5}$

courtesy
G. Onderwater

Three experimental approaches

Spin precession vector in static E and B fields ($\vec{\beta} \cdot \vec{B} = 0, \vec{\beta} \cdot \vec{E} = 0$)

$$\vec{\omega} = -\frac{e}{m} \left[a_\mu \vec{B} - \left(a_\mu - \frac{1}{\gamma^2 - 1} \right) \frac{\vec{\beta} \times \vec{E}}{c} + \frac{\eta}{2} \left(\vec{\beta} \times \vec{B} + \frac{\vec{E}}{c} \right) \right]$$

(1) Magic momentum (g-2 + EDM)

$\gamma=30$ ($P=3$ GeV/c)
(BNL E821, FNAL)

$$\vec{\omega} = -\frac{e}{m} \left[a_\mu \vec{B} + \frac{\eta}{2} \left(\vec{\beta} \times \vec{B} + \frac{\vec{E}}{c} \right) \right]$$

(2) Zero E-field (g-2 + EDM)

$E = 0$ at any γ
(J-PARC E34)

$$\vec{\omega} = -\frac{e}{m} \left[a_\mu \vec{B} + \frac{\eta}{2} (\vec{\beta} \times \vec{B}) \right]$$

(3) Spin frozen (EDM only)

$E_r = a_\mu B c \beta \gamma^2$
to kill g-2 precession

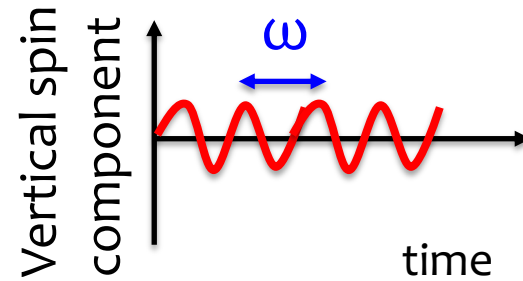
$$\vec{\omega} = -\frac{e}{m} \frac{\eta}{2} \left(\vec{\beta} \times \vec{B} + \frac{\vec{E}}{c} \right)$$

Three experimental approaches

(1) Magic momentum (g-2 + EDM)

(2) Zero E-field (g-2 + EDM)

$$\vec{\omega} = -\frac{e}{m} \left[a_\mu \vec{B} + \frac{\eta}{2} (\vec{\beta} \times \vec{B}) \right]$$



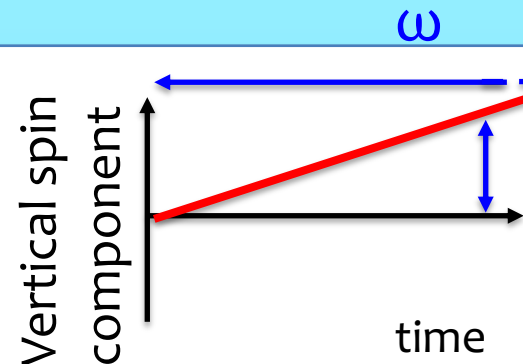
$$\frac{e}{m} \frac{\eta\beta}{4a_\mu}$$

Oscillation with g-2 frequency. Amplitude constrained by g-2

(3) Spin frozen (EDM only)

$E_r = a_\mu B c \beta \gamma^2$
to kill g-2 precession

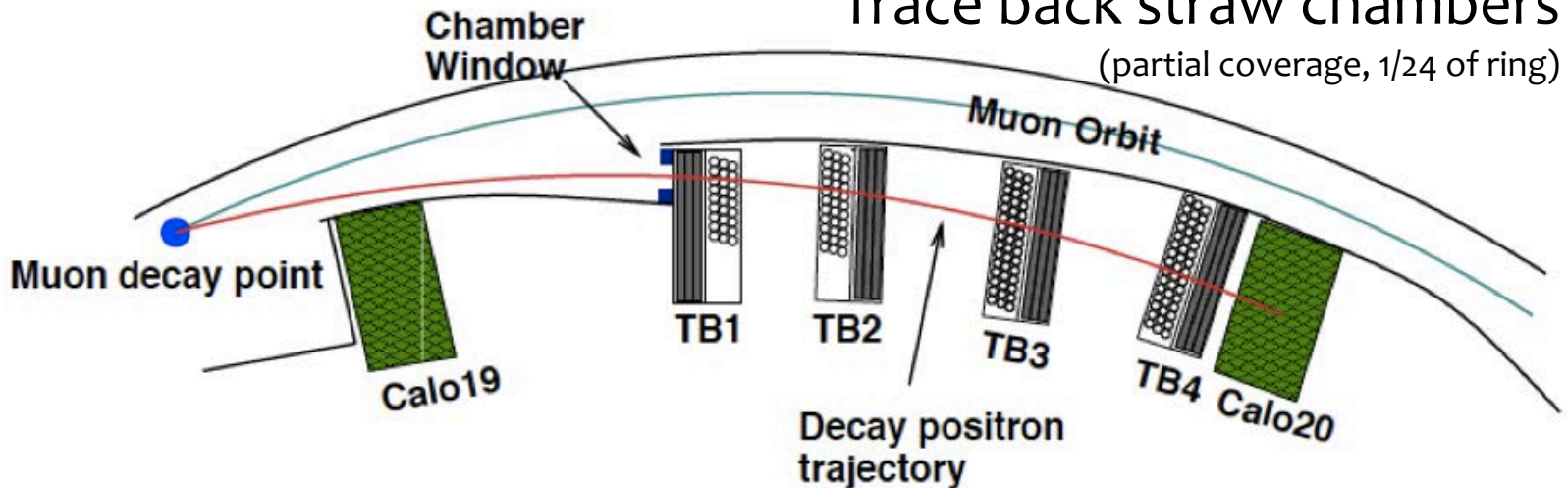
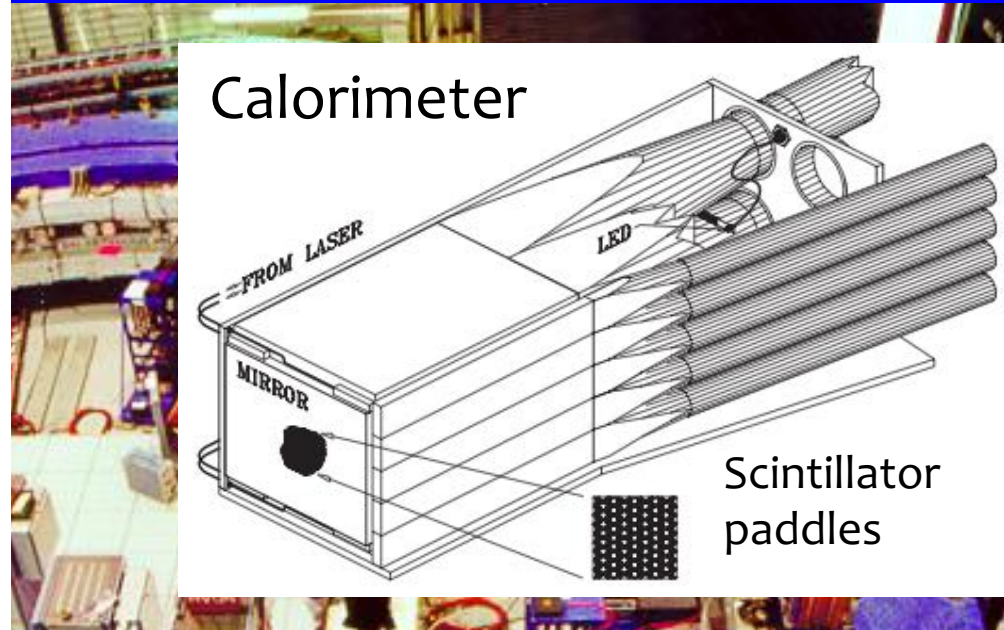
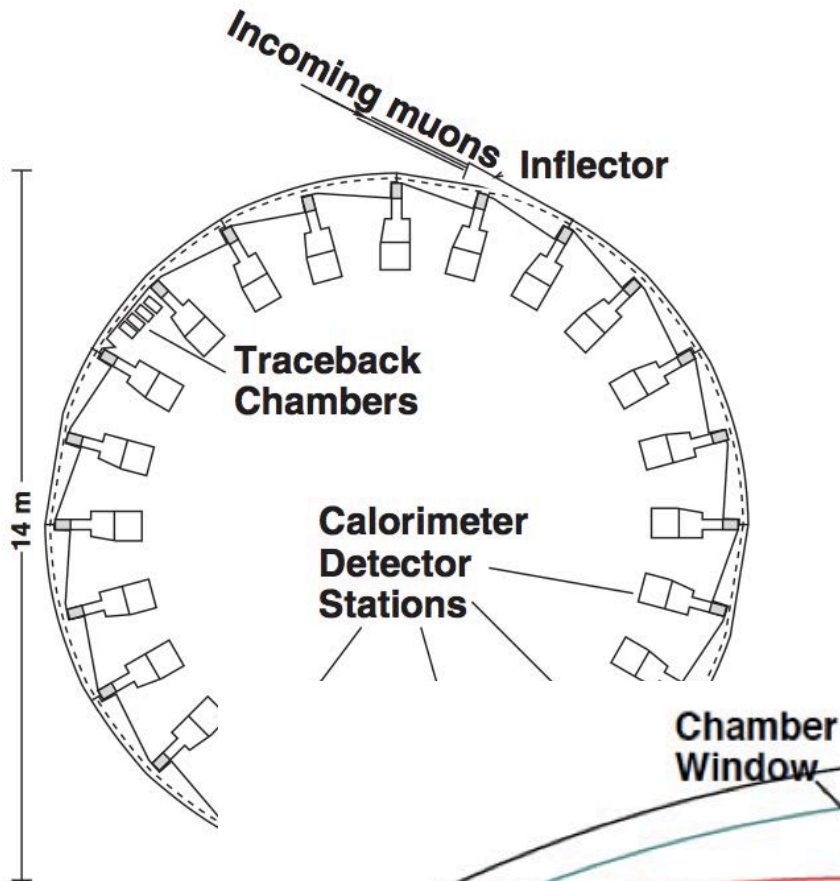
$$\vec{\omega} = -\frac{e}{m} \frac{\eta}{2} \left(\vec{\beta} \times \vec{B} + \frac{\vec{E}}{c} \right)$$



$$\frac{dS}{dt} \approx \frac{e}{m} \frac{\eta\beta}{4} B$$

No constraint in amplitude by g-2 → Better sensitivity

The Experiment at BNL

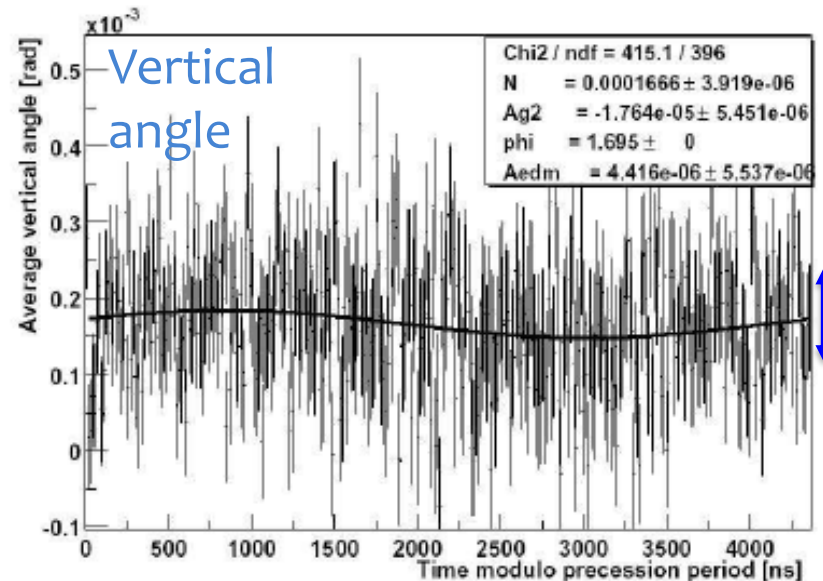
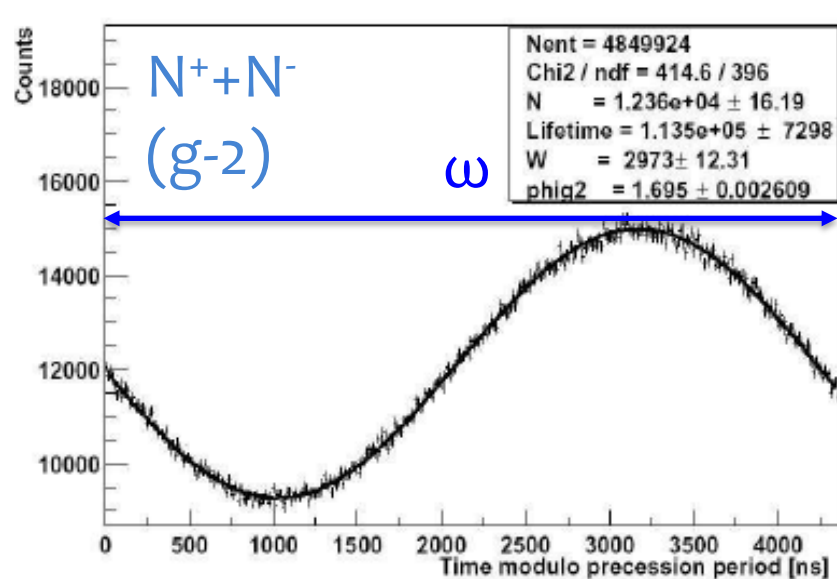


BNL E821 trace-back results

Trace back system

→ Direct measurement of vertical decay angle

$$N^\pm(t) \propto [1 \mp A_{EDM} \sin(\omega t + \phi) + A_\mu \cos(\omega t + \phi)]$$



$$d_{\mu^+} = [-0.04 \pm 1.6(\text{stat}) \pm 0.14(\text{syst})] \times 10^{-19} \text{ ecm}$$

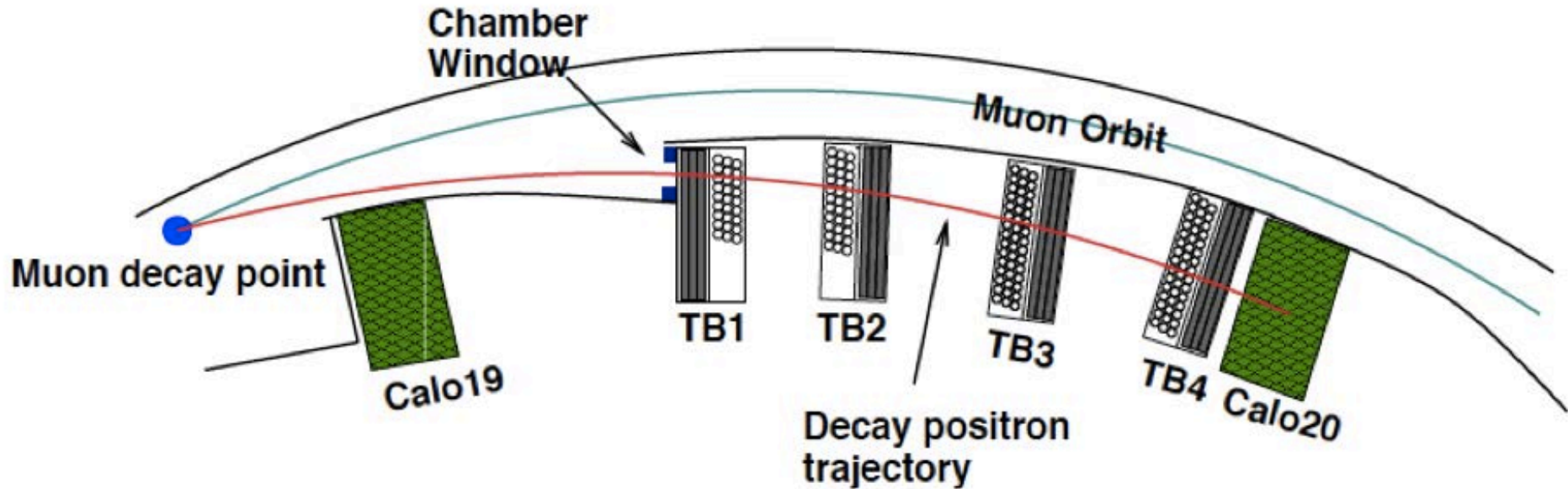
E821 EDM results

| Analysis | Mean value | Stat. error | Syst. error | Total error | 95% C.L. |
|--------------------------------|------------|-------------|-------------|-------------|----------|
| CERN (1978) | | | | | |
| Counting method (μ^+) | 8.6 | 4.0 | 2.0 | 4.5 | |
| (μ^-) | 0.8 | 3.8 | 2.0 | 4.3 | |
| Combined $\mu^+ \mu^-$ | -3.7 | 2.8 | 2.0 | 3.4 | 10.5 |
| E821 | | | | | |
| Traceback (μ^+) | 0.0 | 1.6 | 0.1 | 1.6 | |
| FSD (μ^+) | -0.1 | 0.7 | 1.2 | 1.4 | |
| PSD (μ^-) | -0.1 | 0.3 | 0.7 | 0.7 | |
| Combined $\mu^+ \mu^-$ | 0.0 | 0.2 | 0.9 | 0.9 | 1.8 |

Traceback method :

- Better systematic control than counting methods.
- Statistically limited (partial coverage in the ring)

E821 : systematic uncertainties



G. W. BENNETT *et al.*

PHYSICAL REVIEW D **80**, 052008 (2009)

TABLE II. Table of systematic errors from the traceback analysis.

| Systematic error | Vertical oscillation amplitude (μ rad lab) | Precession plane tilt (mrad) | False EDM generated 10^{-19} (e cm) |
|---------------------------|-------------------------------------------------|------------------------------|------------------------------------------|
| Radial field | 0.13 | 0.04 | 0.045 |
| Acceptance coupling | 0.3 | 0.09 | 0.1 |
| Horizontal CBO | 0.3 | 0.09 | 0.1 |
| No. oscillation phase fit | 0.01 | 0.003 | 0.0034 |
| Precession period | 0.01 | 0.003 | 0.0034 |
| Totals | 0.44 | 0.13 | 0.14 |

Acceptance / CBO coupled with path length difference
(incoming vs outgoing decay)

Future prospect: spin frozen technique



$$\vec{\omega} = -\frac{e}{m} \left[a_\mu \vec{B} - \left(a_\mu - \frac{1}{\gamma^2 - 1} \right) \frac{\vec{\beta} \times \vec{E}}{c} + \frac{\eta}{2} \left(\vec{\beta} \times \vec{B} + \frac{\vec{E}}{c} \right) \right] = \mathbf{0}$$

Apply radial E-field
to eliminate this term

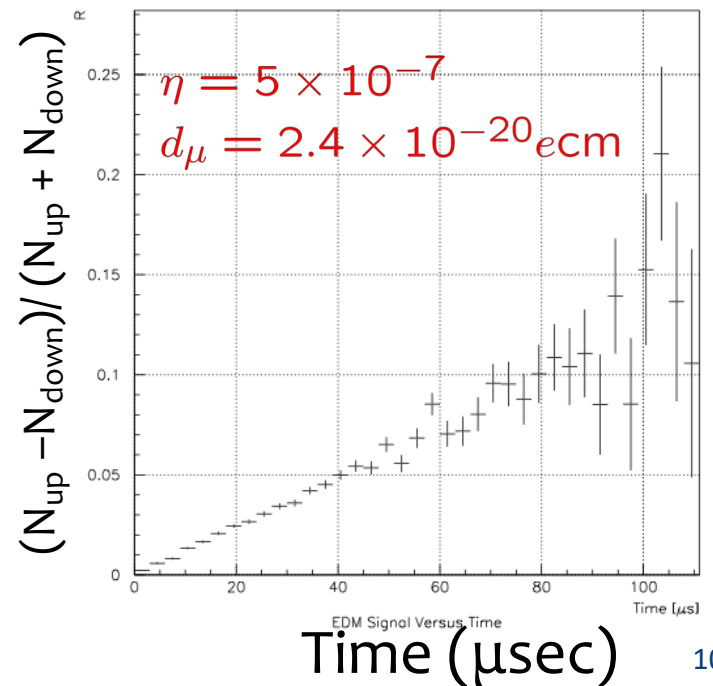
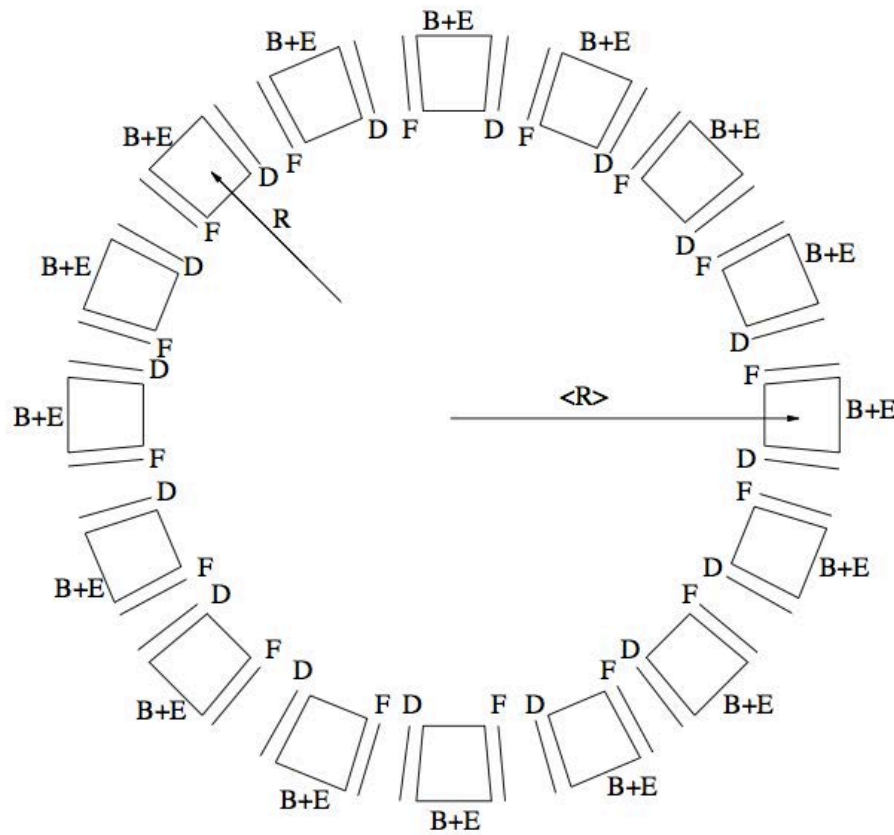
$$E_r = \frac{a_\mu \beta c B}{1 - (1 + a_\mu) \beta^2}$$

- Initially suggested by Yannis Semertzidis, PRL 93, 052001 (2004)
- Muon spin precesses solely by EDM (cf. pEDM experiment)
- Statistical sensitivity:

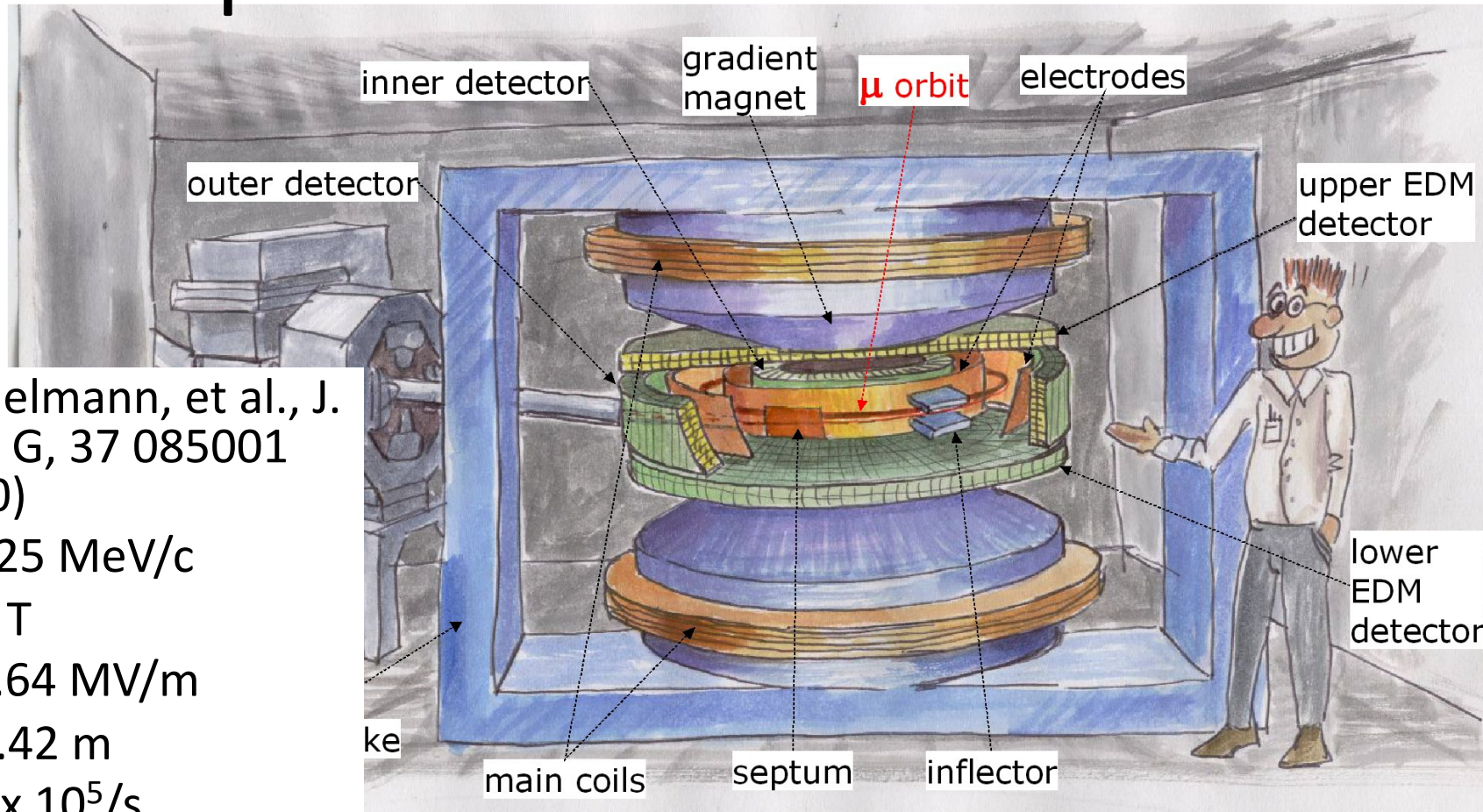
$$\sigma(d_\mu) = \frac{\hbar}{2c(\gamma\tau)(\beta B)A\sqrt{N}}$$

Spin-frozen EDM experiment at J-PARC

- J-PARC LOI 22, A. Silenko et al. (2003)
- $B = 0.25 \text{ T}$
- $E = 2 \text{ MV/m}$
- $R = 7 \text{ m}$
- $NP^2 = 5 \times 10^{16}$ (assume PRISM FFAG)
- sensitivity $\sigma(d_\mu) = 8 \times 10^{-25} \text{ ecm}$



Spin-frozen EDM at PSI



- A. Adelman, et al., J. Phys. G, 37 085001 (2010)
- $p = 125 \text{ MeV}/c$
- $B = 1 \text{ T}$
- $E = 0.64 \text{ MV}/\text{m}$
- $R = 0.42 \text{ m}$
- $N = 2 \times 10^5/\text{s}$
- sensitivity
 $\sigma(d_\mu) = 5 \times 10^{-23} \text{ ecm} / \text{year}$

Summary

- Muon offers rich physics cases to study beyond the standard model in **quantum loops**.
- **BNL muon g-2 results**
 - More than 3σ deviation from the SM.
- **Fermilab muon g-2 experiment** is taking physics run.
- **J-PARC muon g-2/EDM experiment** is in preparation with completely different method.
- **Many new results will come in next 10 years.**